UNIVERSITY OF CALIFORNIA
RIVERSIDE

Air Quality Benefits From Alternative Fuel Vehicles: Ammonia and Nitrous Oxide Emissions From a Fleet of Ethanol Fueled Vehicles and Real-World Emissions From Diesel and Natural Gas-Powered Street-Sweepers

A Thesis submitted in partial satisfaction
of the requirements for the degree of

Master of Science

in

Mechanical Engineering

by

Wei-Zin (Peter) Ho

December 2021

Thesis Committee:

Dr. Georgios Karavalakis, Co-Chairperson
Dr. Heejung Jung, Co-Chairperson
Dr. Lorenzo Mangolini, Member

The Thesis of Wei-Zin (Peter) Ho is approved:

_____

_____

Committee Co-Chairperson

_____

Committee Co-Chairperson

University of California, Riverside

Acknowledgements

I would like to thank many individuals for making this master's thesis possible. First and foremost, I would like to thank God for His never-ending grace, love, and provisions throughout my master's program. I would like to show my gratitude and appreciation to Dr. Georgios Karavalakis and Dr. Kent Johnson for giving me the opportunity to join the Emissions and Fuels Research (EFR) group at the College of Engineering, Center for Environmental Research and Technology (CE-CERT), and for being the best mentors. I would like to thank Dr. Heejung Jung and Dr. Lorenzo Mangolini for their participation in my final thesis defense committee.

I would also like to thank the team members of the EFR group including Mr. Mark Villela, Mr. Daniel Gomez, Mr. Victor Olivares Moran, and Mr. Andrew McCaffery for their help in various chassis dynamometer and PEMS testing. I would like to specially thank the close team members for their support and guidance Dr. Chengguo Li, Dr. Tom Durbin, Mr. Hanwei Zhu, Mr. Tianbo Tang, and Mr. Ma Tiany. I would like to thank Todd Ambriz for his dedication to keeping the lab facilities a safe and conducive environment for conducting research. Lastly, I like to thank my mom Sandy Ho and my brothers WeiJie and WeiLung Ho.

I want to show gratitude to California Air Resources Board (CARB), Renewable Fuels Association (RFA), Growth Energy Inc., USCAR (United States Council for Automotive

Research), and the California Department of Transportation for their financial support and cooperation for each research project.

ABSTRACT OF THE THESIS

Air Quality Benefits From Alternative Fuel Vehicles: Ammonia and Nitrous Oxide Emissions From a Fleet of Ethanol Fueled Vehicles and Real-World Emissions From Diesel and Natural Gas-Powered Street-Sweepers

by

Wei-Zin (Peter) Ho

Master of Science, Graduate Program in Mechanical Engineering
University of California, Riverside, December 2021
Dr. Georgios Karavalakis, Co-Chairperson
Dr. Heejung Jung, Co-Chairperson

Internal combustion engines (ICEs) continue to be a major contributor to environmental air pollution. Emissions from ICEs play a big role in climate change and cause significant human and environmental problems due to both regulated and non-regulated tailpipe emissions. This has prompted the United States Environmental Protection Agency (EPA) to raise the emissions standards for ICEs causing engine manufactures to develop engines more efficient in reducing emissions. These EPA regulations have led some to transition from standard fossil fuels (gasoline and diesel) to alternative fuels and to raise the standard of emissions control technologies. The alternative fuels in this study include ethanol blend gasoline and compressed natural gas (CNG). Emissions technology of interest will include selective reduction catalyst (SCR), diesel oxidation catalyst (DOC), diesel particulate filter (DPF), and three-way catalyst (TWC). With the increasing fleet of vehicles on the road, some non-regulated emissions have become emissions of relevance as some are precursors in the formation of harmful secondary particulate matter (PM).

This study investigates regulated emissions from CNG and diesel street sweepers in the South Coast Basin region of California. Second, this study investigates two non-regulated emissions, ammonia (NH_3) and nitrous oxide (N_2O), in the present fleet of light-duty passenger vehicles (2016-2021) fueled with 10% ethanol blend gasoline (E10) and 15% ethanol blend gasoline (E15).

Table of Contents

List of Figures

List of Tables

1. Introduction

For the last century, internal combustion engines (ICEs) have been used for a variety of applications ranging from automotive transportation to power generation. Even with the rise in electric vehicles (EV), ICEs are still considered the most widely used power-generation device in transportation in the United States. Majority of vehicles in the United States particularly run on two types of fuels, either gasoline or diesel. Gasoline typically utilizes a spark ignition system and diesel utilizes a compressions ignition system with varying direct or indirect fuel injection systems. It is estimated that there are approximately 2 billion internal combustion engines in-use worldwide for a variety of transportation applications ("Internal Combustion Engine—The Road Ahead", 2019).

Research and development in the last century in the automotive industry has uncovered a major downfall of ICEs negative contribution to air quality and global climate change due to harmful emissions. This resulted in the Clean Air Act requiring the Environmental Protection Agency (EPA) to set Nation Ambient Air Quality Standards (NAAQS) for criteria pollutants, particularly with particulate matter (PM), nitrogen oxides (NOx) and carbon dioxide (CO_2), which is a greenhouse gas (GHG) (EPA, 2021).

Particulate matter is a result of the combustion process in both gasoline and diesel engine. PM is a result of incomplete combustion of hydrocarbons in the fuel and lubricant oil (Reşitoğlu, et al., 2014). This formation of particulate matter is dependent on many factors including combustion and expansion process, fuel quality, lubrication oil quality,

combustion temperature and exhaust gas cooling (Reşitoğlu, et al., 2014). It is also shown that diesel engines have considerably higher PM compared to gasoline engines (Reşitoğlu, et al., 2014).

Nitrogen oxides (NOx) is nitrogen oxide (NO) plus nitrogen dioxide (NO_2). NOx formation is attributed to high temperature of burnt gases during combustion and the time duration the gases remain at this temperature (Bindra and Vashist, 2020). NOx is produced from the reaction of nitrogen with oxygen in the combustion chamber (Bindra and Vashist, 2020). This chemical reaction takes place when temperature is 1800 K or higher through dissociation of nitrogen and oxygen molecules as seen below (Bindra and Vashist, 2020):

$$N_2 \rightarrow 2N$$

$$O_2 \rightarrow 2O$$

$$N + OH \rightarrow NO + H$$

$$NO + OH \rightarrow NO_2 + H$$

$$NO_2 + O \rightarrow NO + O_2$$

Therefore, the more time the gases remain at higher temperature (>1800 K), the more NOx produced (Bindra and Vashist, 2020).

Carbon dioxide forms during combustion, where the carbon from the fuel combines with the oxygen from the air (Bindra and Vashist, 2020).

To address the problems of emissions from internal combustion engines, the implementation of catalyst exhaust systems was introduced. Gasoline engines typically use a three-way catalyst (TWC) to control NOx, CO, and THC emissions. Diesel engines generally use diesel oxidation catalyst (DOC) to control CO and THC emissions, diesel particulate filter (DPF) to control PM emissions, and selective catalytic reduction (SCR) to control NOx emissions. The result of the TWC in gasoline engine is that it creates a chemical reaction in the catalyst downstream, producing ammonia (NH_3) (Żółtowski and Gis, 2021). NH_3 is not a regulated or heavily studied pollutant, but recently has drawn some attention due to its health and environmental concerns (Żółtowski and Gis, 2021).

Another solution to address emissions from internal combustion engines is the use of alternative fuels such as biomass-derived liquid fuels and compressed natural gas (CNG). Ethanol, the biofuel of choice in the United States (US), is produced from biomass sources and is currently used at 10% in volume in all commercial gasoline sold in the US (Roth, et al., 2020). CNG has proven to offer life cycle GHG emissions benefits and reduction of some engine emissions, depending on vehicle type, duty cycle, and engine calibration ("Alternative Fuels Data Center: Natural Gas Vehicle Emissions"). Since natural gas is a low-carbon fuel, switching from traditional gasoline to natural gas in some automotive applications can result in reduction in hydrocarbons, CO, NOx, and GHG emissions ("Alternative Fuels Data Center: Natural Gas Vehicle Emissions"). At the same time, natural gas vehicles have the capability to meet stringent emissions

standards with less complicated emissions controls ("Alternative Fuels Data Center: Natural Gas Vehicle Emissions").

1.1 Chapter 1: Investigation of Caltrans Sweeper Emissions

Concerns with adverse health effects due to high emissions of oxides of nitrogen (NOx) and particulate matter (PM) from heavy-duty engines has prompted the United States Environmental Protection Agency's (EPA) to raise emissions standards for heavy-duty engine to reduce NOx and PM to near-zero levels (ARB). Diesel engines continue to be the most popular type of engines in the trucking industry in both passenger and vocational vehicles. An alternative to meet air quality standards more easily is the use of natural gas engines. Natural gas engines, particularly compressed natural gas (CNG) engines, operate on a spark-ignition and a three-way catalyst (TWC) after treatment system with stoichiometric air-fuel ratio to reduce CO and NOx (Thiruvengadam, et al., 2015).

Due to EPA emissions standards and California region specific emissions standards, CNG engines become common in street sweepers in the South Coast Basin. The purpose of this study is to evaluate and compare the exhaust emissions from CNG and diesel street sweepers in their normal day to day operations in the South Coast Basin region of California.

1.2 Chapter 2: NH_3 and N_2O Emissions for E10 CaRFG and Splash Blended E15

According to the U.S. Department of Energy, ethanol is a renewable, alternative fuel made from various plant material known as "biomass", produced from starch in corn grains. Over 98% of U.S. gasoline contains ethanol, most widely used is E10 (10% ethanol, 90% gasoline), which oxygenates the fuel to reduce air pollution (U.S. Department of Energy). Ethanol fuel is also available as E15 (10.5% to 15% ethanol), which has been approved for use in model year 2001 and newer for all light-duty vehicles (U.S. Department of Energy). These ethanol blends vary depending on geographic location and seasons to help reduce emissions (U.S. Department of Energy).

Previous studies (Durbin, et al. (2007), Clairotte, et al., (2013), Graham, et al., (2008), Andrade, et al., (1998)) have shown that an increase in the ethanol content in fuel blends reduces some regulated emissions including carbon monoxide (CO), total hydrocarbons (THC) and carbon dioxide (CO_2). Yet, limited studies have been conducted for ethanol blends and its relation to NH_3, an unregulated emission, produced in the catalyst. With the resulting health risk due to NH_3 emissions, there is the need for ethanol blend fuels and resulting NH_3 emissions to be evaluated. The purpose of this study is to further evaluate ethanol blend fuels in the current fleet of on-road light-duty vehicles (model year 2016-2021). Two blends of ethanol gasolines were utilized in this study including, E10 California Reformulated Gasoline (CaRFG), and E15 by adding denatured ethanol to the E10 CaRFG. Additional emissions sampling was conducted for NH_3 precursor pollutants.

1.3 References

"Alternative Fuels Data Center: Natural Gas Vehicle Emissions." *EERE: Alternative Fuels Data Center*, afdc.energy.gov/vehicles/natural_gas_emissions.html.

Andrade, Jailson B., et al. "Atmospheric levels of formaldehyde and acetaldehyde and their relationship with the vehicular fleet composition in Salvador, Bahia, Brazil." *Journal of the Brazilian Chemical Society*, vol. 9, no. 3, 1998, www.scielo.br/j/jbchs/a/b85CyLTnwQqzJHTX9WYHj9G/abstract/?lang=en.

Bindra, Manu, and Devendra Vashist. "Particulate Matter and NOx Reduction Techniques for Internal Combustion Engine: A Review." *Journal of The Institution of Engineers (India): Series C*, vol. 101, no. 6, 2020, pp. 1073-1082, link.springer.com/article/10.1007/s40032-020-00607-1.

Clairotte, M., et al. "Effects of low temperature on the cold start gaseous emissions from light duty vehicles fuelled by ethanol-blended gasoline." *Applied Energy*, vol. 102, 2013, pp. 44-54, www.sciencedirect.com/science/article/pii/S0306261912005806.

Durbin, Thomas D., et al. "Effects of Fuel Ethanol Content and Volatility on Regulated and Unregulated Exhaust Emissions for the Latest Technology Gasoline Vehicles." *Environmental Science & Technology*, vol. 41, no. 11, 2007, pp. 4059-4064, pubs.acs.org/doi/full/10.1021/es061776o.

EPA. "Criteria Air Pollutants." *US EPA*, 22 Mar. 2021, www.epa.gov/criteria-air-pollutants.

Graham, Lisa A., et al. "Emissions from light duty gasoline vehicles operating on low blend ethanol gasoline and E85." *Atmospheric Environment*, vol. 42, no. 19, 2008, pp. 4498-4516, www.sciencedirect.com/science/article/pii/S1352231008001209.

"Internal Combustion Engine—The Road Ahead." *Https://www.industr.com*, 22 Jan. 2019, www.industr.com/en/internal-combustion-engine-the-road-ahead-2357709.

Reşitoğlu, İbrahim A., et al. "The pollutant emissions from diesel-engine vehicles and exhaust aftertreatment systems." *Clean Technologies and Environmental Policy*, vol. 17, no. 1, 2014, pp. 15-27, *https://link.springer.com/article/10.1007/s10098-014-0793-9*.

Roth, Patrick, et al. "Evaluating the relationships between aromatic and ethanol levels in gasoline on secondary aerosol formation from a gasoline direct injection

vehicle." Science of The Total Environment, vol. 737, 2020, p. 140333, www.sciencedirect.com/science/article/pii/S0048969720338559.

Suarez-Bertoa, R., et al. "Impact of ethanol containing gasoline blends on emissions from a flex-fuel vehicle tested over the Worldwide Harmonized Light duty Test Cycle (WLTC)." Fuel, vol. 143, 2015, pp. 173-182, www.sciencedirect.com/science/article/pii/S0016236114010710.

Thiruvengadam, Arvind, et al. "Emission Rates of Regulated Pollutants from Current Technology Heavy-Duty Diesel and Natural Gas Goods Movement Vehicles." *Environmental Science & Technology*, vol. 49, no. 8, 2015, pp. 5236-5244, pubs.acs.org/doi/full/10.1021/acs.est.5b00943.

U.S. Department of Energy. "Alternative Fuels Data Center: Ethanol Benefits and Considerations." *EERE: Alternative Fuels Data Center*, afdc.energy.gov/fuels/ethanol_benefits.html.

Żółtowski, Andrzej, and Wojciech Gis. "Ammonia Emissions in SI Engines Fueled with LPG." Energies, vol. 14, no. 3, 2021, p. 691.

2. CNG and Diesel Street Sweeper Emissions

2.1 Abstract

In-use gaseous and particulate emissions were assessed utilizing portable emissions measurement systems (PEMS) for two CNG and two diesel medium-heavy duty utility street sweepers. Testing was conducted in the South Coast Basin, California. Results showed that the TWC equipped stoichiometric natural gas street sweeper emitted on average 76% lower NOx emissions and similar PM emissions as compared to the SCR equipped diesel street sweepers. NOx emissions from the CNG street sweepers were well below engine certification standards, while NOx emissions from the diesel street sweepers were generally within the certification standards. PM emissions from both the CNG and diesel street sweepers were all well below certification standards. The CNG experiments showed significantly higher soot mass or black carbon emissions compared to the test routes of the diesel street sweepers. The NOx emission results from both the diesel and CNG street sweepers showed some consistency with the EMFAC model NOx emissions speed profile. This study is to provide a better understanding of the real-world emissions from CNG and diesel-powered street sweeper utility vehicles, as this is novelty study. There are only very few studies available in open literature and the results of this work can better inform regulatory and environmental agencies on the actual emission impacts of street sweeper.

2.2 Introduction

Heavy-duty and medium-duty diesel engines are major contributors to urban air pollution due to emissions of NOx, which can contribute to various environmental issues such as smog, secondary PM formation, acid deposition, in addition to negative effects to human health (Misra, et al., 2017). The reduction of both NOx and PM in parts of California has shown improvement due to stringent emission standards for on-road heavy-duty diesel fleet adopted by the EPA and the California Air Resource Board (CARB) (Misra, et al., 2017). Vehicle emissions are often estimated using mobile source emission models such as EMission FACtors (EMFAC) by the California Air Resources Board (CARB), yet mobile emission models may deviate from real-world conditions (Wang, et al., 2021). Therefore, studies of real-world heavy-duty diesel emissions measurements have been carried out with various methods including chassis dynamometer, remote sensing and PEMS testing to validate and compare with model estimates.

To meet stringent NOx emissions standards, diesel engine manufactures have been utilizing SCR systems to reduce engine out NOx emissions for engine year 2010 and newer (Misra, et al., 2017). SCR is an advanced exhaust after treatment system (Figure 3-1) that spreads aqueous urea solution (AUS 32) into the exhaust stream, which reacts with heat and converts to NH_3 (Cummins). The ammonia then reacts with the NOx and passes over the catalyst to form harmless by-products that is nitrogen and water vapor (Cummins).

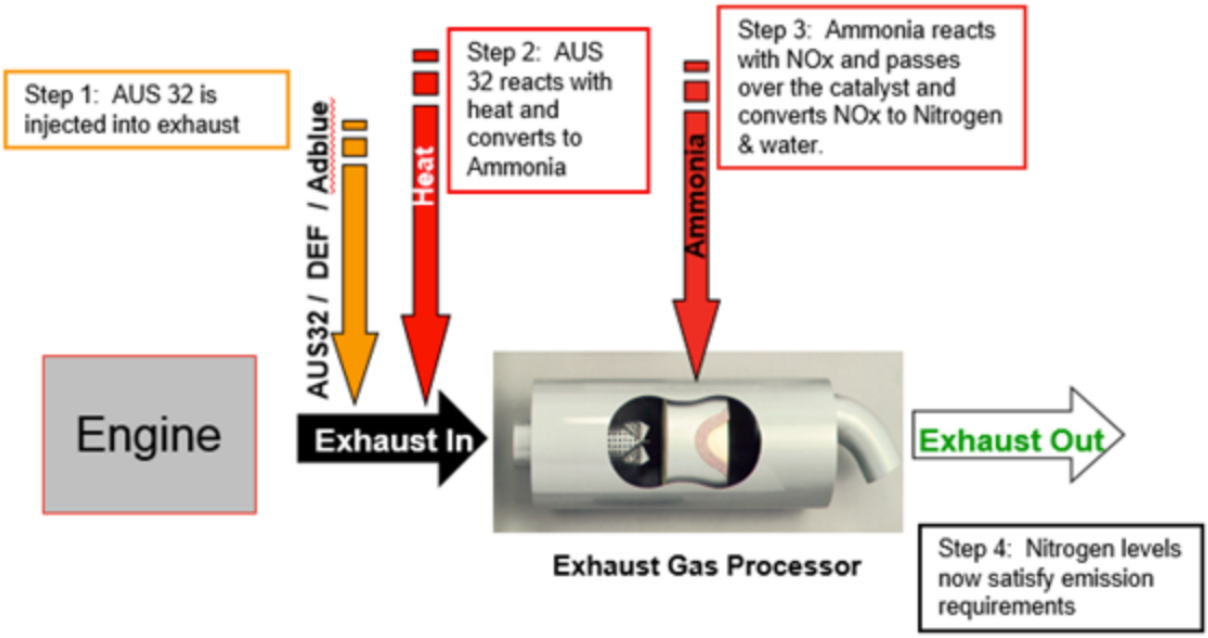

Figure 2-1: SCR System Working

Even with the use of SCR systems, there is the possibility that NOx can exceed certified emissions standards due to various operational characteristics such as idling time as well as duty cycles affecting emissions (ARB). As vehicles age and accumulate miles, emissions control systems can deteriorate over time, which can lead to emissions being much higher than their certification standards (ARB). In a 200-vehicle study, CARB researchers showed that NOx emissions for some vehicles with higher milage to significantly exceed their respective engine emissions standard (ARB).

As of 2017, the U.S. refuse truck fleet account for 120,000 – 136,000 trucks power by heavy-duty diesel engines burning billions of gallons of fuel each year (Misra, et al.,

2017). The refuse truck industry has taken the initiative to decrease dependence of petroleum and shift to alternative fuels to reduce emissions (Misra, et al., 2017).

One growing alternative for heavy-duty applications is stoichiometric natural gas engines due to lower NOx and PM emissions (Misra, et al., 2017). Natural gas engines typically use TWC to remove HC, CO, and NOx (Misra, et al., 2017). TWC has been shown to be more effective than lean combustion in controlling NOx emissions (Misra, et al., 2017). Grigoratos, et al. (2016) showed CNG trucks with 3 – 4 times lower NOx when compared to the same model/year diesel counterparts (Misra, et al., 2017). Another advantage of natural gas engines over diesel engines is that natural gas has 25% lower CO_2 production per unit of energy (Misra, et al., 2017). All these benefits of emission reduction make natural gas engines a good choice, yet presents challenges like maintenance, refueling and lower energy density (Misra, et al., 2017).

The University of California, Riverside (UCR) research team collaborated with California Department of Transportation (CalTrans) to conduct a PEMS field test for four selected street sweepers (2 CNG sweepers, 2 Diesel sweepers) to obtain emissions data during different modes of operations. This information collected will be used to compare street sweeper technologies (CNG and Diesel), specifically comparing emissions of NOx, CO, total hydrocarbons (THC), methane (CH_4), CO_2, PM, and soot mass. Currently, there are minimal studies specifically analyzing street sweeper exhaust emissions outside of some heavy-duty diesel vocational vehicles studies that briefly include a street sweeper in

the study (Carder, et al. 2002, Gautam et al. 2002) and a test of a mobile participatory sensing emissions technology used on a diesel street sweeper (Aoki et al.).

The motivation behind this study is due to strict emissions standards by the South Coast Air Quality Management District, which has led CalTrans to using CNG-powered sweepers. The problem with CNG sweepers is that they are not as reliable and have lower production rates.

2.3 Experimental Procedures

2.3.1 Test Vehicles

Table 2-1 describes the main technical specifications for each of the four street sweepers in this study. All tests are with Class 7 vehicles equipped with Cummins engines of model year 2014 or newer. All street sweepers were equipped with exhaust gas recirculation (EGR), which is used to reduce in-cylinder NOx formation by lowering combustion temperatures. The CNG street sweepers were equipped with TWCs. The diesel street sweepers were equipped with selective catalytic reduction (SCR), diesel particulate filters (DPF), and diesel oxidation catalysts (DOC). All CNG and diesel street sweepers were certified to CARB's optional 0.2 g/bhp-hr ultra-low emissions NOx limit, CARB's 15.5 g/bhp-hr emissions CO limit, and CARB's 0.01 g /bhp-hr emissions PM limit.

Table 2-1: Technical specifications of the test vehicles

UCR ID	**CNG 1**	**CNG 2**	**Diesel 1**	**Diesel 2**
Vehicle ID	7011373	7011374	7005947	7008055
Vehicle Type	Class-7 CNG	Class-7 CNG	Class-7 Diesel	Class-7 Diesel
Manufacturer	Cummins	Cummins	Cummins	Cummins
Engine model year	2015	2015	2012	2012
Engine Family	FCEXH0540LBF	FCEXH0540LBF	CCEXH0408BAH	CCEXH0408BAH
Ignition Type	Spark	Spark	Compression	Compression
Mileage	40,017	31,263	255,057	295,177
Aftertreatment	EGR, TWC	EGR, TWC	EGR, SCR, DPF	EGR, SCR, DPF
Displacement (L)	8.9	8.9	6.7	6.7
Engine model	ISLG250	ISLG250	ISB280	ISB280
Torque	1600lb-ft @ 500	1600lb-ft @ 500	1600lb-ft @ 660	1600lb-ft @ 660
Max power (HP)	250	250	280	280
Certification Standards (US EPA)				
NOx (g/bhp-hr)	0.2	0.2	0.2	0.2
NMHC (g/bhp-hr)	0.14	0.14	0.14	0.14
CO_2 (g/bhp-hr)	618	618	-	-
CO (g/bhp-hr)	15.5	15.5	15.5	15.5
PM (g/bhp-hr)	0.01	0.01	0.01	0.01
N_2O (g/bhp-hr)	-	-	-	-
CH_4 (g/bhp-hr)	-	-	-	-

2.3.3 PEMS Emissions Testing

A gaseous PEMS unit (Semtech DS, Sensors Inc., Saline, MI) was used throughout the test campaign for all 4 street sweepers. Measurements were made for carbon monoxide (CO), total hydrocarbons (THC), carbon dioxide (CO_2), and nitrogen oxides (NOx). The Semtech DS unit is equipped with a non-dispersive infrared (NDIR) analyzer for CO and CO_2 measurements, a non-dispersive ultraviolet (NDUV) analyzer for NO and NO_2 measurements, and a hot flame ionization detector (HFID) for THC measurements. This unit is recognized by the US EPA as being capable of meeting accuracy requirements for in-use regulatory testing requirements. Figure 2-2 shows a picture of the gas-phase PEMS unit.

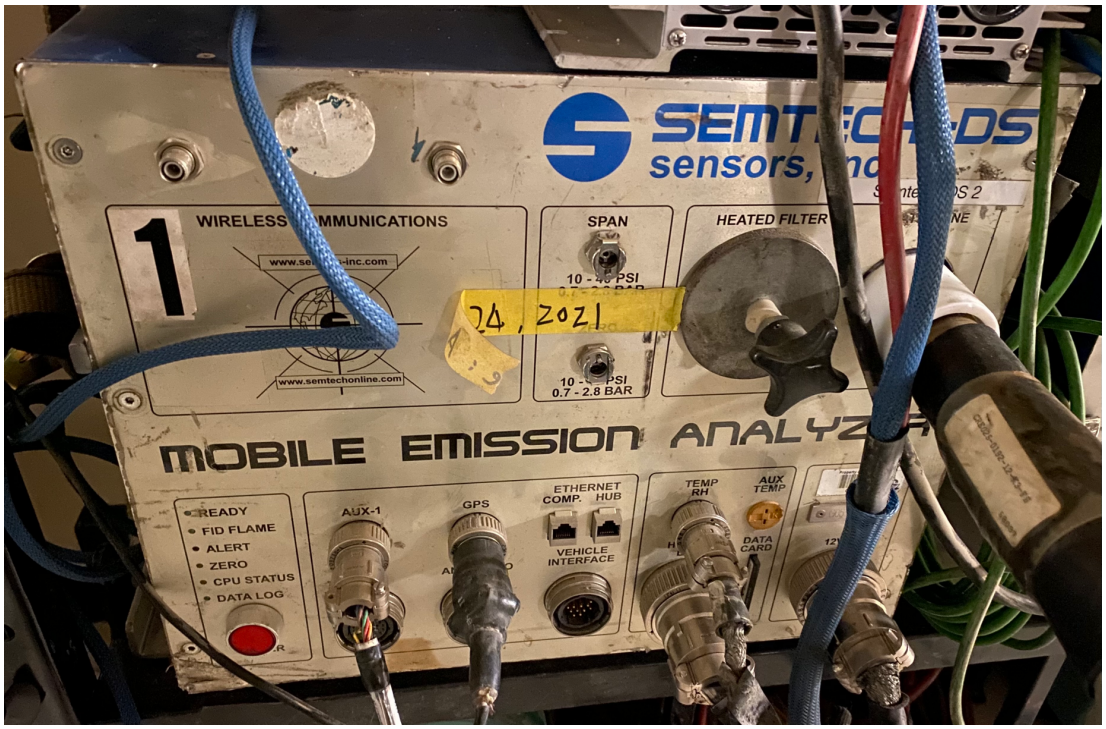

Figure 2-2: Gas PEMS unit

A Sensors, Inc. exhaust flow meter (EFM) compatible with the PEMS unit was used to provide integrated mass emissions and second by second emissions data. The EFM system was equipped with an averaging pitot tube and thermocouples to obtain the exhaust mass flow. The EFM system was calibrated following procedures according to CFR40 Part 1065.307. Figure 2-3 shows a picture of the EFM. The exhaust flow rates are multiplied by the concentration levels on a second-by-second basis after time alignment to provide emission rates in grams per second.

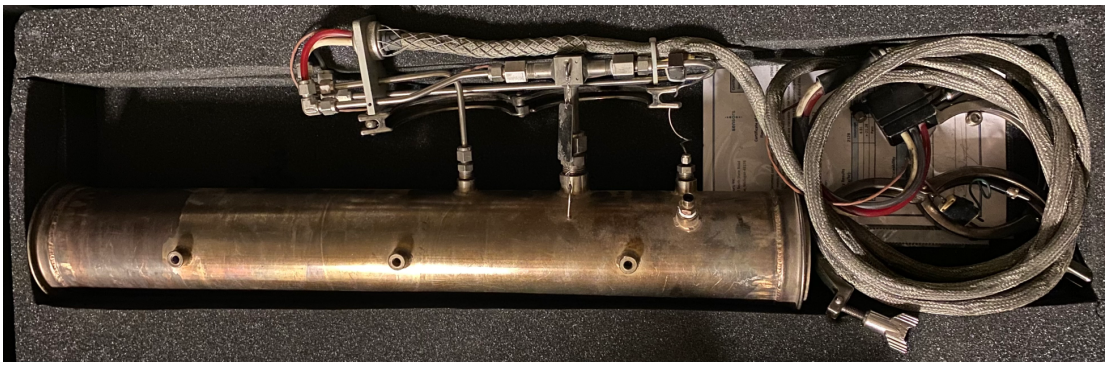

Figure 2-3: PEMS exhaust flow meter measurement system

PM emissions were measured using the AVL 494 PM system. The unit combines AVL's 483 micro soot sensor (MSS) with a gravimetric filter module (GFM) option (Figure 2-4). The AVL 483 MSS measures the modulated laser light absorbed by particles from an acoustical microphone. The measurement principle is directly related to elemental carbon (EC) mass (also called soot), and is robust and has been shown to have good agreement with the reference gravimetric method for EC dominated PM. The GFM is then utilized in conjunction with a post processor that utilizes the filter to estimate (or calibrate) the total PM from the soot and gravimetric filter measurements. One gravimetric filter can be sampled per day, depending on PM loading for different vehicles. Continuous PM concentration is recorded at 1 Hz with an option of 10 Hz data. The combined MSS+GFM system received type approval by EPA as a total PM measurement solution for in-use testing, thus making it one of the few 1065 compliant PM PEMS systems.

Figure 2-4: PM PEMS unit

Each individual PEMS unit was fixed on a custom rack. The rack was then mounted on the back of the street sweepers on custom rails. The entire PEMS rack was powered by a gasoline generator for the duration of the test. The PEMS setup is shown in Figure 2-5.

Figure 2-5: PEMS rack installed on street sweeper

Testing of each street sweeper was conducted over a typical day during in-use operation for their specific location. The test routes corresponded to the normal routes for each street sweeper's vocation. CNG Sweeper 1 and 2 operated in Bloomington, California, Diesel 1 Sweeper operated in Victorville, California, and Diesel 2 Sweeper operated in Yucca Valley, California. Testing of each vehicle varied in length from 24 to 90 miles with testing duration of 4 to 8 hours. The PEMS unit was zeroed and spanned to check

for drift before and after every test. Table 2-2 shows the length and duration for each vehicle's test route. Maps of each test route for CNG and diesel street sweepers (Diesel1_Route1 GPS data lost due to technical difficulties) are shown in Figure 2-6 and Figure 2-7.

Table 2-2: Length and duration for each vehicle during typical operation

Vehicle type	Engine MY	Route/Test #	Naming	Miles	Hours
CNG Sweeper 1	2017	1	CNG1_Route1	42.6	6.93
CNG Sweeper 1	2017	2	CNG1_Route2	27.09	6.54
CNG Sweeper 2	2017	1	CNG2_Route1	56.91	5.49
CNG Sweeper 2	2017	2	CNG2_Route2	85.43	7.95
Diesel Sweeper 1	2014	1	Diesel1_Route1	89.88	6.09
Diesel Sweeper 1	2014	2	Diesel1_Route2	24.32	4.08
Diesel Sweeper 2	2014	1	Diesel2_Route1	24.15	6.11
Diesel Sweeper 2	2014	2	Diesel2_Route2	39.76	4.21

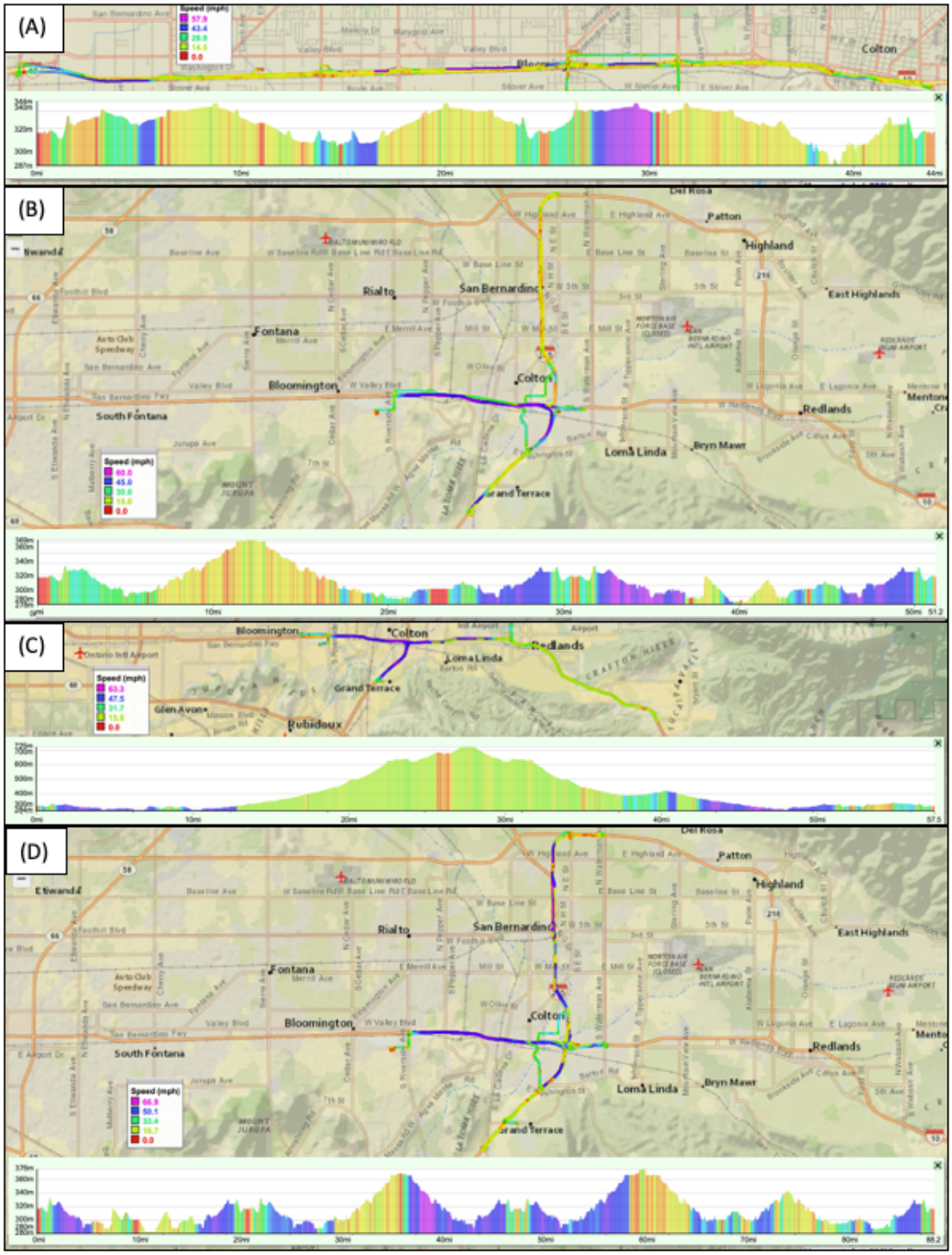

Figure 2-6: Test route map for (a) CNG1_Route1, (b) CNG1_Route2, (c) CNG2_Route1, and (d) CNG2_Route2

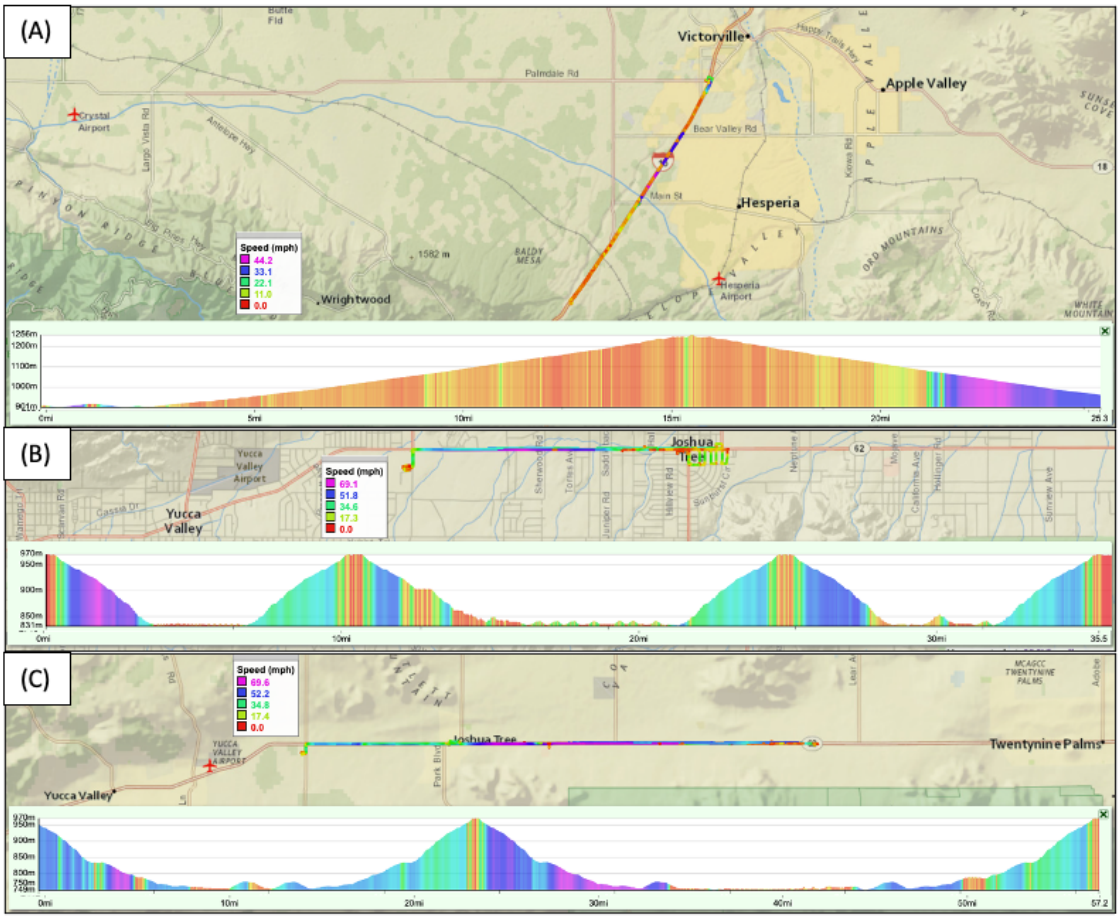

Figure 2-7: Test route map for (a) Diesel1_Route2, (b) Diesel2_Route1, and (c) Diesel2_Route2

2.5 Results and Discussion

2.5.1 NOx Emissions

Figure 2-8 shows the brake-specific NOx emissions for all sweeper tests in g/bhp-hr, while Appendix A shows NOx emissions in units of grams per mile (g/mile), grams per hour (g/hr), grams per gallon (g/gal), and grams per day (g/day). For the SCR-equipped diesel street sweepers, in-use NOx emissions generally met EPA engine certification limit of 0.2 g/bhp-hr. An exemption was observed for diesel 1 over route 1 (0.26 g/bhp-hr) and diesel 2 over route 2 (0.22 g/bhp-hr). In-use NOx emissions were 30% higher for Diesel1_Route1, 50% lower for Diesel1_Route2, 55% lower for Diesel2_Route1, and 10% higher for Diesel2_Route2, respectively, than engine certification limit. For the CNG street sweepers, in-use NOx emissions were all well below EPA engine certification limit compared to the diesel NOx emissions, with CNG in-use NOx emissions being 78% lower for CNG1_Route1, 125% lower for CNG1_Route2, 78% for CNG2_Route1, and 108% lower for CNG2_Route2, respectively.

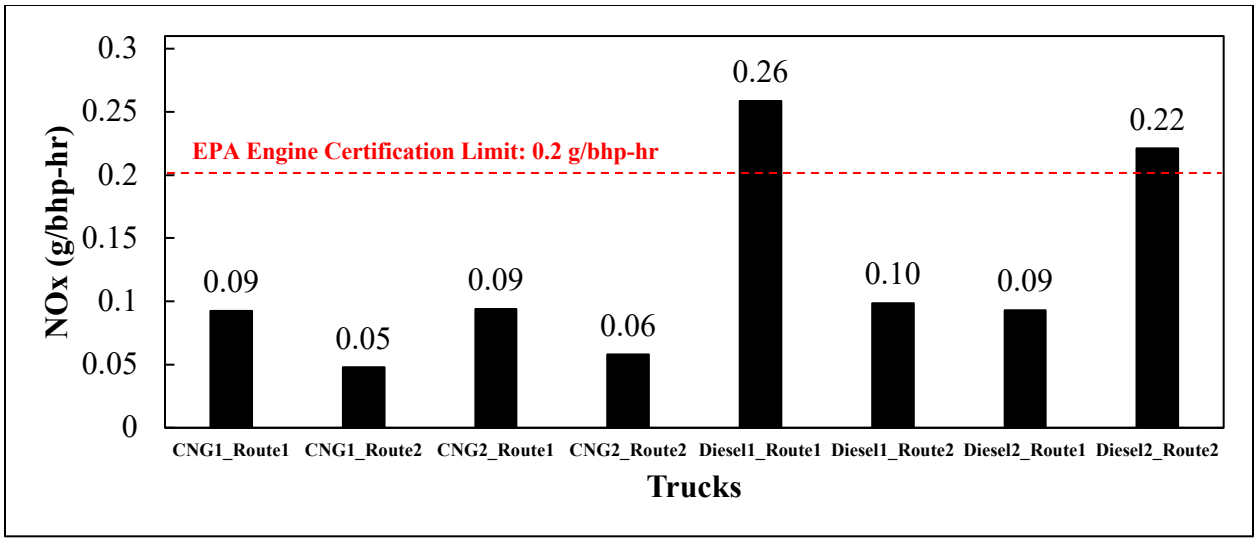

Figure 2-8: Brake-specific NOx emissions for the diesel and CNG sweepers

2.5.2 Real-time NOx Emissions

Elevated real-time NOx emissions were observed during cold starts for all street sweepers (diesel and CNG), likely due to the aftertreatment system being below its light-off temperature (Misra, et al., 2017). CNG sweepers proved to have consistent NOx emissions in all test runs. Real-time NOx emissions for all CNG sweepers showed peaks coinciding with acceleration and elevated load events. CNG1_Route1 showed slightly higher NOx emissions that CNG1_Route2. This is likely due to the many elevation changes seen in Figure 2-6 (a), which resulted in significantly more load changes and spikes in NOx emissions. CNG1_Route2 (Figure 2-6, (b)) showed a relatively constant elevation during the duration of the test, resulting in lower spikes of NOx emissions (Figure 2-9). Similar to CNG1_Route1, CNG2_Route2 showed many elevation and load

changes (Figure 2-6, (d); Figure 2-12), which resulted in higher NOx emissions compared to CNG2_Route1 that only had one big elevation change (Figure 2-6, (c); Figure 2-11).

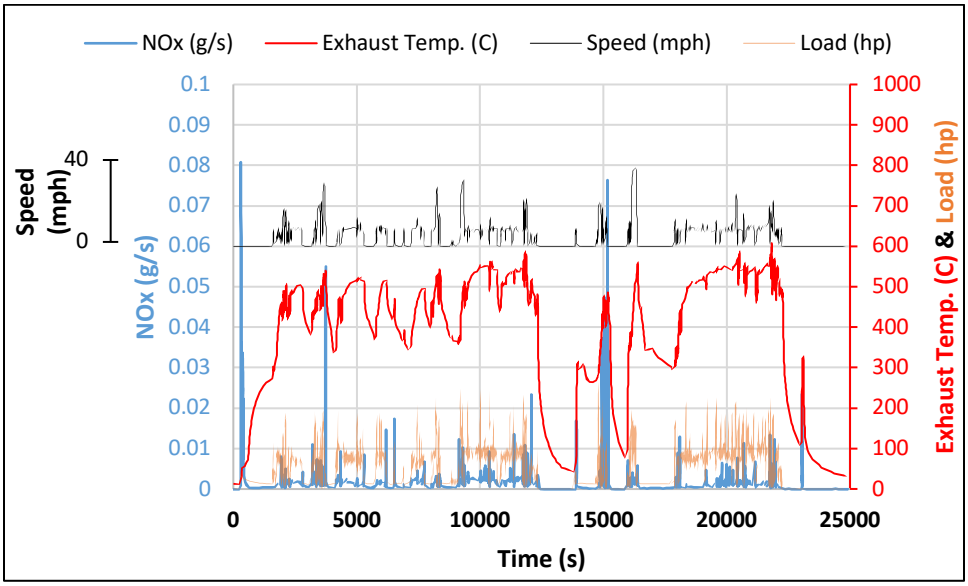

Figure 2-9: Real-time NOx emissions as a function of exhaust temperature, vehicle speed, and load for CNG1_Route1

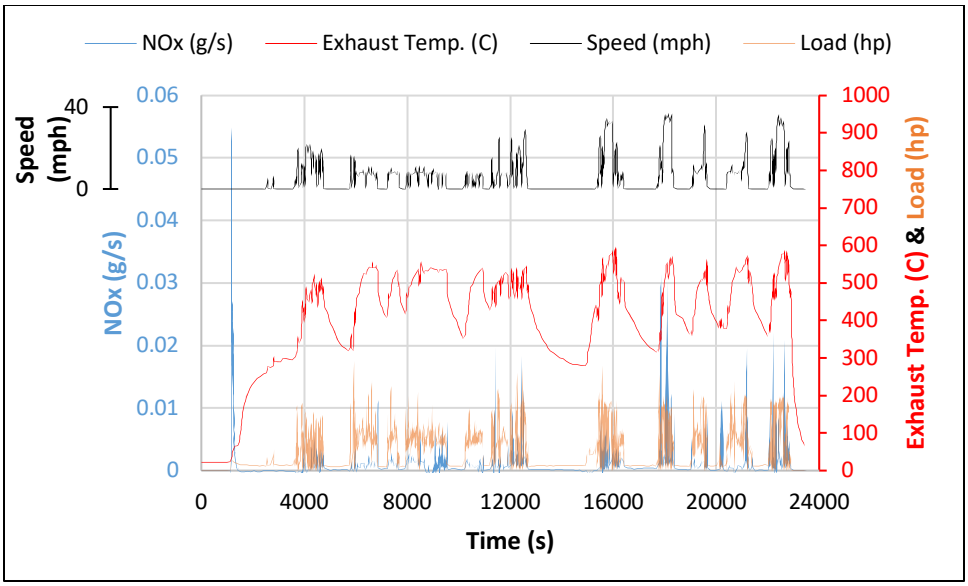

Figure 2-10: Real-time NOx emissions as a function of exhaust temperature, vehicle speed, and load for CNG1_Route2

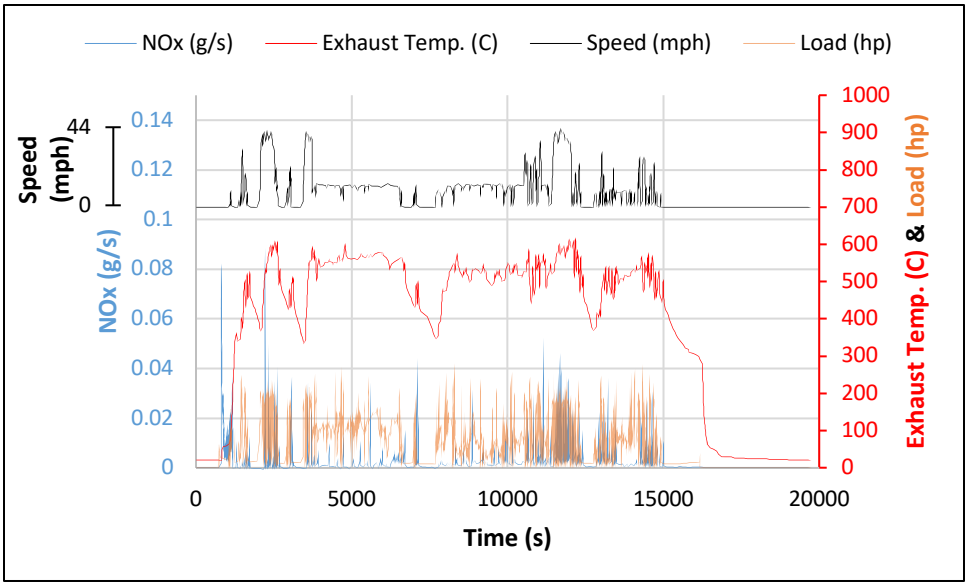

Figure 2-11: Real-time NOx emissions as a function of exhaust temperature, vehicle speed, and load for CNG2_Route1

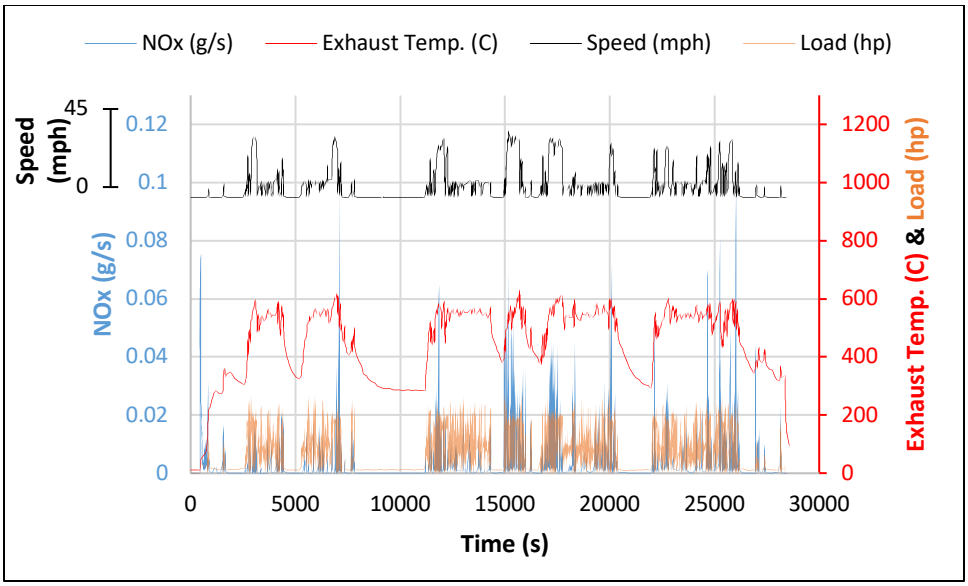

Figure 2-12: Real-time NOx emissions as a function of exhaust temperature, vehicle speed, and load for CNG2_Route2

Figure 2-8 showed in-use NOx emissions were significantly higher for the diesel sweepers compared to the CNG sweepers, which is consistent with previous heavy-duty PEMS studies (Quiros et al., 2016 and Thiruvengadam, et al., 2015). Lower NOx emissions for the CNG sweepers compared to the diesel sweepers were likely due to the effectiveness of the TWC in removing NOx during stoichiometric operating conditions. Higher NOx emissions for the diesel sweepers than the CNG sweepers are likely due to the higher compression ratio in the diesel engines compared to the spark ignition engines in the CNG sweepers, which means higher pressure and temperature, promoting NOx emission (Datta and Mandal, 2016). The CNG street sweepers also showed higher average exhaust temperature (40% higher) than the diesel street sweepers, so the TWC generally remained active to remove NOx even in lower loads of operations. All CNG

street sweepers demonstrated in-use NOx emissions 2-4 times lower than the CARB optional standard of 0.2 g/bhp-hr and resulted in consistent NOx emissions in all tests.

The SCR-equipped diesel sweeper demonstrated NOx emissions generally below the CARB optional standard of 0.2 g/bhp-hr (Figure 2-6) with exception of two diesel tests being slightly higher. Real-time NOx as a function of exhaust gas temperature and vehicle speed for the SCR-equipped diesels sweepers are shown in Figure 2-13 and Figure 2-15. Real-time NOx emissions were quite different for Diesel1_Route1 and Diesel1_Route2, as the route and speed profile were significantly different. Diesel1_Route1 included many acceleration changes and higher engine load, while Diesel1_Route2 included lower speeds and less transient operation. Diesel1_Route2 showed low NOx emissions and showed very consistent exhaust temperature of about 250 ℃ throughout the entire duration of the test with very low NOx emission spikes. Diesel1_Route1 showed high spikes of NOx and exhaust temperature ranging from 200 ℃ to over 400 ℃ with abrupt acceleration changes.

A previous study (Misra, et al., 2013) showed that exhaust temperature is generally sufficient to reduce NOx emissions in diesel vehicles during highway cruise conditions, where exhaust temperatures are above SCR light-off conditions. Therefore, NOx emissions are greatly dependent on exhaust temperature for SCR operation. Typically, SCR needs to be at least 200-250 ℃ to achieve a significant level of NOx reduction (Boriboonsomsin, et al., 2018). Several studies show elevated in-use NOx emissions

during low-speed driving as a result of exhaust gas temperatures being below 200 °C, making the SCR ineffective in reducing NOx emissions (Misra et al., 2013; Misra et al., 2017; Thiruvengadam et al., 2015; Grigoratos et al., 2019). On the contrary, Diesel1_Route2 shows that it is possible that a constant exhaust temperature of 250 °C at lower speeds may be more effective than a fluctuating temperature of 200-400 °C at higher speeds in reducing NOx emissions, where Diesel1_Route2 showed significantly lower NOx emissions at a lower speed and lower average exhaust temperature than Diesel1_Route2.

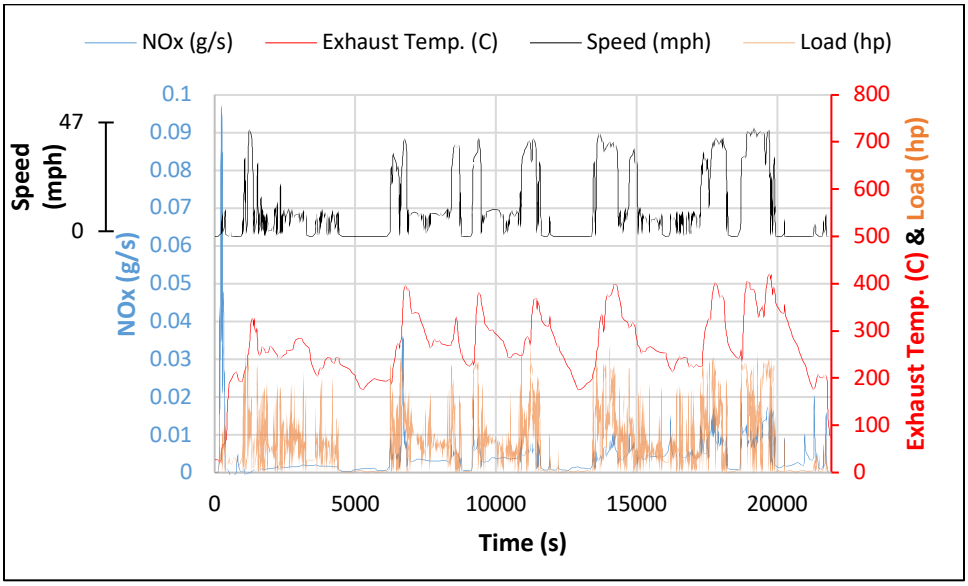

Figure 2-13: Real-time NOx emissions as a function of exhaust temperature, vehicle speed, and load for Diesel1_Route1

Further investigating, Figure 2-14 shows Diesel1_Route1 emitting high NOx with exhaust temperature well above catalyst light-off temperature during a hard acceleration.

This shows acceleration plays a bigger role than SCR light-off temperature in NOx emissions. This explains the significantly higher NOx emissions from Diesel1_Route1 compared Diesel1_Route2. Both routes show exhaust temperatures above SCR light-off conditions, yet Diesel1_Route1 show driving conditions with more aggressive accelerations and higher vehicle speeds compared to Diesel1_Route2.

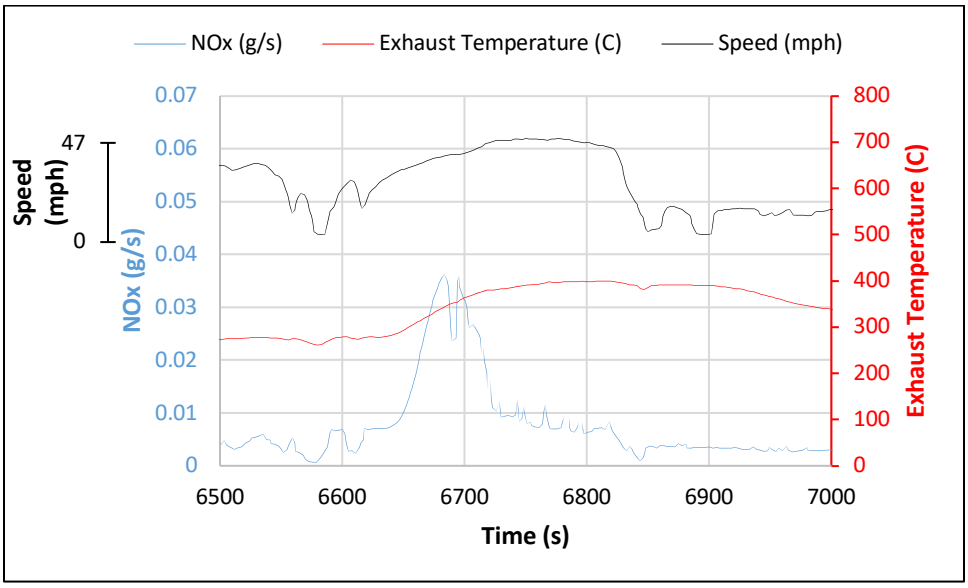

Figure 2-14: Real-time NOx emissions as a function of exhaust temperature and vehicle speed for Diesel1_Route1 from 6500 - 7000 seconds

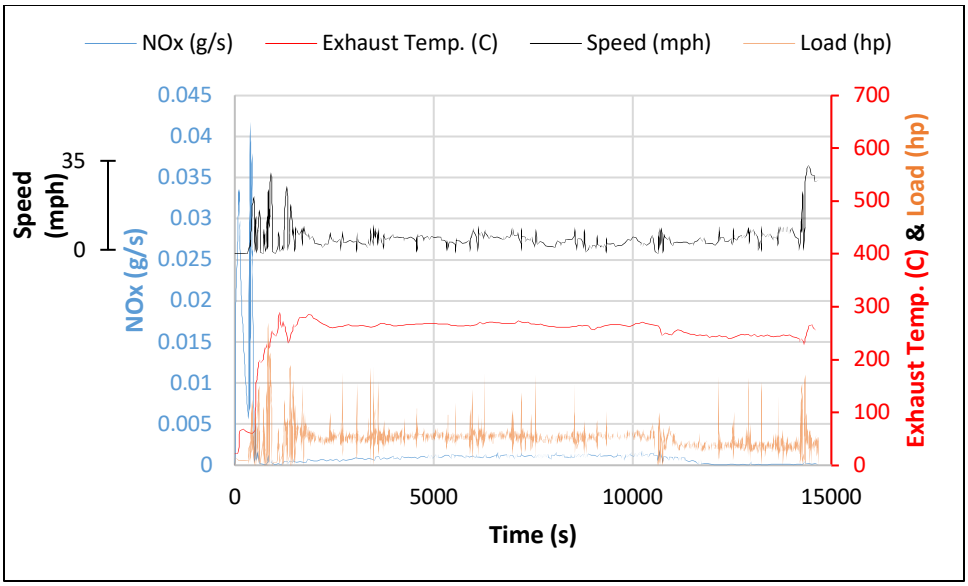

Figure 2-15: Real-time NOx emissions as a function of exhaust temperature, vehicle speed, and load for Diesel1_Route2

Figure 2-7 shows Diesel2 with similar routes for both tests. Diesel2_Route2 shows one major elevation change, while Diesel2_Route1 shows multiple elevation changes in Figure 2-7. Figure 2-16 and Figure 2-17 shows Diesel2_Route1 and Diesel2_Route2 NOx emissions to be below 0.02 g/s sec, with one high NOx peak for Diesel_Route2 at 6000 seconds. At 6000 seconds, Diesel2_Route2 shows a hard acceleration as seen by the high engine load in Figure 2-17, resulting in a NOx spike of 0.1 g/s.

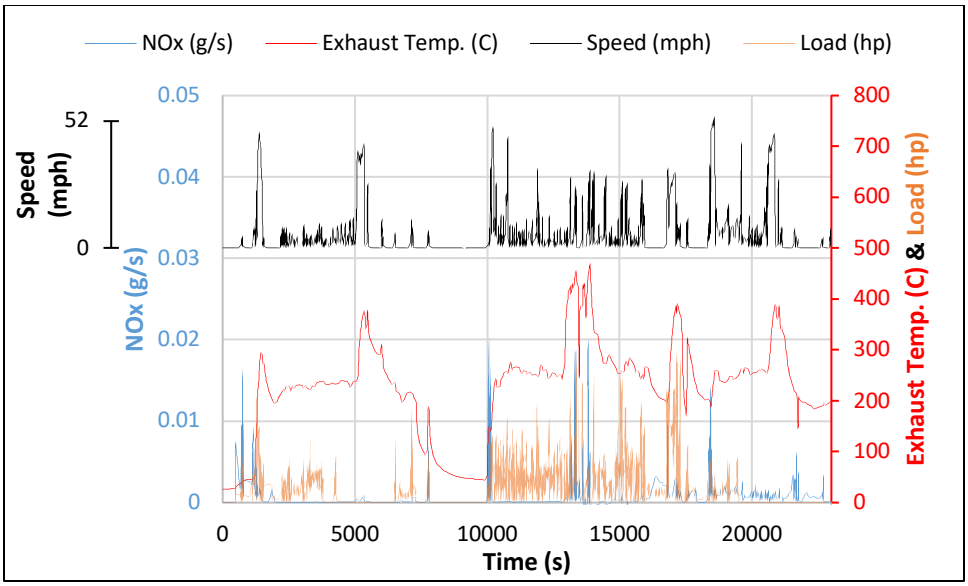

Figure 2-16: Real-time NOx emissions as a function of exhaust temperature, vehicle speed, and load for Diesel2_Route1

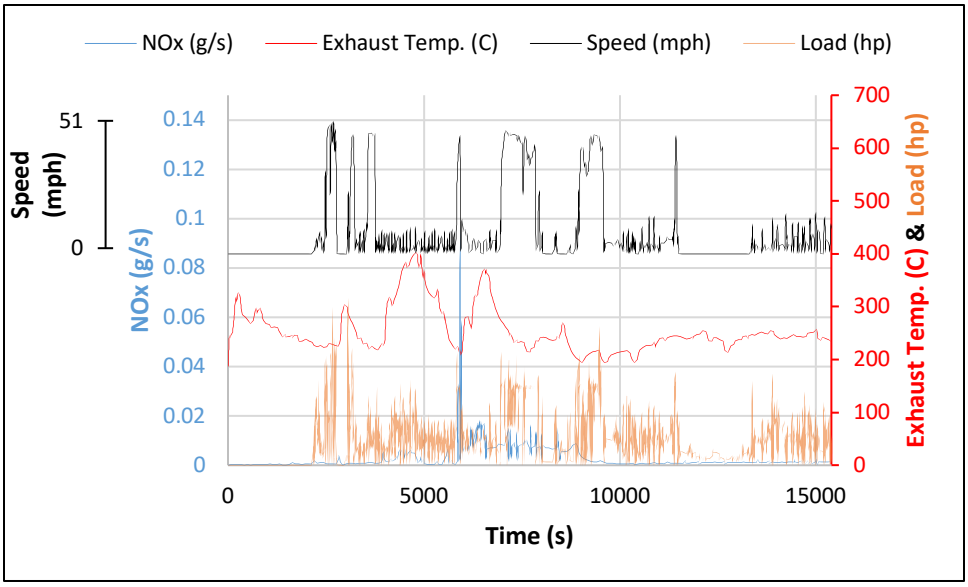

Figure 2-17: Real-time NOx emissions as a function of exhaust temperature, vehicle speed, and load for Diesel2_Route2

2.5.3 THC and CH_4 Emissions

Figure 2-18 shows the brake-specific THC emissions for all street sweeper tests in g/bhp-hr, while Appendix A shows THC emissions in units of grams per mile (g/mile), grams per hour (g/hr), grams per gallon (g/gal), and grams per day (g/day). Figure 2-19 shows the brake-specific CH_4 emissions for all street sweeper tests in g/bhp-hr, while Appendix A shows CH_4 emissions in units of grams per mile (g/mile), grams per hour (g/hr), grams per gallon (g/gal), and grams per day (g/day). The CNG-powered street sweepers showed significantly higher THC emissions than the diesel street sweeper, consistent with past studies (Guo et al., 2014; Thiruvengadam et al., 2014). Similarly, CNG-powered street sweepers showed higher CH_4 emissions compared to the diesel street sweepers. Looking at CNG1 and CNG2, CNG1 showed higher THC and CH_4 emissions than CNG2, which is possibly due to the higher mileage and the more aged catalyst for this vehicle.

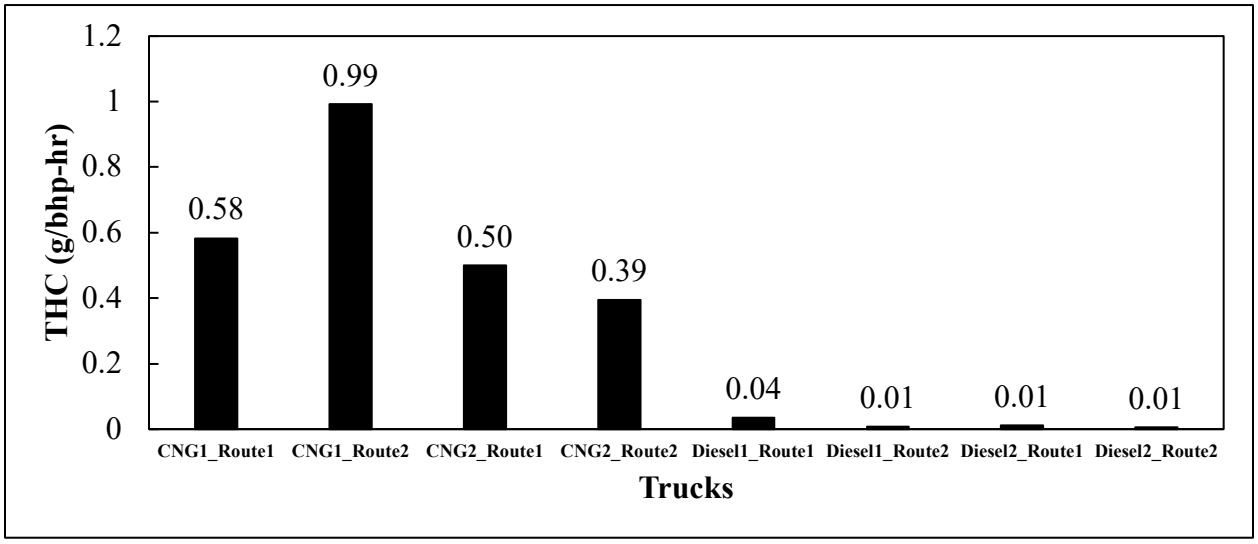

Figure 2-18: Brake-specific THC emissions for the diesel and CNG sweeper

Typically, in natural gas engines THC emissions are predominantly CH_4 with some concentrations of heavier hydrocarbons (Da Pan, et al., 2020). Natural gas is composed mainly of CH_4 (typically 70–90%) with variable proportions of other hydrocarbons (Matthey, 2021). Unburnt CH_4 is a potent greenhouse gas and a byproduct of combustion in natural gas engines due to incomplete combustion (Matthey, 2021). Unburnt CH_4 is typicaly due to the incomplete combustion of natural gas in the crevices and squish volume in the engine's combustion chamber. Figure 2-12 shows CH_4 emissions for the CNG street sweepers being 98% of the THC emissions, while CH_4 concentrations for the diesel sweepers were almost negligible (< 0.0007 g/bhp-hr).

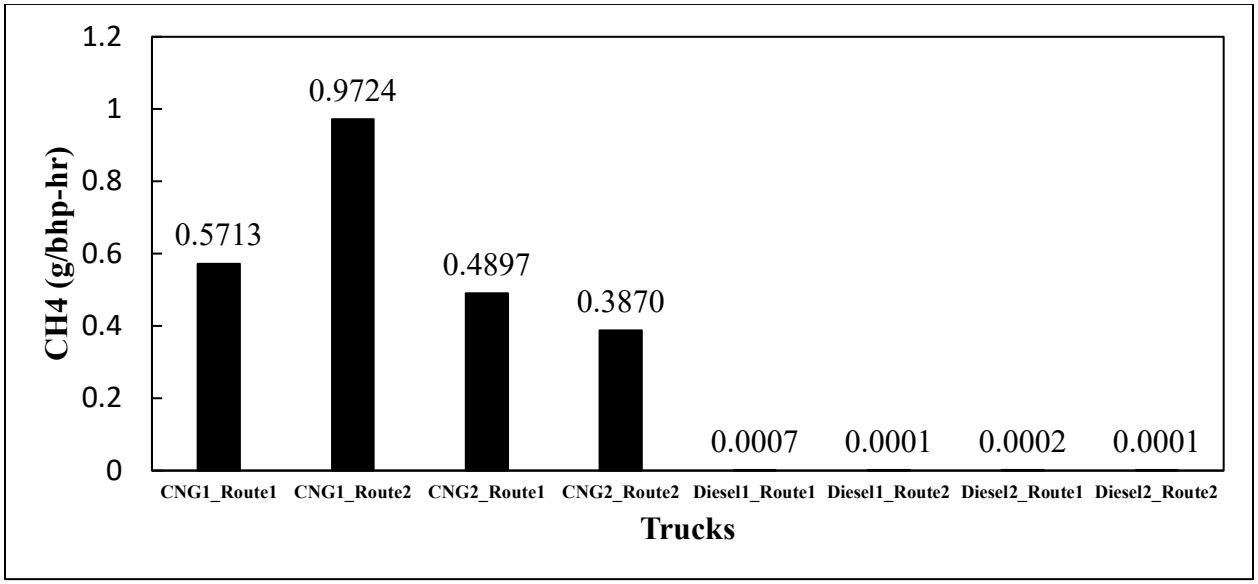

Figure 2-19: Brake-specific CH_4 emissions for the diesel and CNG sweepers

2.5.4 CO Emissions

Figure 2-20 shows the brake-specific CO emissions for all street sweeper tests in g/bhp-hr, while Appendix A shows CO emissions in units of grams per mile (g/mile), grams per hour (g/hr), grams per gallon (g/gal), and grams per day (g/day). For all street sweeper tests, in-use CO emissions were much lower than the U.S. EPA engine certification limit of 15.5 g/bhp-hr. Consistent to previous studies (Thiruvengadam et al., 2015; Quiros et al., 2016; Zhu et al., 2020), these results exhibited significantly higher CO emissions for the natural gas vehicles compared to the diesel vehicles. The higher CO for the CNG street sweepers was likely due to the stoichiometric combustion of spark ignition engines and the strategy of engine manufactures to tune natural gas engines to be slightly rich to reduce NOx emissions. The EPA's more stringent regulation on NOx emissions certification limit of 0.20 g/bhp-hr possibly contributes to the much less stringent CO engine emissions certification limit of 15.5 g/bhp-hr. Stoichiometric combustion during high-speed conditions for CNG street sweepers result in higher CO emissions due to the lack of oxygen during combustion (Karavalakis et al., 2013; Grigoratos et al., 2019; Zhu et al., 2020). At the same time, diesel street sweepers have leaner combustion and a DOC, which oxidizes CO to CO_2, leading to much lower CO emissions (Zhu, et al., 2020).

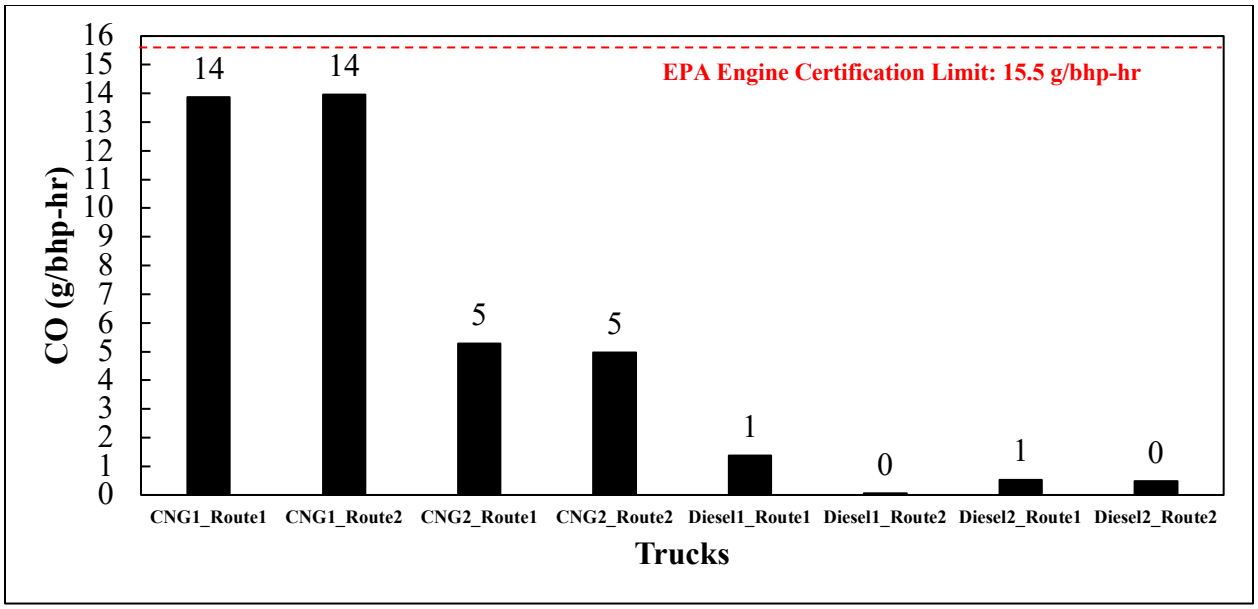

Figure 2-20: Brake-specific CO emissions for the diesel and CNG sweepers

2.5.5 CO_2 Emissions

Figure 2-21 shows the brake-specific CO_2 emissions for all street sweeper tests in g/bhp-hr, while Appendix A shows CO_2 emissions in units of grams per mile (g/mile), grams per hour (g/hr), grams per gallon (g/gal), and grams per day (g/day). For the TWC-equipped CNG street sweepers, in-use CO_2 emissions met EPA engine certification limit of 618 g/bhp-hr. CNG street sweepers in-use CO_2 emissions are 12% lower for CNG1_Route1, 13% lower for CNG1_Route2, 16% lower for CNG2_Route1, and 16% lower for CNG2_Route2 than the engine certification limit, respectively.

Overall, CO_2 tailpipe emissions trended higher for the diesel-powered sweepers compared to the CNG-powered sweepers, which is similar to a previous study (Guo et. al., 2014). CO_2 emissions for the diesel-powered street sweepers substantially varied from 709.46 to 1020.90 g/bhp-hr with less than a 36% difference between tests, while CNG-power street sweepers consistently ranged from 526.93 to 548.89 g/bhp-hr with less than a 4% difference between each test.

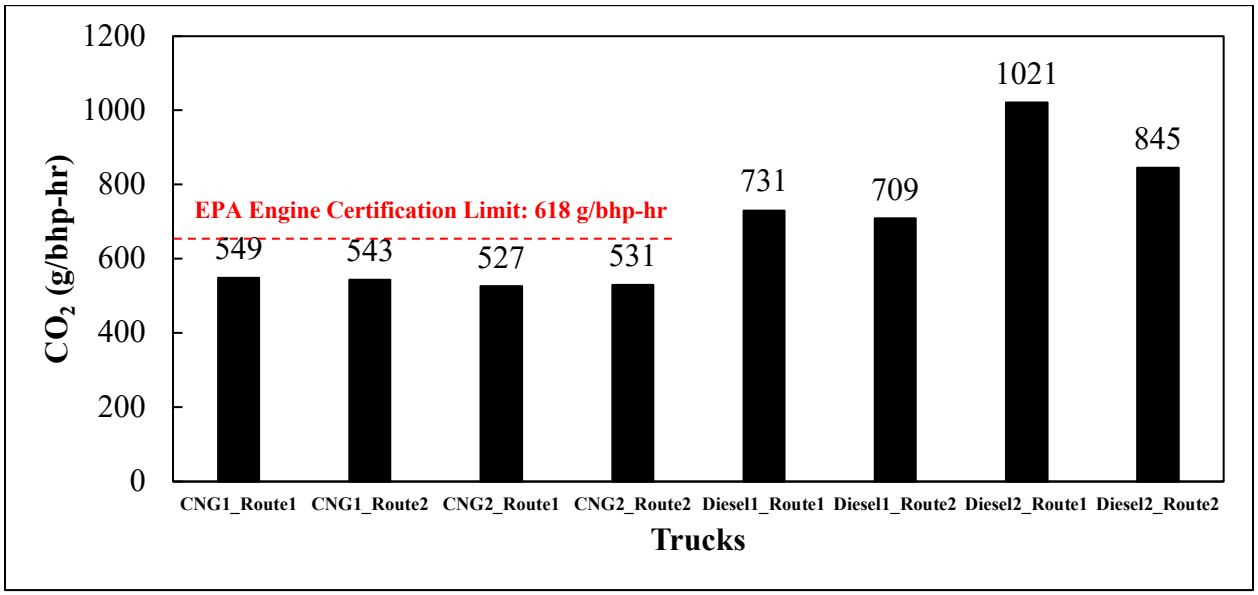

Figure 2-21: Brake-specific CO_2 emissions for the diesel and CNG sweepers

2.5.6 PM Mass and Soot Mass Emissions

Figure 2-22 shows the brake-specific PM mass emissions for all sweeper tests in mg/bhp-hr, while Appendix A shows soot mass emissions in units of milligrams per mile (mg/mile), milligrams per hour (mg/hr), milligrams per gallon (mg/gal), and milligrams

per day (mg/day). Overall, PM mass emissions showed similar variations for both CNG-powered and diesel-powered street sweepers, where CNG-powered street sweepers emitted slightly lower PM mass, almost identical to a heavy-duty natural gas and diesel engine study (Khalek, et al., 2018). Natural gas lacks C-C bonds, which is likely why the CNG-power street sweepers resulted in PM emission levels slightly lower than diesel-powered street sweepers (Thiruvengadam et al., 2015).

For the SCR-equipped diesel street sweeper, in-use PM emissions were significantly lower than EPA engine certification limit of 10 mg/bhp-hr. Diesel1_Route1, Diesel1_Route2, Diesel2_Route1, and Diesel2_Route2 in-use PM emissions were 157%, 166%, 190%, and 198% lower than engine certification limit.

For the TWC-equipped CNG street sweeper, in-use PM emissions met EPA engine certification limit of 10 mg/bhp-hr. CNG1_Route1, CNG1_Route2, CNG2_Route, and CNG2_Route2 in-use PM emissions were 173%, 185%, 131%, and 185% lower than engine certification limit, respectively. Overall, the CNG and diesel street sweepers in-use PM emissions were all well below EPA engine certification limits.

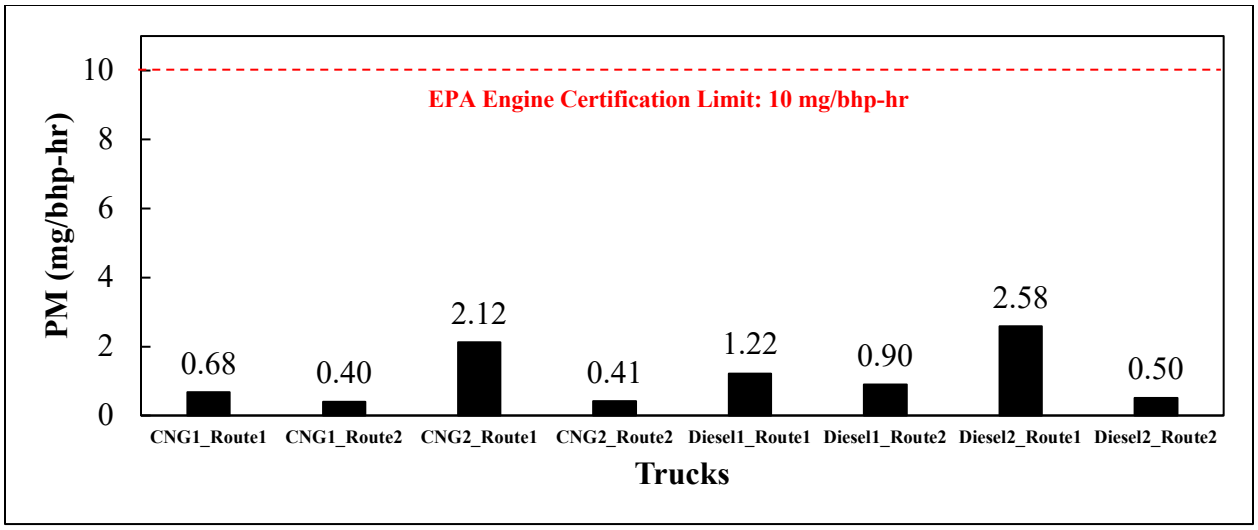

Figure 2-22: Brake-specific PM emissions for the diesel and CNG sweepers

Figure 2-23 shows the brake-specific soot mass for all street sweeper tests in mg/bhp-hr, while Appendix A shows soot mass emissions in units of milligrams per mile (mg/mile), milligrams per hour (mg/hr), milligrams per gallon (mg/gal), and milligrams per day (mg/day). Comparing the street sweeper tests, the CNG-powered street sweepers showed higher soot mass emissions compared to the diesel-powered street sweepers. These findings contradict those of a past study (Zhou, et al., 2019), which showed lower soot mass emissions for CNG-powered heavy-duty vehicles when tested on a chassis dynamometer. For the CNG-powered street sweepers, soot mass emissions ranged from 0.29 to 0.33 mg/bhp-hr, while soot emissions for the diesel-powered street sweepers ranged from 0.18 to 0.31 mg/bhp-hr. The CNG-powered sweepers showed consistent soot emissions with less a 16% difference in all tests. The diesel-powered sweepers showed consistent soot emissions except for one test (Diesel2_Route1) that was 53% higher while

the other three tests were less than 3% different. The lower soot mass for the diesel-powered street sweepers compared to the CNG street sweepers was likely due to the presence of the DPF system, which can effectively reduce soot by periodically burning it off the filter. The higher soot mass from the CNG street sweepers is likely because the main function of the TWC is to control HC, CO, and NOx emissions, while the soot emissions are uncontrolled (Misra, et al., 2017). The main contributor to CNG engine soot emissions is due to the lubricant oil entering the combustion chamber, resulting in metal ash particles (Zhu et al., 2020; Thirunvengadam et al., 2014).

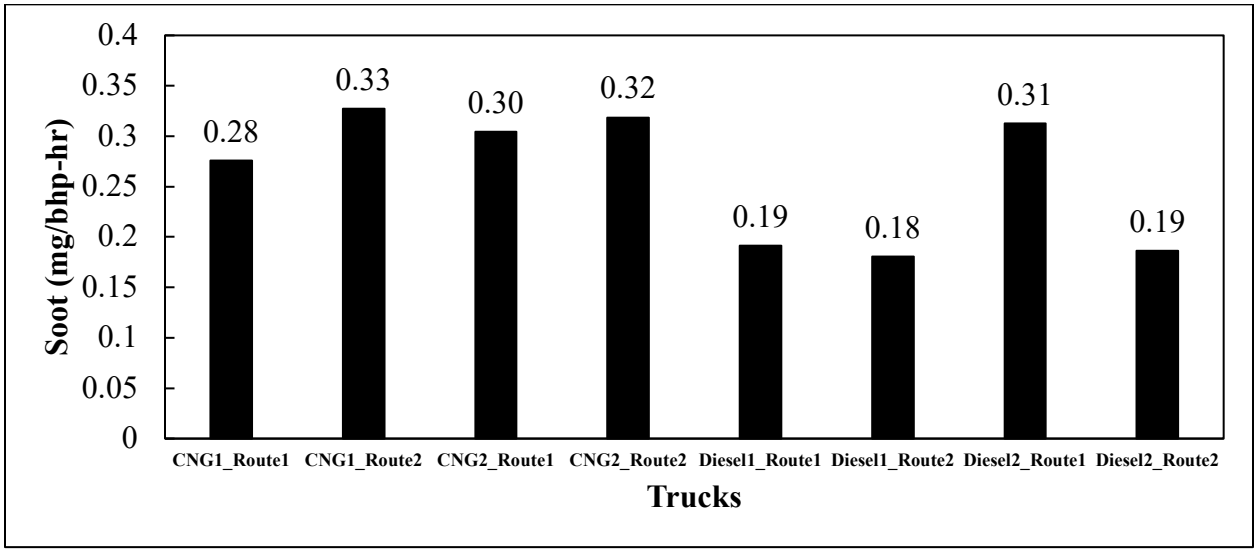

Figure 2-23: Brake-specific Soot emissions for the diesel and CNG sweepers

Figure 2-24 shows the real-time soot emissions in grams per second (g/s) as a function of exhaust gas temperature (°C) and vehicle speed (miles per hour) for the TWC-equipped CNG street sweeper (CNG1_Route1). Real-time soot emissions were quite similar for

both CNG street sweepers. From the CNG1_Route1 sweeper real-time soot emissions, a typical soot emission profile shows that large spikes occurred during acceleration and deceleration events. The results from this study are consistent with previous studies that also show high soot emissions during deceleration events due to motor oil entering the combustion chamber (Tonegawa et al., 2006).

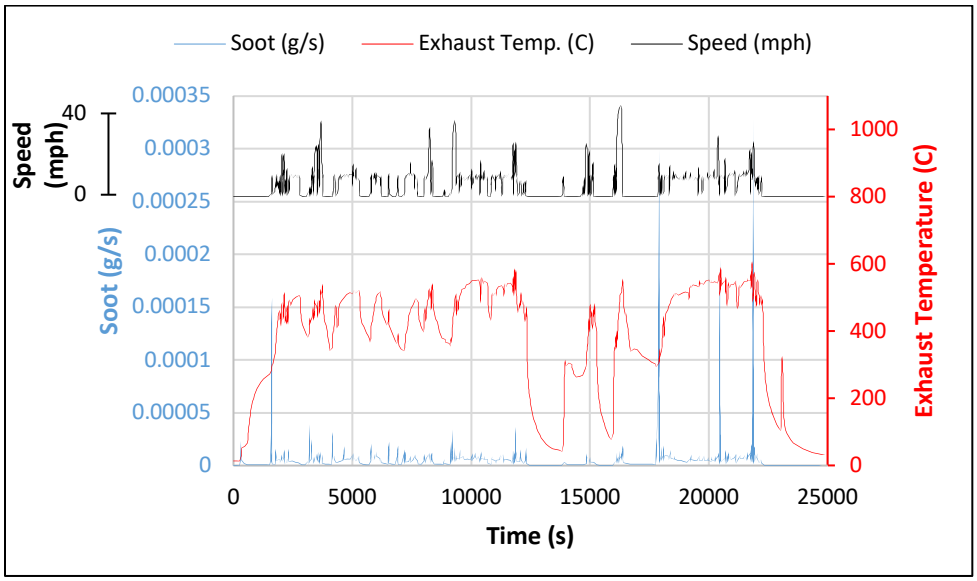

Figure 2-24: Real-time Soot emissions as a function of exhaust temperature and vehicle speed for CNG1_Route1

Real-time soot emissions in grams per second (g/s) as a function of exhaust gas temperature (°C) and vehicle speed (miles per hour) for the SCR-equipped Diesel2_Route1 and Diesel1 (Diesel1_Route1, Diesel1_Route1) are shown below in Figure 2-25, Figure 2-27, and Figure 2-27, respectively. Due to technical difficulties,

Diesel2_Route2 lost cold start emissions data. Therefore, Diesel1 real-time data will be used to compare the Diesel2_Route1 soot emission discrepancies.

Figure 2-25 shows real-time soot emissions for Diesel2_Route1 with large peaks during cold start, between 14000 -15000 seconds, and around 17000 seconds. Figure 2-26 shows that a DPF regeneration event took place for Diesel2_Route1 from 13,200-13,500 seconds indicated by the high exhaust temperature, NOx, THC and CO_2 emissions as seen in other studies (Keramydas, et al.; 2019, Chen, et al., 2020; Dwyer, et al., 2010). Previous studies (Keramydas, et al., 2019; Dwyer, et al., 2010) showed that during regeneration events, there are periodic increases in PM emissions. In a DPF regeneration study (Dwyer, et al., 2010), PM emissions proved to be the highest during regeneration, and this is likely due to semi-volatile matter passing through a more porous filter material due to the unloading of the filter (Dwyer, et al., 2010). Before regeneration, the filter material is less porous due to the PM collected on the filter material, contributing to semi-volatile PM collecting on the filter material (Dwyer, et al., 2010). In other words, after a DPF regeneration, the filter efficiency was likely reduced due to the lack of soot accumulation. At the same time, DPF's have a filter efficiency of 90-95% and likely lose efficiency with age (Deng, et al., 2019). Therefore, this DPF regeneration is a plausible explanation for the elevated soot emissions for Diesel2_Route1.

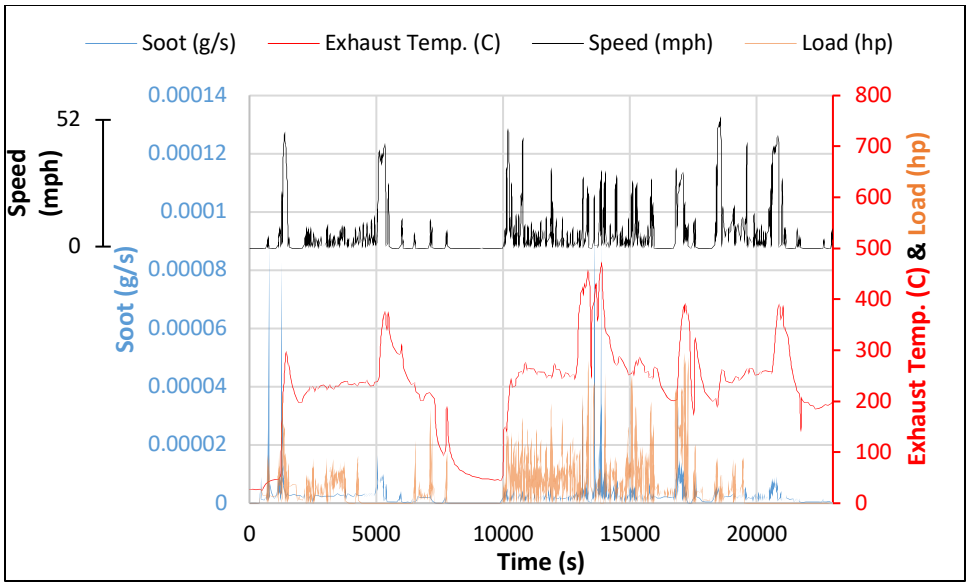

Figure 2-25: Real-time Soot emissions as a function of exhaust temperature, vehicle speed, and load for Diesel2_Route1

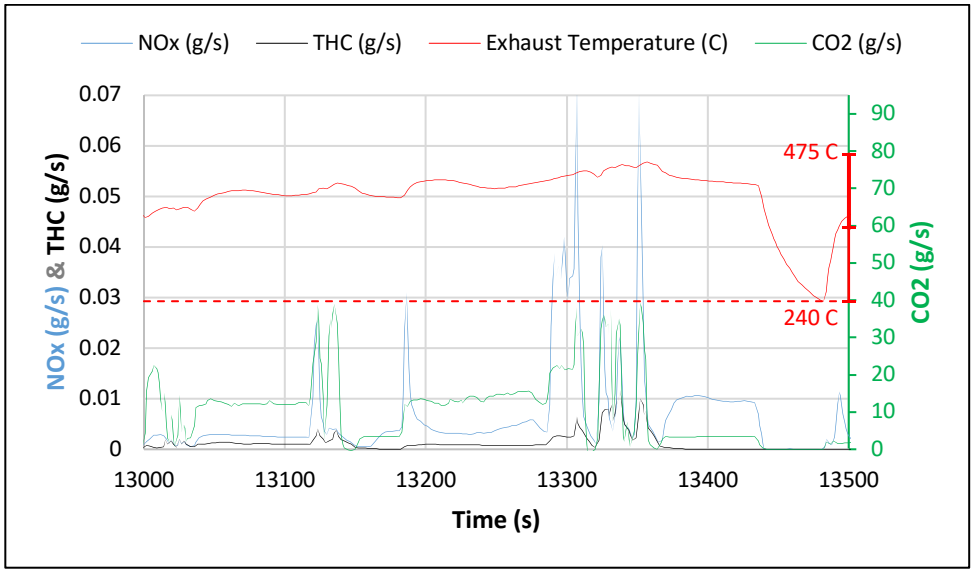

Figure 2-26: Diesel regeneration event for Diesel2_Route1

Figure 2-27 showed Diesel1_Route1 with relatively low real-time soot emissions with spikes during cold-start, at around 14,000 seconds, and at around 17,000-20,000 seconds. The soot emissions were below 0.0002 g/s for the entire test with no DPF regeneration events. Apart from the cold-start, Figure 2-28 showed Diesel1Route2 with close to zero real-time soot emissions, with soot emissions less than 0.00002 g/s during the entire test and no observed DPF regeneration events. From these real-time soot emissions, Diesel1 showed significantly lower soot mass (<0.0002 g/s) apart from the cold start, whereas Diesel2_Route1 showed spikes of soot emissions up to 0.00093 g/s during cold-start and the DPF regeneration event.

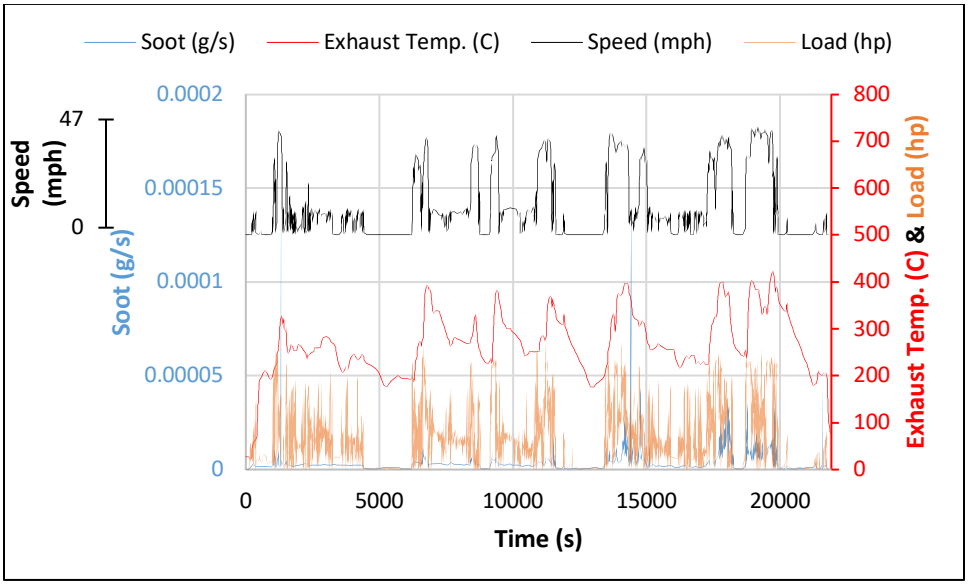

Figure 2-27: Real-time Soot emissions as a function of exhaust temperature, vehicle speed, and load for Diesel1_Route1

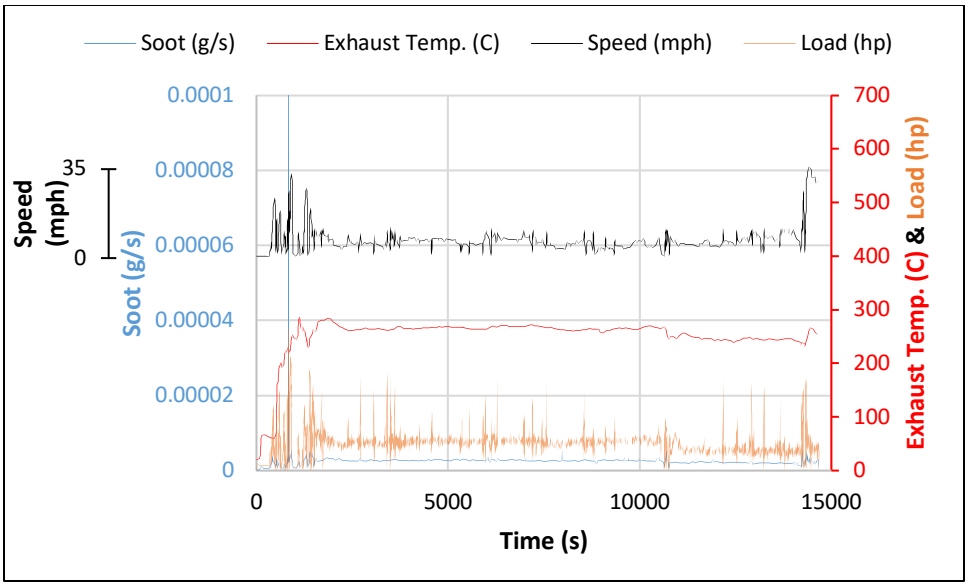

Figure 2-28: Real-time Soot emissions as a function of exhaust temperature, vehicle speed, and load for Diesel1_Route2

2.5.7 Measured and modeled emission factor comparison for NOx, CO, CO_2, and PM

The California Air Resource Board Emissions Factor (EMFAC) 2021 Model was used to estimate official on-road emissions for the CNG (2017) and diesel (2014) street sweepers in South Coast Air Basin based on the average speed of every test run. Due to the lack of street sweeper emissions studies, the EMFAC model is used as a comparison for this study.

Figure 2-29 shows the comparison of NOx emissions from the EMFAC model. The CNG street sweepers showed NOx emissions that were slightly lower than the EMFAC model,

whereas diesel street sweepers showed varying results with three out of the four tests being significantly lower than the EMFAC model.

CNG1_Route1, CNG1_Route2, CNG2_Route1, and CNG2_Route2 show the PEMS NOx emissions being 5% lower, 50% lower, 3% lower, and 59% lower than the EMFAC model. Diesel1_Route1, Diesel1_Route2, Diesel2_Route1, and Diesel2_Route2 show the PEMS NOx emissions being 13% higher, 104% lower, 243% lower, and 25% lower than the EMFAC model.

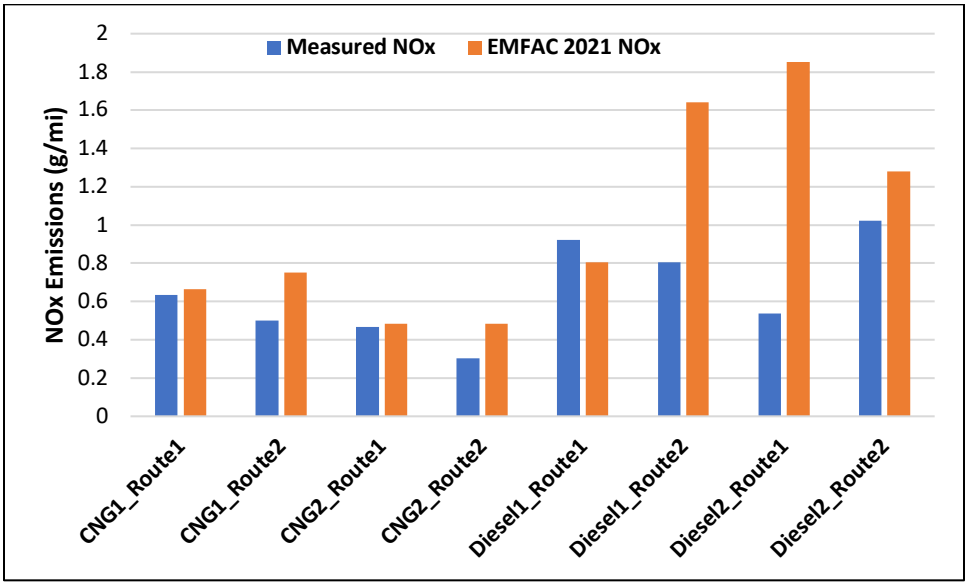

Figure 2-29: Comparison of NOx emissions by EMFAC model and PEMS measurement

Figure 2-30 shows the CNG and diesel street sweepers CO emissions. Our results show that EMFAC model underestimates the in-use CO emissions measured with PEMS.

CNG1_Route1, CNG1_Route2, CNG2_Route1, and CNG2_Route2 show the PEMS CO emissions being 92% higher, 85% higher, 75% higher, and 74% lower than the EMFAC model. Diesel1_Route1, Diesel1_Route2, Diesel2_Route1, and Diesel2_Route2 show the PEMS CO emissions being 98% higher, 61% higher, 93% higher, and 93% higher than the EMFAC model.

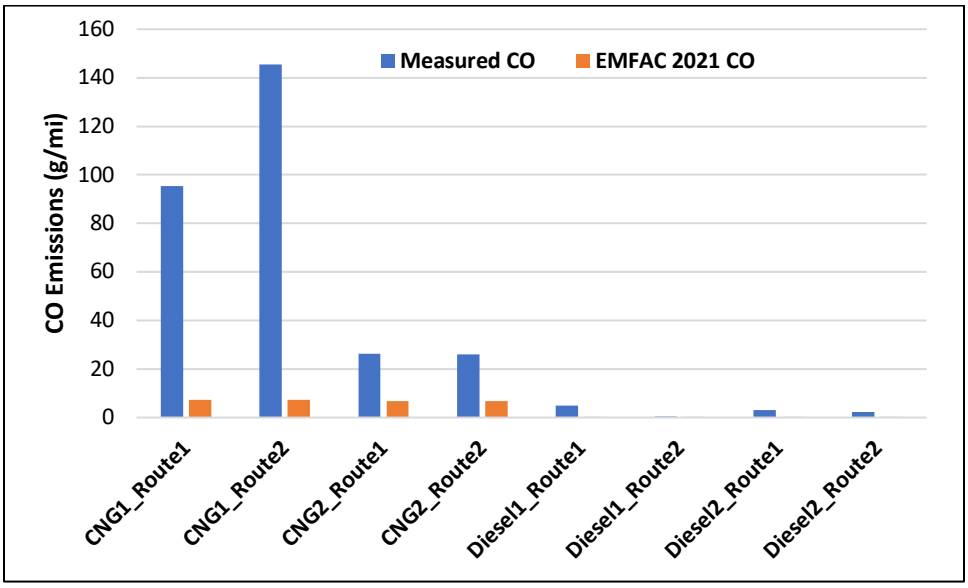

Figure 2-30: Comparison of CO emissions by EMFAC model and PEMS measurement

Figure 2-31 shows both the CNG and diesel street sweepers producing more CO_2 emissions compared to the EMFAC model. CNG1_Route1, CNG1_Route2, CNG2_Route1, and CNG2_Route2 show the PEMS CO_2 emissions being 35% higher, 53% higher, 23% higher, and 27% higher than the EMFAC model. Diesel1_Route1,

Diesel1_Route2, Diesel2_Route1, and Diesel2_Route2 show the PEMS CO_2 emissions being 38% higher, 59% higher, 57% higher, and 48% higher than the EMFAC model.

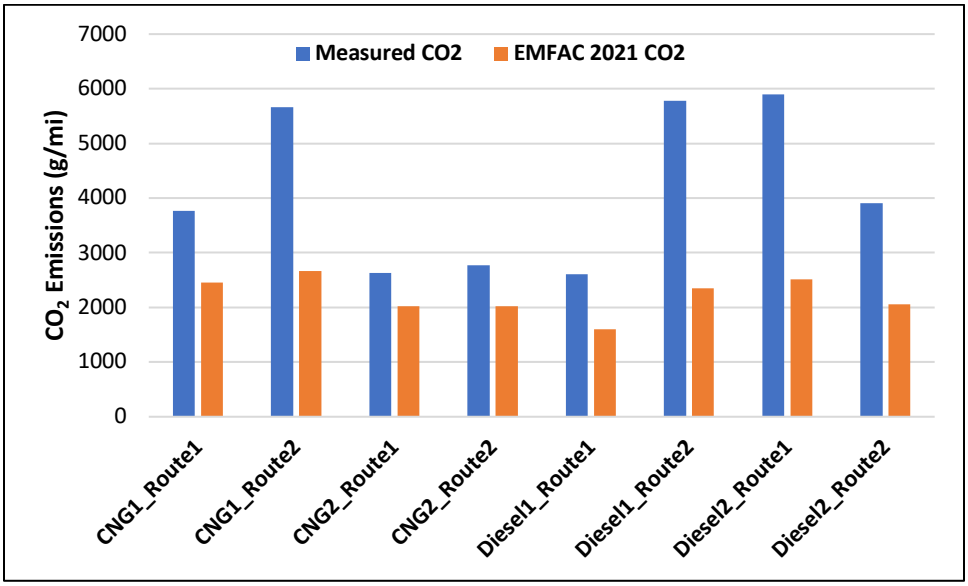

Figure 2-31: Comparison of CO_2 emissions by EMFAC model and PEMS measurement

Figure 2-32 compares the PEMS PM emissions with the EMFAC model for both the CNG and diesel sweeper. Measured PM emissions showed three of the four CNG test runs being higher, and two out of the four diesel test runs being higher than the EMFAC model. CNG1_Route1, CNG1_Route2, CNG2_Route1, and CNG2_Route2 show the PEMS PM emissions being 35% higher, 23% higher, 73% higher, and 30% lower than the EMFAC model. Diesel1_Route1, Diesel1_Route2, Diesel2_Route1, and Diesel2_Route2 show the PEMS PM emissions being 52% higher, 51% higher, 116% lower, and 27% lower than the EMFAC model.

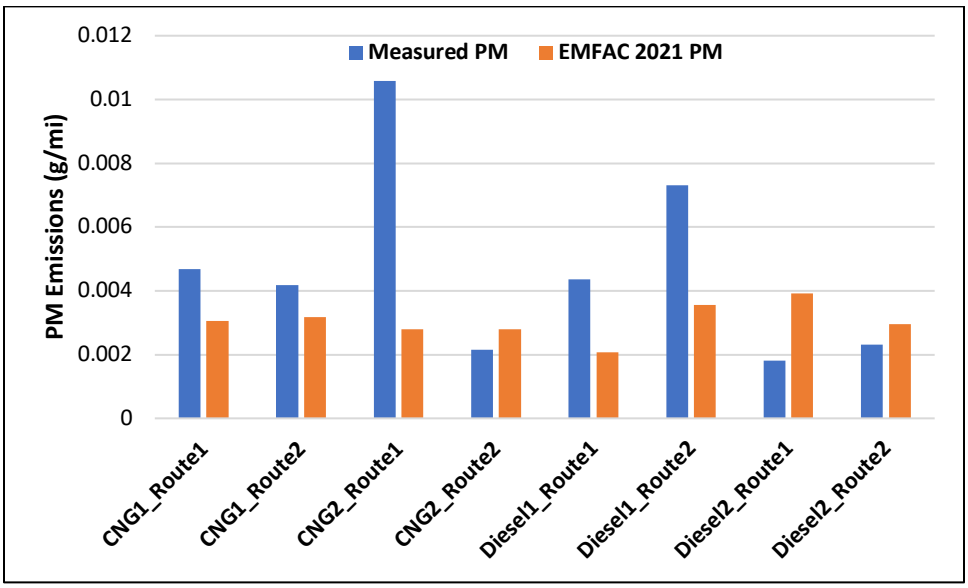

Figure 2-32: Comparison of PM emissions by EMFAC model and PEMS measurement

2.5.8 Measured and modeled emission factor comparison for NOx at different speeds

To further analyze NOx emissions, the EMFAC model estimations is used to compare with the PEMS NOx results within a speed range of 0-60 mph for both the CNG and diesel sweepers. The EMFAC NOx model and both the CNG and diesel show high NOx during low speeds of around 0-15 mph, which resembles other literature that has shown that vehicle operation at speeds of less than 25 mph results in NOx emissions more than five times the certification for heavy-duty vehicles (Badshah, et al., 2019). Overall, both the CNG and diesel sweeper generally show a linear downward trend as speeds increase like the EMFAC model.

Figure 2-33 shows CNG1_Route1 with NOx emissions level lower than the EMFAC model only when sweeper speed is at 0-5 mph, while speeds from 10-45 mph showed NOx emissions levels higher than the model. CNG1_Route2 show NOx emissions to be very close to the EMFAC model with majority of the different speeds emitting lower NOx emissions than the model. These two routes for the CNG traveled at average vehicle speeds of 6 mph (CNG1_Route1) and 4 mph (CNG1_Route2) for the duration of the test.

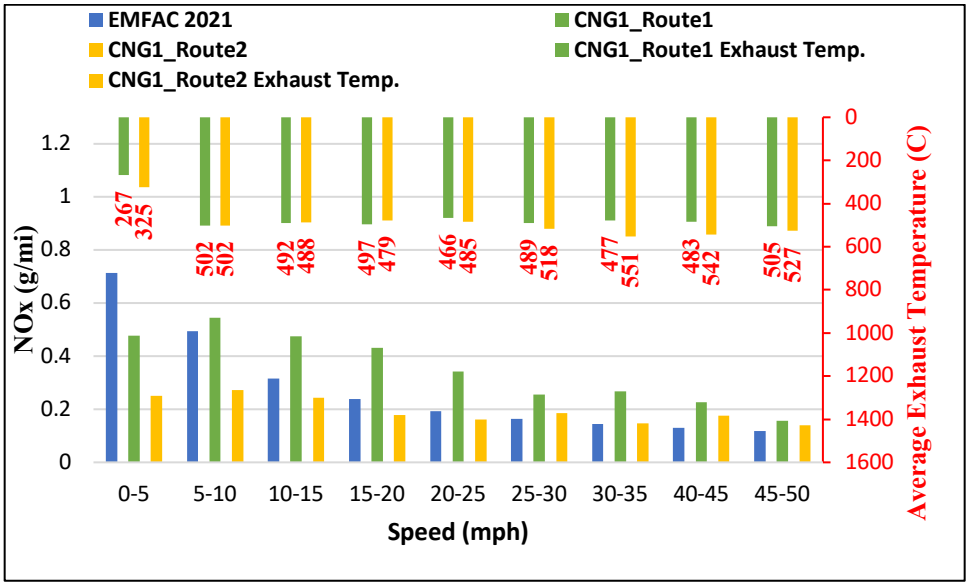

Figure 2-33: Comparison of NOx emissions by EMFAC model and CNG1 PEMS measurement within speed profile

Figure 2-34 shows CNG2_Route2 NOx emissions to be only lower than the EMFAC model from 0-15 mph and 50-55 mph, where CNG2_Route1 only showed NOx

emissions lower than the model from 10-15 mph. These two routes tested with CNG2 traveled at an average vehicle speed of 10 mph for the duration of the test.

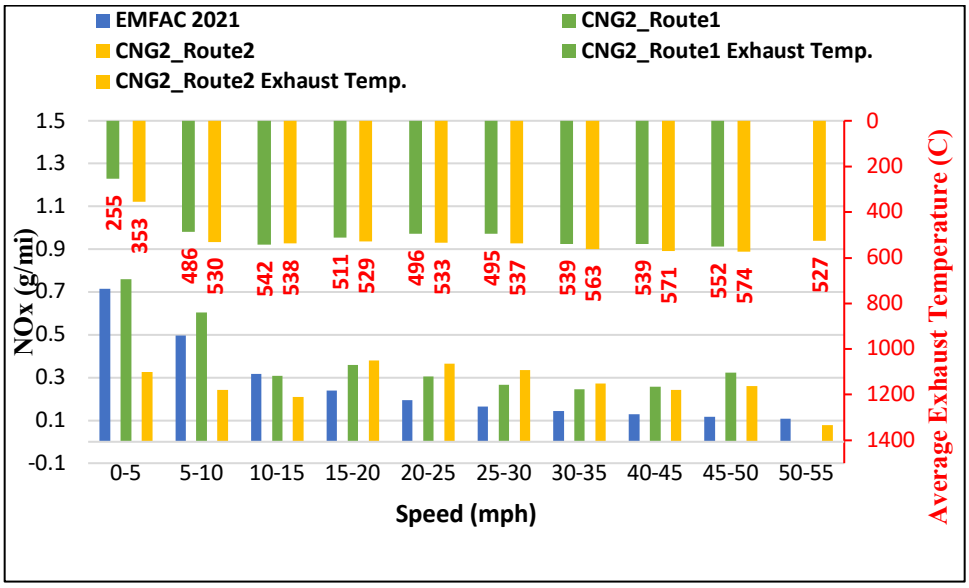

Figure 2-34: Comparison of NOx emissions by EMFAC model and CNG2 PEMS measurement within speed profile

Figure 2-35 shows Diesel1_Route2 to have comparable NOx emissions trends as the EMFAC model, where the PEMS NOx is significantly lower except at 15-20 mph. Diesel_Route1 shows measured NOx emissions going down in the lower speeds (0-10 mph) and NOx increases as speed increase, where NOx emissions are only below EMFAC model emissions from 5-15 mph. These two routes for the Diesel1 traveled at average vehicles speeds of 15 mph (Diesel1_Route1) and 6 mph (Diesel1_Route2) for the duration of the test.

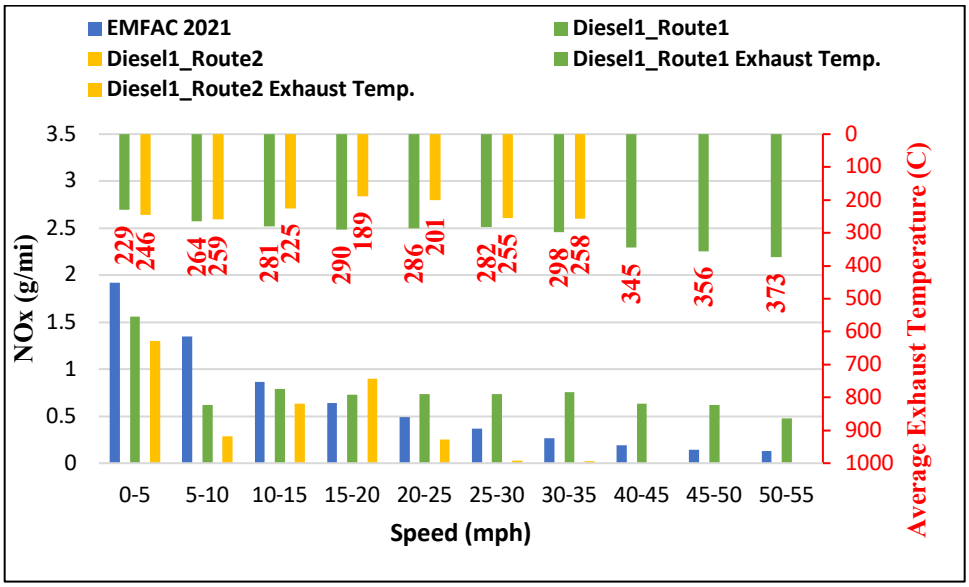

Figure 2-35: Comparison of NOx emissions by EMFAC model and Diesel1 PEMS measurement within speed profile

Figure 2-36 shows Diesel2_Route1 NOx emissions being significantly lower than the EMFAC model and the Diesel2_Route2 NOx emissions during the entire speed profile. Diesel2_Route2 NOx emissions show a consistent trend with the EMFAC model with lower NOx emissions except at the higher speeds of 30-50 mph. These two routes for the Diesel1 traveled at average vehicles speeds of 4 mph (Diesel2_Route1) and 9 mph (Diesel2_Route1) for the duration of the test.

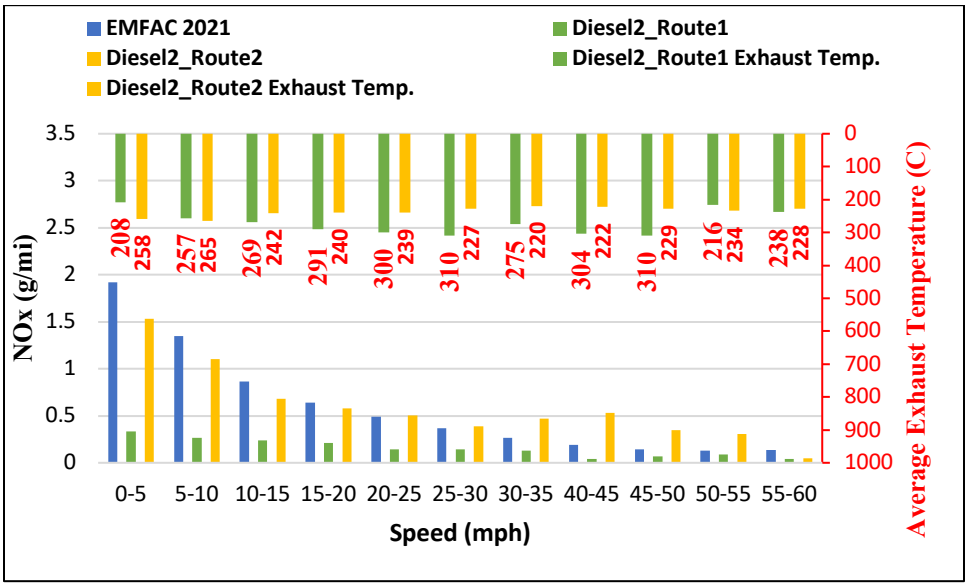

Figure 2-36: Comparison of NOx emissions by EMFAC model and Diesel2 PEMS measurement within speed profile

The EMFAC model showed some varying emission estimations compared to the PEMS results likely due to the method and procedure used in the model estimation. According to ARB's EMFAC2021 Volume III Technical Document, medium heavy-duty CNG and diesel trucks emission models were estimated by applying scaling factors to the rates of EMFAC2021 HHD CNG and diesel trucks. The EMFAC2021 HHD CNG and diesel model exhaust emissions were based on the test data from CARB's Truck and Bus Surveillance Program and those from a project carried out by the Engine and Truck Manufacturers Association and University of California Riverside (ARB, 2021). This scaling factor applied to the medium heavy-duty emissions model is most likely what

caused the model estimations to be significantly higher or lower than some the PEMS results. Some other reasons for varying emissions comparison include real-world driving conditions(elevation), ambient air temperature, weather, catalyst age, malmaintenance and engine deterioration. Overall, the EMFAC model still showed that the PEMS results are reasonable and comparable despite the uncontrollable variables.

2.5.9 Influence of speed and load on NOx emission rates

Figure 2-37 and Figure 2-38 shows the NOx emissions for each CNG and diesel sweeper test as a function of engine load and vehicle speed bins. Engine loads below 25% were consider at low load, between 25%-45% were considered as medium loads, and above 45% were considered as high loads. Within each load bin, three speed bins were categorized for low speed (0-25 mile/h), medium speed (25-45 mile/hr), and high speed (>45 miles/hr). Idle was considered as a vehicle with its engine running and no speed (0 mile/hr). CNG sweepers dedicated most of their time of operation idling (47-60% of their time). For CNG1_Route1, a total of 43% of NOx emissions were generated during the 31% of total time operating in the medium load and low speed bin and a total of 31% of NOx emissions generated during 53% of its total time in idle. For CNG1_Route1, a total of 35% of NOx emissions were generated during the 60% of total time operating in idle and a total of 18% of NOx emissions generated during the 24% of total time operating in the medium load and low speed bin. For CNG2_Route1, a total of 37% of NOx emissions were generated during the 50% of total time operating in idle and a total of 20% of NOx emissions generated during both low speed bins (16% of total time) in the low and

medium load bin (20% of total time), individually. For CNG2_Route2, a total of 22% of NOx emissions were generated during idle (22% of total time) and during medium speed and high load bin (9% of total time), individually.

Diesel sweepers dedicated most of their operating time in idle and in the low speed and low load bin, while also generating majority of NOx emissions with those same operating conditions. For Diesel1_Route1, a total of 30% of NOx emissions were generated during the 30% of total time operating in the low load and low speed bin and a total of 24% of NOx emissions generated during 10% of its total time in high load and medium speed bin. For Diesel1_Route2, a total of 53% of NOx emissions were generated during the 78% of total time operating in the low load and low speed bin and a total of 33% of NOx emissions generated during 10% of its total time in idle. During idle Diesel1_Route2 showed an average exhaust temperature, 166 °C, below SCR light-off condition. For Diesel2_Route1, a total of 47% of NOx emissions were generated during the 50% of total time operating in idle and a total of 37% of NOx emissions generated during 40% of its total time in low load and low speed bin. During idle Diesel2_Route1 showed an average exhaust temperature, 184 °C, below SCR light-off condition. For Diesel2_Route2, a total of 36% of NOx emissions were generated during the 42% of total time operating in idle and a total of 33% of NOx emissions generated during 39% of its total time in low load and low speed bin.

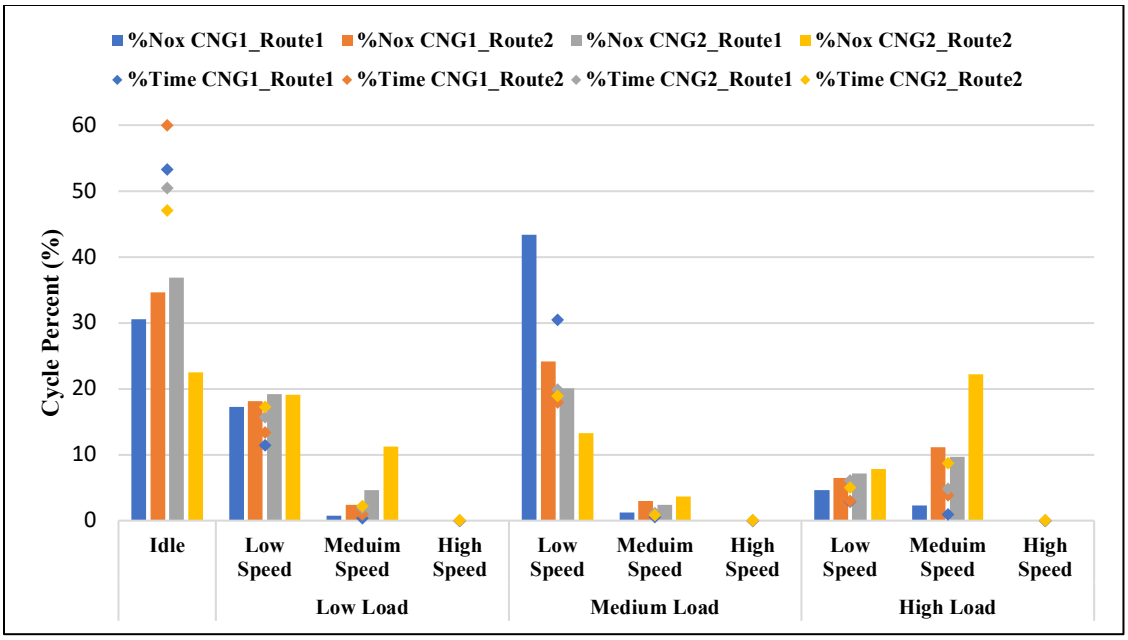

Figure 2-37: Percentage of NOx emissions and time spend at each speed and power bin for CNG sweepers

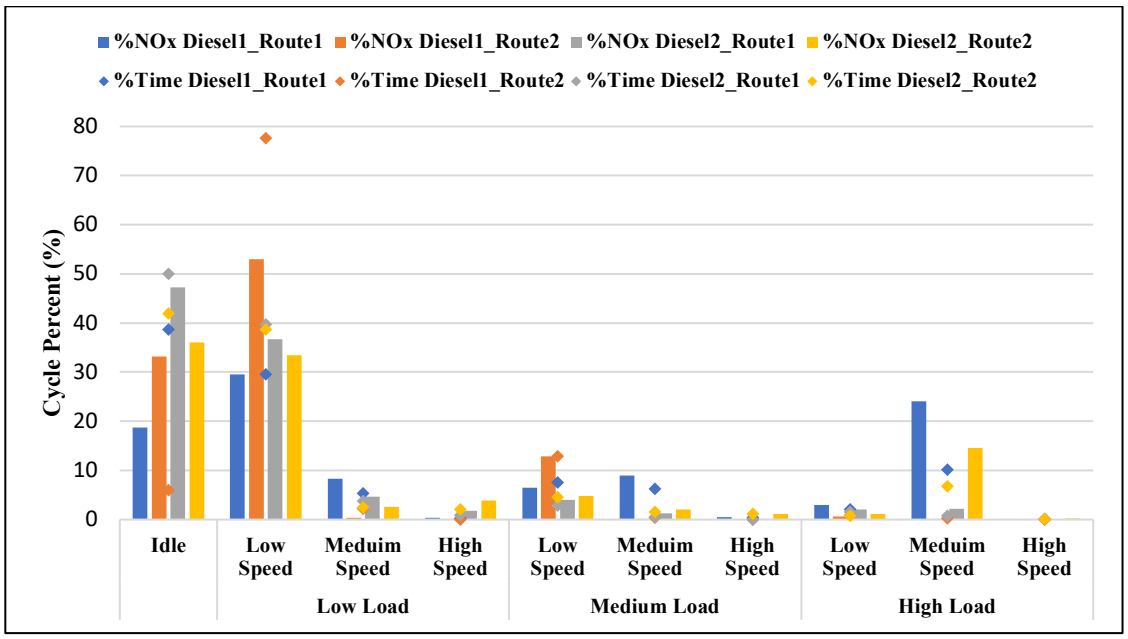

Figure 2-38: Percentage of NOx emissions and time spend at each speed and power bin for diesel sweepers

2.6 Conclusion

In this study, on-road emissions of NOx, THC, CH_4, CO, CO_2, PM, and soot from two CNG street sweeper and two diesel street sweepers were examined using a PEMS. The rate of emissions, in gram per brake-horsepower (g/bhp-hr), of NOx, CO, and PM measured was generally within the engine certification standard with some test runs being slightly higher. The emissions from this study were also compared with the EMFAC model, where NOx is lower, CO is higher, CO_2 is lower, and PM showed varying emissions compared to the EMFAC model. A comparisons of NOx emissions with the EMFAC model and the PEMs data showed that NOx was higher during lower speeds apart from the Diesel2 data. Most NOx emissions for both CNG and diesel sweepers were produced during the idle and low speed operation due to the nature of sweeper use.

The four street sweepers analyzed confirms what is reported in literature that CNG sweepers present a significant advantage with regards to NOx and a slight advantage with PM emissions, but lack in efficiency when it comes to CO, THC, and CH_4 emissions compared to its diesel counterpart (Fontaras, et al., 2012). Contrary to what is presented in current literature, this study shows CNG-powered sweepers emitting noticeably higher soot emissions than the diesel-powered sweepers. Generally, this PEMS study showed varying results compared to the EMFAC model. Therefore, further studies are necessary to determine if a city or region should shift toward either technology, as the study of CNG and diesel street sweeper emissions is still a novelty study.

2.7 Appendix

Appendix A

In-use emission pollutants for the street sweeper test

Vehicle	CO_2	CO	kNOx	CH_4	NMHC	THC	Soot	PM
	g/bhp-hr						mg/bhp-hr	
CNG1_Route 1	548.89	13.87	0.09	0.5713	0.57	0.58	0.28	0.68
CNG1_Route 2	543.31	13.96	0.05	0.9724	0.97	0.99	0.33	0.40
CNG2_Route 1	526.93	5.28	0.09	0.4897	0.49	0.50	0.30	2.12
CNG2_Route 2	530.67	4.97	0.06	0.3870	0.39	0.39	0.32	0.41
Diesel1_Route1	730.77	1.36	0.26	0.0007	0.00	0.04	0.19	1.22
Diesel1_Route2	709.46	0.06	0.10	0.0001	0.00	0.01	0.18	0.90
Diesel2_Route1	1020.90	0.52	0.09	0.0002	0.00	0.01	0.31	2.58
Diesel2_Route2	845.00	0.47	0.22	0.0001	0.00	0.01	0.19	0.50
	g/mi						mg/mi	
CNG1_Route 1	3771.89	95.29	0.63	5.5184	5.52	5.63	1.90	4.68
CNG1_Route 2	5665.80	145.60	0.50	10.1409	10.14	10.35	3.41	4.17
CNG2_Route 1	2629.31	26.35	0.47	2.4434	2.44	2.49	1.52	10.59
CNG2_Route 2	2775.15	26.02	0.30	2.0237	2.02	2.07	1.67	2.15
Diesel1_Route1	2609.56	4.87	0.92	0.0026	0.00	0.13	0.68	4.36
Diesel1_Route2	5779.60	0.50	0.80	0.0012	0.00	0.06	1.47	7.32
Diesel2_Route1	5893.49	3.02	0.54	0.0013	0.00	0.06	1.81	14.91
Diesel2_Route2	3911.47	2.18	1.02	0.0005	0.00	0.03	0.86	2.32
	g/hr						mg/hr	
CNG1_Route 1	23186.87	585.75	3.90	33.6366	33.64	34.32	11.65	28.77
CNG1_Route	23480.01	603.40	2.08	42.0255	42.03	42.88	14.13	16.31

2								
CNG2_Route 1	27239.57	272.98	4.85	25.3133	25.31	25.83	15.73	86.97
CNG2_Route 2	29832.77	279.68	3.26	21.7549	21.75	22.20	17.91	26.49
Diesel1_Route1	38513.69	71.92	13.63	0.0378	0.04	1.89	10.08	56.61
Diesel1_Route2	34453.97	2.96	4.80	0.0071	0.01	0.35	8.76	25.67
Diesel2_Route1	23291.29	11.93	2.13	0.0051	0.01	0.26	7.13	51.96
Diesel2_Route2	36940.82	20.59	9.67	0.0051	0.01	0.25	8.16	13.30
g/gal							**mg/gal**	
CNG1_Route 1	7166.22	181.03	1.21	11.1754	11.18	11.40	3.60	8.89
CNG1_Route 2	7058.47	181.39	0.62	12.6335	12.63	12.89	4.25	5.04
CNG2_Route 1	6752.30	67.67	1.20	6.2748	6.27	6.40	3.90	26.88
CNG2_Route 2	6680.02	62.62	0.73	4.8713	4.87	4.97	4.01	8.19
Diesel1_Route1	10800.78	20.17	3.82	0.0106	0.01	0.53	2.83	17.50
Diesel1_Route2	10282.52	0.88	1.43	0.0021	0.00	0.11	2.61	7.93
Diesel2_Route1	14016.78	7.18	1.28	0.0031	0.00	0.15	4.29	16.06
Diesel2_Route2	10298.06	5.74	2.69	0.0014	0.00	0.07	2.27	4.11
g/day							**mg/day**	
CNG1_Route 1	160685.04	4059.22	27.03	102.2551	102.26	104.34	80.75	199.36
CNG1_Route 2	153513.61	3945.06	13.58	274.7653	274.77	280.37	92.38	113.03
CNG2_Route 1	149643.59	1499.65	26.64	139.0615	139.06	141.90	86.40	602.73
CNG2_Route 2	237087.67	2222.64	25.89	172.8909	172.89	176.42	142.35	183.58
Diesel1_Route1	234548.36	437.99	83.00	0.2303	0.23	11.52	61.37	392.33
Diesel1_Route2	140553.05	12.07	19.57	0.0288	0.03	1.44	35.74	177.92

Diesel2_Route1	142335.63	72.89	13.00	0.0312	0.03	1.56	43.59	360.10
Diesel2_Route2	155520.86	86.70	40.69	0.0214	0.02	1.07	34.34	92.20

2.9 References

Aoki, Paul M., et al. "Common Sense: Mobile Environmental Sensing Platforms to Support Community Action and Citizen Science." citeseerx.ist.psu.edu/viewdoc/download?doi=10.1.1.443.7944&rep=rep1&type=pdf#page=67.

ARB. "EMFAC2021 Volume III Technical Document." *California Air Resources Board*, ARB, ww2.arb.ca.gov/sites/default/files/2021-08/emfac2021_technical_documentation_april2021.pdf.

---. "In-Use Emission Performance of Heavy Duty Natural Gas Vehicles Lessons Learned from 200 Vehicle Project." *California Air Resources Board*, 2021, ww2.arb.ca.gov/sites/default/files/2021-04/Natural_Gas_HD_Engines_Fact_Sheet.pdf.

Badshah, Huzeifa, et al. "Current state of NOx emissions from in-use heavy-duty diesel vehicles in the United States." 2019, theicct.org/publications/nox-emissions-us-hdv-diesel-vehicles.

Boriboonsomsin, Kanok, et al. "Real-world exhaust temperature profiles of on-road heavy-duty diesel vehicles equipped with selective catalytic reduction." *Science of The Total Environment*, vol. 634, 2018, pp. 909-921, www.ncbi.nlm.nih.gov/pmc/articles/PMC6698901/.

Carder, Daniel K., et al. "Determination of In-Use Brake-Specific Emissions from Off-Road Equipment Powered by Mechanically Controlled Diesel Engines." *SAE Technical Paper Series*, 2002, ww2.arb.ca.gov/sites/default/files/classic/research/apr/past/98-317.pdf.

Chen, Chao, et al. "Experimental study of the active and passive regeneration procedures of a diesel particulate filter in a diesel methanol dual fuel engine." *Fuel*, vol. 264, 2020, p. 116801, www.sciencedirect.com/science/article/pii/S0016236119321556.

Cummins. "BSIV Selective Catalytic Reduction (SCR)." *Cummins Inc*, www.cummins.com/en/in/engines/bsiv-selective-catalytic-reduction-scr.

Da Pan, et al. "Methane emissions from natural gas vehicles in China." *Nature Communications*, vol. 11, no. 1, 2020, www.nature.com/articles/s41467-020-18141-0.

Datta, Ambarish, and Bijan K. Mandal. "Effect of compression ratio on the performance, combustion and emission from a diesel engine using palm biodiesel." 2016, aip.scitation.org/doi/pdf/10.1063/1.4958396.

Deng, Yangbo, et al. "Experimental Study on a Diesel Particulate Filter with Reciprocating Flow." *ACS Omega*, vol. 4, no. 17, 2019, pp. 17098-17108, pubs.acs.org/doi/10.1021/acsomega.9b01164.

Dieselnet. "Emission Standards: USA: HD Vehicles Fuel Economy." *DieselNet: Engine & Emission Technology Online*, 2017, dieselnet.com/standards/us/fe_hd.php#co2.

Dwyer, Harry, et al. "Emissions from a diesel car during regeneration of an active diesel particulate filter." *Journal of Aerosol Science*, vol. 41, no. 6, 2010, pp. 541-552, www.sciencedirect.com/science/article/pii/S0021850210000960.

EPA. "Heavy-Duty Highway Compression-Ignition Engines and Urban Buses: Exhaust Emission Standards." *EPA for the Search Site*, nepis.epa.gov/Exe/ZyPDF.cgi?Dockey=P100O9ZZ.pdf.

Fontaras, Georgios, et al. "Assessment of on-road emissions of four Euro V diesel and CNG waste collection trucks for supporting air-quality improvement initiatives in the city of Milan." *Science of The Total Environment*, vol. 426, 2012, pp. 65-72, www.sciencedirect.com/science/article/pii/S0048969712003993.

Gautam, Mridul, et al. "Testing for Exhaust Emissions of Diesel Powered Off- Road Engines." 2002, citeseerx.ist.psu.edu/viewdoc/download?doi=10.1.1.1019.6707&rep=rep1&type=pdf.

Grigoratos, Theodoros, et al. "A study of regulated and green house gas emissions from a prototype heavy-duty compressed natural gas engine under transient and real life conditions." *Energy*, vol. 103, 2016, pp. 340-355, www.sciencedirect.com/science/article/pii/S0360544216302195.

Guo, Jiadong, et al. "On-road measurement of regulated pollutants from diesel and CNG buses with urea selective catalytic reduction systems." *Atmospheric Environment*, vol. 99, 2014, pp. 1-9, www.sciencedirect.com/science/article/pii/S1352231014005548.

Keramydas, Christos, et al. "Characterization of Real-World Pollutant Emissions and Fuel Consumption of Heavy-Duty Diesel Trucks with Latest Emissions Control." *Atmosphere*, vol. 10, no. 9, 2019, p. 535, www.researchgate.net/publication/335729175_Characterization_of_Real-

World_Pollutant_Emissions_and_Fuel_Consumption_of_Heavy-Duty_Diesel_Trucks_with_Latest_Emissions_Control.

Khalek, Imad A., et al. "Solid Particle Number and Ash Emissions from Heavy-Duty Natural Gas and Diesel w/SCRF Engines." *SAE Technical Paper Series*, 2018.

Matthey, Johnson. "Methane Emission Control | Abatement Review Natural Gas Engines." *Johnson Matthey Technology Review*, 27 Jan. 2021, www.technology.matthey.com/article/60/4/228-235/.

Misra, Chandan, et al. "In-Use NOx Emissions from Model Year 2010 and 2011 Heavy-Duty Diesel Engines Equipped with Aftertreatment Devices." *Environmental Science & Technology*, vol. 47, no. 14, 2013, pp. 7892-7898, pubs.acs.org/doi/full/10.1021/es4006288.

---. "In-Use NOx Emissions from Diesel and Liquefied Natural Gas Refuse Trucks Equipped with SCR and TWC, Respectively." *Environmental Science & Technology*, vol. 51, no. 12, 2017, pp. 6981-6989, pubs.acs.org/doi/full/10.1021/acs.est.6b03218.

Quiros, David C., et al. "Real-World Emissions from Modern Heavy-Duty Diesel, Natural Gas, and Hybrid Diesel Trucks Operating Along Major California Freight Corridors." *Emission Control Science and Technology*, vol. 2, no. 3, 2016, pp. 156-172, link.springer.com/article/10.1007/s40825-016-0044-0.

Thiruvengadam, Arvind, et al. "Emission Rates of Regulated Pollutants from Current Technology Heavy-Duty Diesel and Natural Gas Goods Movement Vehicles." *Environmental Science & Technology*, vol. 49, no. 8, 2015, pp. 5236-5244, pubs.acs.org/doi/full/10.1021/acs.est.5b00943.

---. "Characterization of Particulate Matter Emissions from a Current Technology Natural Gas Engine." *Environmental Science & Technology*, vol. 48, no. 14, 2014, pp. 8235-8242, pubs.acs.org/doi/abs/10.1021/es5005973.

Tonegawa, Yoshio, et al. "Evaluation of Regulated Materials and Ultra Fine Particle Emission from Trial Production of Heavy-Duty CNG Engine." *SAE Technical Paper Series*, 2006.

US EPA. *Greenhouse Gas Emissions Standards and Fuel Efficiency Standards for Medium- and Heavy-Duty Engines and Vehicles; Final Rule*. 2011, www.govinfo.gov/content/pkg/FR-2011-09-15/pdf/2011-20740.pdf.

Wang, Xiaoliang, et al. "Comparison of vehicle emissions by EMFAC-HK model and tunnel measurement in Hong Kong." *Atmospheric Environment*, vol. 256, 2021, p. 118452, www.sciencedirect.com/science/article/pii/S1352231021002739.

Zhou, Haiqin, et al. "Investigation on soot emissions from diesel-CNG dual-fuel." *International Journal of Hydrogen Energy*, vol. 44, no. 18, 2019, pp. 9438-9449, www.researchgate.net/publication/331653984_Investigation_on_soot_emissions_from_diesel-CNG_dual-fuel.

Zhu, Hanwei, et al. "Characterizing emission rates of regulated and unregulated pollutants from two ultra-low NOx CNG heavy-duty vehicles." *Fuel*, vol. 277, 2020, p. 118192, www.sciencedirect.com/science/article/pii/S0016236120311881.

3. Light-Duty Vehicle NH_3 and N_2O Emissions Using E10 CaRFG and Splash Blended E15

3.1 Abstract

Emissions of NH_3 and N_2O were measured with the federal testing procedure (FTP) cycle for 20 vehicles, including light-duty passenger cars and light-duty trucks with emissions technology groups from SULEV 30, ULEV 125, ULEV 70, and ULEV 50. The NH_3 and N_2O emissions measurements were carried out using Fourier Transform Infrared spectroscopy (FTIR). The goal of this study is to compare the NH_3-w and N_2O-w emissions concentration for a variety of vehicles fueled with 10 percent ethanol and 15 percent ethanol gasoline concentration. NH_3 and N_2O emissions is a by-product formed in the TWC due to catalytic reaction with conventional pollutant exhaust gases. Under FTP driving cycle, average weighted NH_3 and N_2O emissions after TWC are 4.38 and 17.13 mg/mi for E10 fuel and 4.72 and 14.69 mg/mi for E15 fuel.

3.2 Introduction

Earlier this year, the EPA approved the use of higher ethanol blend fuel of up to 15 percent ethanol (E15) by volume year-round. Before this approval, gasoline in California contained up to 10 percent of ethanol by volume. The major benefit of a higher ethanol fuel would be the reduced reliance on fossil fuels, which results in reduced greenhouse gas (GHG) and criteria pollutant emissions (Dale and Pimental, 2008). With this

increased ethanol in fuel, the CARB has received request from the ethanol industry to adopt specifications for E15 gasoline. “CARB's mission is to promote and protect public health, welfare, and ecological resources through effective reduction of air pollutants while recognizing and considering effects on the economy” (California Air Resource Board, 2021). Therefore, before adopting the E15 specification, CARB has requested Bourns College of Engineering, Center for Environmental Research & Technology (CE-CERT) of Riverside to carry out a study to better understand emissions related to ethanol volume increase in gasoline. This study will be conducted with a total of twenty light-duty vehicle’s using E10 California Reformulated Gasoline (CaRFG) and E15 by adding denatured ethanol to the E10 CaRFG.

The primary objective of this study will be to determine the impact of NH_3 and N_2O emissions after the ethanol content of gasoline is increased from 10 percent to 15 percent for LDVs. Although NH_3 is not a regulated criteria pollutant, NH_3 is considered a toxic compound and a precursor in the formation of atmospheric secondary aerosols (Behera and Sharma, 2010). The exposure to higher NH_3 concentration can cause irritation of the skin, eyes, nose, or throat due to direct contact (Żółtowski and Gis, 2021). On the other hand, even at low concentrations, NH_3 has an unpleasant odor when released into the air and most notably harms vegetation, particularly at high concentrations (Żółtowski and Gis, 2021). The particulate matter (PM) formed due to NH_3 emissions, namely ammonium nitrate and ammonium sulphate, is also associated with similar adverse health effects, impoverishes air quality, and negatively effects nitrogen-containing ecosystems

(Suarez-Bertoa, et al., 2014). This means that NH_3 plays a major role in the impact of air pollution on human health and the environment, therefore effects to understand and control emissions are essential (Farren, et al. 2020).

Generally, NH_3 gas is associated with rural environments, yet it has been observed that some urban areas have NH_3 levels similar to what is usually observed in rural areas (Livingston, et al., 2009). It has been observed that vehicles with internal combustion engines contribute to a majority of NH_3 emissions in the urban environments (Livingston et al., 2009, Battye, 2003). This vehicle related NH_3 emissions is mainly produced because of the widely used TWC in LDVs.

In the TWC, NH_3 formation has been attributed to the reactions of nitric oxide with hydrogen gas as a result from a water-gas shift reaction between CO and H_2O as shown in reaction 1 (Livingston, et al., 2009). The hydrogen gas produced in reaction 1 reacts with the NO by either the pathway of reaction 2a or 2b to produce NH_3 (Livingston, et al., 2009).

$$CO + H_2O \rightarrow CO_2 + H_2 \quad (1)$$

$$2NO + 2CO + 3H_2 \rightarrow 2NH_3 + 2CO_2 \quad (2a)$$

$$2NO + 5H_2 \rightarrow 2NH_3 + 2H_2O \quad (2b)$$

N_2O is an unregulated emission yet is a powerful greenhouse gas with 298 times the global warming potential of CO_2 over 100 years (Suarez-Bertoa, et al., 2016). Furthermore, N_2O is considered the single most important ozone-depleting substance (Suarez-Bertoa, et al., 2016). The interest in this study is due to the contribution of LDVs to the global N_2O inventory due to the ethanol volume increase of 5%.

All combustion processes have N_2O emissions as a by-product. N_2O is formed by two general chemical reaction in the combustion. First, through a homogeneous gas-phase reaction of NO with isocynate (NCO) (reaction 3a) or imidogen (NH) (reaction 3b) (Wallington and Wiesen, 2014). Yet, this gas-phase combustion reaction is not typically an effective source of N_2O from engines because there is little nitrogen in fuel and N_2O that is formed will thermally decompose at high temperatures (Wallington and Wiesen, 2014).

$$NO + NCO \rightarrow N_2O + CO \quad (3a)$$

$$NO + NH \rightarrow N_2O + H \quad (3b)$$

Second, N_2O is typically formed in heterogeneous reactions of NOx in exhaust emissions treatment system (Wallington and Wiesen, 2014). In short, engine-out NOx is absorbed onto the catalyst surface resulting in the weakening of the N-O bonds and increasing the mobility of nitrogen atom on the catalyst surface (Wallington and Wiesen, 2014). When

two nitrogen atoms encounter each other, they form N_2 and when a nitrogen atom encounters a molecule of NO a molecule of N_2O is formed and released from the catalyst surface (Wallington and Wiesen, 2014).

Therefore, before adopting a higher ethanol specification, it is important to understand the resulting NH_3 and N_2O emissions from internal combustion engines. It is also important to collect emissions data from a broad range of in-use vehicles. The objective of this study was to measure the emissions level of NH_3 and N_2O from a fleet of 20 in-use vehicles over the FTP cycle. These vehicles included light-duty passenger cars and light-duty trucks with technology groups of SULEV 30, ULEV 125, ULEV 70, and ULEV 50. Measurements were taken using FTIR at 1 Hz, which has the capability to capture emissions of compounds like NH_3 and N_2O in real-time on a mass per second basis. The result of this study is further discussed in this paper.

3.3 Experimental Procedures

3.3.1 Test Fuels

Two fuels were used in this program, namely an E10 and an E15 fuel. Fuels samples were taken at C3 Fuels facility, where fuel mixture will take place. Three samples from three separate drums of E10 and three samples from three separate drums of E15 were collected and shipped to SWRI for fuel properties analysis and detailed hydrocarbon analysis. The table below lists the fuel properties and method to be analyzed for the E10 and E15 samples.

Table 3-1: Main properties and methods for the Analysis of Test Fuels

Property	Method	Cap Limits Ca RFG3 (all maxima)
Reid Vapor Pressure (psi)	ASTM D5191	7.2
Sulfur Content (ppmw)	ASTM D5453	20
Benzene Content (%vol)	ASTM D5580	1.1
Aromatics Content (%vol)	ASTM D5580	35.0
Olefins Content (%vol)	ASTM D6550	10.0
T50 (°F)	ASTM D86	220
T90 (°F)	ASTM D86	330
Oxygen Content (%w)	ASTM D4815	3.5% (not applicable to E15)
Ethanol Content	ASTM D4815	NA
T5, T10, T20, T30, T40, T60, T80, T95, FBP	ASTM D86	NA
RON	ASTM D2699	NA
MON	ASTM D2700	NA
MTBE Content	ASTM D7754	NA
Specific gravity	ASTM D4052	NA
DHA	ASTM D6730	NA
Carbon	ASTM D5291	NA
Net Heating Value	ASTM D4809	NA

Table 3-2: Main Physicochemical Properties of the Test Fuels

Property		Test Method	E10 Drum#2	E10 Drum#3	E10 Drum#4	E15 Drum#1	E15 Drum#2	E15 Drum#3
RVP (EPA Equation)	psi	D5191	7.43	7.44	7.41	7.33	7.35	7.36
DVPE (ASTM Equation)	psi		7.31	7.32	7.28	7.20	7.22	7.23
CARVP (California Equation)	psi		7.20	7.21	7.17	7.09	7.11	7.12
Research Octane Number	ON	D2699Mdp	91.1	91.2	91.1	94.1	93.4	93.4
Motor Octane Number	ON	D2700Mdp	83.6	83.5	83.5	85.1	85.1	85.0
API Gravity		D4052	59.15	59.15	59.15	58.48	58.48	58.48
Specific Gravity			0.7422	0.7422	0.7422	0.7448	0.7448	0.7448
Density at 15C	g/ml		0.7420	0.7419	0.7420	0.7446	0.7445	0.7445
Heat of Combustion , Gross	BTU/lb	D4809	19255	19264	19274	18883	18862	18887
	MJ/kg		44.787	44.809	44.831	43.922	43.873	43.931
	cal/g		10697.2	10702.5	10707.8	10490.6	10478.9	10492.8
Heat of Combustion , Net	BTU/lb		17970	17980	17996	17609	17592	17615
	MJ/kg		41.799	41.823	41.860	40.959	40.919	40.972
	cal/g		9983.6	9989.2	9998.1	9782.8	9773.3	9786.1
Methanol	Vol%	D4815	<0.2	<0.2	<0.2	<0.2	<0.2	<0.2
Ethanol	Vol%		9.61	9.70	9.68	14.54	14.59	14.21
Isopropanol	Vol%		<0.2	<0.2	<0.2	<0.2	<0.2	<0.2
tert-Butanol	Vol%		<0.2	<0.2	<0.2	<0.2	<0.2	<0.2
n-Propanol	Vol%		<0.2	<0.2	<0.2	<0.2	<0.2	<0.2
Methyl tert-butyl ether	Vol%		<0.2	<0.2	<0.2	<0.2	<0.2	<0.2
sec-Butanol	Vol%		<0.2	<0.2	<0.2	<0.2	<0.2	<0.2
Diisopropylether	Vol%		<0.2	<0.2	<0.2	<0.2	<0.2	<0.2
Isobutanol	Vol%		<0.2	<0.2	<0.2	<0.2	<0.2	<0.2
Ethyl tert-butylether	Vol%		<0.2	<0.2	<0.2	<0.2	<0.2	<0.2
tert-Pentanol	Vol%		<0.2	<0.2	<0.2	<0.2	<0.2	<0.2
n-Butanol	Vol%		<0.2	<0.2	<0.2	<0.2	<0.2	<0.2
tert-amyl methyl ether	Vol%		<0.2	<0.2	<0.2	<0.2	<0.2	<0.2
Total Oxygen	Wt%		3.57	3.60	3.59	5.38	5.40	5.26
Carbon	wt%	D5291 CH	82.80	82.76	82.85	81.08	80.71	80.93
Hydrogen	wt%		14.08	14.08	14.00	13.96	13.92	13.94
Sulfur	ppm	D5453	6.23	5.79	6.74	4.47	4.62	4.33
Benzene	Vol%	D5580	0.59	0.60	0.60	0.56	0.56	0.56
Toluene	Vol%		4.03	4.04	4.04	3.81	3.81	3.81
Ethylbenzene	Vol%		0.94	0.94	0.94	0.89	0.89	0.89
p,m-Xylene	Vol%		3.85	3.85	3.85	3.65	3.65	3.64

o-Xylene	Vol%		1.36	1.36	1.37	1.29	1.29	1.29
C9 plus Aromatics	Vol%		8.73	8.74	8.74	8.27	8.27	8.25
Total Aromatics	Vol%		19.52	19.53	19.53	18.47	18.47	18.45
Olefin	Mass %	D6550	5.0	5.0	5.1	4.6	4.7	4.6
DHA		D6730	File Attached	File Attached	File Attached	File Attached	File Attached	File Attached
Distillation		D86						
IBP	deg F		100.8	101.9	102.2	101.9	102.9	102.0
5%	degF		129.2	130.0	129.4	130.7	128.5	128.7
10%	degF		134.8	135.8	135.4	136.8	135.8	135.4
15%	degF		138.6	139.3	139.3	140.7	139.8	139.4
20%	degF		142.3	143.1	142.7	144.3	143.4	143.1
30%	degF		148.8	149.7	149.1	150.8	150.5	149.8
40%	degF		156.4	157.7	157.7	156.4	156.3	155.5
50%	degF		204.1	205.3	204.1	162.0	161.8	159.6
60%	degF		227.5	228.5	228.2	219.4	219.1	218.4
70%	degF		248.1	249.4	248.6	244.7	244.8	242.5
80%	degF		274.8	275.7	275.1	272.6	271.5	269.8
90%	degF		313.7	314.2	313.0	310.5	310.9	310.1
95%	degF		341.8	342.6	341.8	340.6	339.3	338.8
Final Boiling Point	degF		392.6	397.0	392.6	394.8	394.2	392.8
Recovered	mL		99.0	99.2	99.0	98.8	97.9	98.5
Residue	mL		0.7	0.7	0.7	0.7	0.7	0.7
Loss	mL		0.3	0.1	0.3	0.5	1.4	0.8

One sample of denatured ethanol will also be collected and shipped to SWRI for analysis.

The table below shows the properties to be analyzed for the denatured ethanol sample.

Table 3-3: Main properties and methods for the Analysis of Denatured ethanol

Property	Test Method	Limit
Ethanol (Vol%, min)	ASTM D5501-94(1998)	92.1
Methanol (Vol%, max)	ASTM-D5501	0.5
Solvent-washed gum, mg/100 ml, max.	ASTM D381-00 air jet apparatus	5.0
Water content, vol% max.	ASTM E203-96 or E1064-00	1
Denaturant content vol.%	Reported by Source of Ethanol	Between 1.96 and 5.00
Inorganic chloride content, mass ppm (mg/l)	Modification of ASTM D512-89 (1999) Procedure C	40 (32)
Copper content mg/kg	Modification of ASTM D1688-95, Test Method A	0.1
Acidity (as acetic acid) mass % (mg/l), max	ASTM D1613-96 (1999)	0.007(56)
pHe	ASTM D 6423-99	Between 6.5 and 9.0
Appearance	Determined at indoor ambient temperature	Visibly free of suspended or precipitated contaminants (clean and bright)
Sulfur, ppm, max	D5453-93	10 ppm
Benzene, vol%, max	D7576--10	0.06
Olefins content, vol%, max	D7347-07	0.5
Aromatic hydrocarbons, vol%, max	D7576-10	1.7

Table 3-4: Denatured ethanol properties

Test method	Property	Unit	Denatured Ethanol
D1613	Acidity	mgKOH/g	0.0353
	Acidity as Acetic Acid	wt%	0.0038
D1688 M	Copper	mg/L	<0.05
D381	Unwashed Gum	mg/100 mL	0.50
	Washed Gum	mg/100 mL	<0.5
D4176	Clear and Bright		Pass
	Particulate		Pass
	Free Water		Pass
	Haze Rating		1
	Temperature of Sample	°C	6.0
D5453	Sulfur	ppm	0.75
D5501	Ethanol	Vol%	97.49
	Methanol	Vol%	0.02
D6423	pHe		8.55
D7319	Total Chloride	ppm	<0.5
	Total Sulfate	ppm	<0.5
	Potential Sulfate	ppm	<1.0
D7347	Olefin Content	mass%	<0.1
D7576	Benzene	Vol%	0.01
	Toluene	Vol%	<0.01
	Ethylbenzene	Vol%	<0.01
	p,m-Xylene	Vol%	<0.01
	o-Xylene	Vol%	<0.01
	C9 plus Aromatics	Vol%	<0.01
	Total Aromatics	Vol%	<0.29
E1064	Water	Wt%	0.6913

No lubricant changes will be performed on the test vehicles.

3.3.3 Test Vehicles

Twenty passenger cars were acquired for testing. A list of the vehicles that were used for this testing is provided in Table 3-5. The test matrix included vehicles with direct injection engines and port fuel injection systems that are representative of the current US fleet. All vehicles were equipped with three-way catalysts (TWCs).

The test matrix included a mix of different manufacturers and passenger cars. The test matrix included 9 vehicles from domestic manufacturers (Chevrolet, Ford, Dodge, Jeep, Buick and GMC) and 11 vehicles from foreign manufacturers (Kia, Honda, Nissan, Toyota, Mazda and Hyundai). The vehicles also represented a range of different engine displacements.

The vehicles were certified to meet the Federal Tier 3 exhaust emission standards or the California LEV-III, SULEV exhaust emissions standards.

The primary source for vehicles was rental fleets. Vehicle odometers at the onset of testing ranged from 7,352 miles (Ford F150) to 63,491 miles (Nissan Rogue). All vehicles acquired for testing were inspected to ensure that they were in sound mechanical and operational condition using a standard checklist. Each vehicle was also tested over a preliminary emissions test to ensure that its emissions are acceptable for that class of vehicle. Vehicle preconditioning will be performed as specified below using 2 HWFET (highway fuel economy test cycles), 2 LA4s, and two additional drain and 40% fills.

During the prep procedure, side fan cooling will be applied to the fuel tank. Following the prep cycle, the vehicle will be idled for two minutes, then shut down in preparation for the soak. After the 12 to 24 hours soak the first FTP test cycle will be performed.

Table 3-5: Test Vehicle Specifications

	PFI# 1	GDI# 1	PFI# 2	PFI# 3	PFI+ GDI# [illegible]	GDI# 2	GDI# 3	GDI# 4	GDI# 5	PFI# 4	GDI# 6	PFI# 5	GDI# 7	PFI_ Hybr [illegible]	GDI# 8	GDI# 9	GDI# 10	PFI+ GDI# [illegible]	PFI# 6	GDI# 11
Year	2019	2018	2020	2016	2019	2018	2016	2020	2019	2021	2020	2020	2020	2020	2020	2020	2021	2017	2021	2018
Make	Dodge	Honda	Jeep	Nissan	Toyota	Honda	Mazda	Ford	Chevrolet	Chevrolet	KIA	Jeep	Nissan	Toyota	GMC	Buick	Chevrolet	Ford	Hyundai	Chevrolet
Model	Ram 1500	Fit	Compass	Rogue	Rav4	Civic	Mazda3	Fusion	Impala	Spark	Optima	Cherokee	Armada	Prius	Acadia	Enclave	Colorado	F-150	Accent	Suburban
vehicle class (EPA)	LDT	LDV	LDT	LDT1	LDT1	LDV	LDV	LDV	LDV	LDV	LDV	LDT	LDT4	LDV	LDT	LDT	LDT	LDT	LDV	LDT
Miles at start (mi)	3223	3554	2917	6349	3732	3577	7433	3302	2572	4073	2937	2327	3273	1001	3494	3262	1760	7352	1222	3447
Engine size (L)	5.7	1.5	2.4	2.5	2.5	1.5	2.5	2	3.6	1.4	2.4	3.6	5.6	1.8	3.6	3.6	3.6	3.5	1.6	5.3
Fuel injection [illegible]	SFI	DFI	SFI	SFI	DFI+ SFI	DFI	DFI	DFI	DFI	SFI	DFI	SFI	DFI	SFI	DFI	DFI	DFI	DFI/ SFI	SFI	DFI
Air intake system	Natural aspir	Natural aspir	Turb	Natural aspir	Natural aspir	Turbo-char	rally aspir	Turbo-char	rally aspir	Natural aspir	Natural aspir	Natural aspir	Natural aspir	Natural aspir	Natural aspir	Natural aspir	Natural aspir	Turbo-char	Natural aspir	Natural aspir
Number of cylinders	8	4	4	4	4	4	4	4	6	4	4	6	8	4	6	6	6	6	4	8
Engine compression ratio	10.5-1	11.5:1	10:0	10:0 in states with California emission standard	13:0	10.3:1	13:0	9.3:1	11.5:1	10.6:1	11.3:1	10.2:1	11.2:1	13:0	11.5:1	11.5:1	11.5:1	10.5:1	11.2:1	11:0
Emission standard	USEPA: T3 B70 CA: ULEV70	USEPA: T3B30 CA: SULEV30 PC	USEPA: T3 B50 CA: ULEV50	USEPA: Calif orni a emis sion stan dard	USEPA: T3B5 0 CA: ULEV50	USEPA: IT3B 125 CA: ULEV 5 PC	USEPA: N/A CA: SULEV30/ PZEV	USEPA: T3B7 0 CA: ULEV70 PC	USEPA: TIER 3 CA: PC/S ULEV V30	USEPA: TIER 3 CA: PC/U LEV7 0	USEPA: T3B7 0 CA: ULEV70 PC	USEPA: T3 B30 CA: SULEV30		USEPA: T3 B30 CA: SULEV30 PC	USEPA: TIER 3 CA: ULEV50	USEPA: TIER 3 CA: ULEV50	USEPA: TIER 3 CA: ULEV50	USEPA: T2B5 25 CA: ULEV 5	USEPA: T3B1 25 CA: ULEV 5 PC	USEPA: TIER 3 CA: ULEV12 5
Aftertreatment systems	HO2S TWC	WU-TWC HO2S TWC	HO2S	TWC (2) HO2S WR-HO2S	EGR	TWC	WU-TWC	TWC	HO2S	HO2S	WR-HO2S	EGR	2TWC (2)	EGR	HO2S	HO2S	HO2S	TWC	WR-HO2S	HO2S
		TWC	TWC	HO2S	EGR C WR-HO2S TWC (2)	WR-HO2S	WU-TWC	HO2S WR-HO2S CAC	TWC	TWC	HO2S	EGR	2HO 2S 2WK	EGR C WR-HO2S TWC (2)	TWC	TWC	TWC	WR-HO2S	HO2S	TWC
		WR-HO2S	WR-HO2S	WR-HO2S		HO2S					WU-TWC	HO2S	- HO2					HO2S	WU-TWC	
		EGR				TC		TC			TWC	TWC						TC	TWC	
						CAC								HO2S				CAC	EGR	
																			EGR C	

3.3.4 Test Sequence, Randomization, and Fuel Conditioning

Each vehicle/fuel combination was tested three times using the FTP emissions test cycle. The FTP test cycle is shown in Figure 3-1.

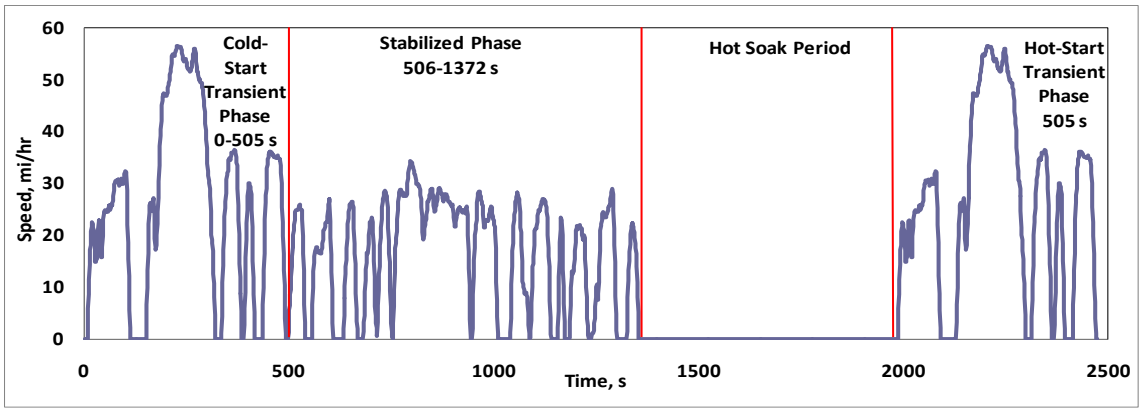

Figure 3-1: FTP cycle

The actual randomization sequence for each vehicle is provided in Table 3-6.

Table 3-6: Actual Test matrix randomization sequence

Vehicle		
Dodge Ram1500	A	B
Honda Fit	A	B
Jeep Compass	A	B
Nissan Rogue	B	A
Toyota Rav4	A	B
Honda Civic	B	A
Mazda3	B	A
Ford Fusion	B	A
Chevrolet Impala	A	B
Chevrolet Spark	A	B
KIA Optima	A	B
Jeep Cherokee	A	B
Nissan Armada	B	A
Toyota Prius	A	B
GMC Acadia	B	A
Buick Enclave	A	B
Chevrolet Colorado	A	B
Ford F-150	A	B
Hyundai Accent	B	A
Chevrolet Suburban	B	A

Where: A=E10 and B=E15

Details of the test procedure are provided below:

A. Upon receiving the vehicle, CE-CERT's technical staff performed vehicle check-in and inspection, as well prepared the vehicle for testing.

B. The existing fuel in the tank was drained from the vehicle and the tank was flushed with the test fuel using the procedure shown in Figure 3-2. The tank was filled 40% full with the test fuel in CE-CERT's outdoor prep area.

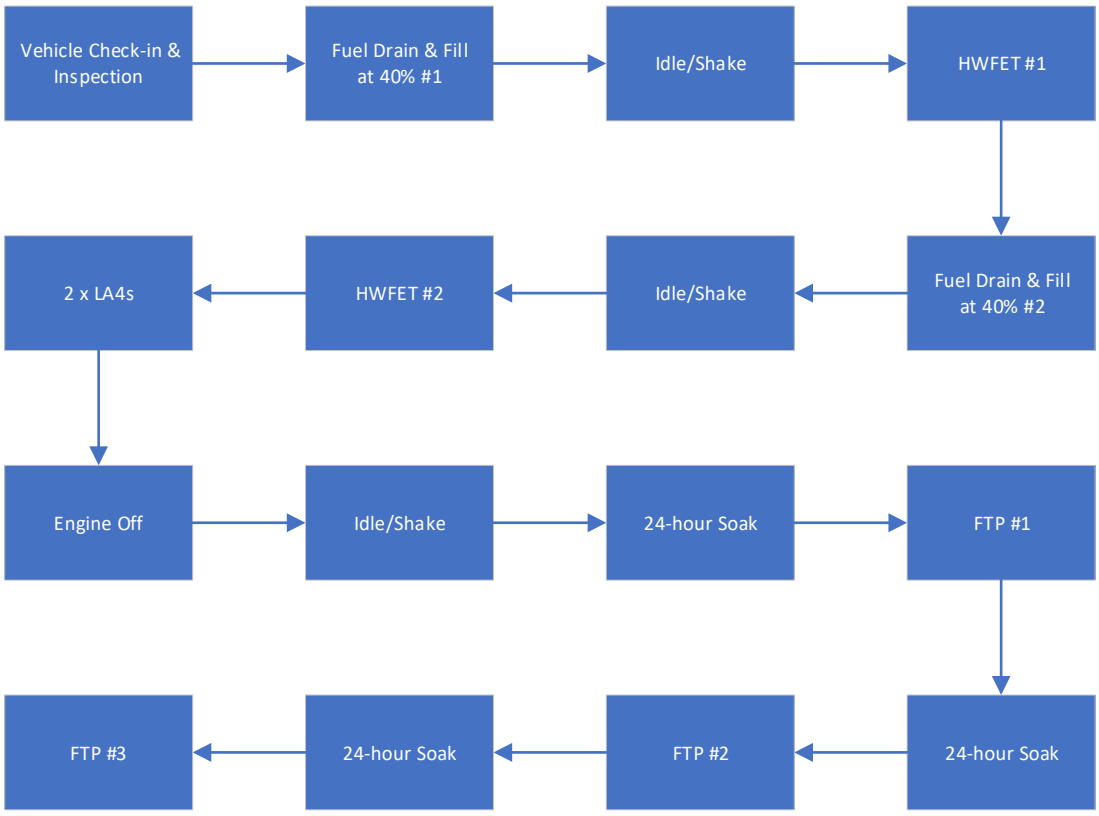

Figure 3-2: Prep and test procedure

C. Vehicle preconditioning was performed as specified below using 2 HWFET (highway fuel economy test cycles), 2 LA4s, and two additional drain and 40% fills. During the prep procedure, side fan cooling was applied to the fuel tank. Following the prep cycle, the vehicle was idled for two minutes, then shut down in preparation for the soak. After the 12 to 24 hours soak the first FTP test cycle was performed.

Fuel Change, Conditioning, and Test Procedure

1. Drain vehicle fuel completely by disconnecting the fuel fill hose at the tank and then inserting a small plastic tube to pump out the residual fuel. Reattach the fuel fill hose.
2. Turn vehicle ignition to RUN position for 30 seconds to allow controls to allow fuel level reading to stabilize. Confirm the return of fuel gauge reading to zero.
3. Turn ignition off. Put 12 gals of next test fuel in sequence in fuel tank. Shake and then allow the vehicle to idle for two minutes.
4. Drain fuel and refill to 40% with test fuel. Start vehicle an idle for 10 minutes to purge fuel lines.
5. Move vehicle in the test lab without starting the engine. Start vehicle and perform a HWFET cycle.
6. Drain fuel again and refill to 40% with test fuel. Shake and then allow the vehicle to idle for two minutes.

7. Move vehicle in the test lab without starting the engine. Start vehicle and perform a HWFET cycle.
8. Perform the preconditioning 2 LA4 cycles. During the prep cycle, apply side fan cooling to the fuel tank to alleviate the heating effect of the exhaust system. Following the prep cycle, allow the vehicle to idle for two minutes, then shut down the engine in preparation for the soak.
9. Move vehicle to soak area without starting the engine.
10. Park vehicle in soak area at proper temperature (75°F) for at least 8 hours and no more than 24 hours.
11. Move vehicle to test area without starting engine.
12. Perform FTP cycle emissions test.
13. Move vehicle to soak area without starting the engine.
14. Park vehicle in soak area of proper temperature for 12-36 hours.
15. Move vehicle to test area without starting the engine.
16. Perform FTP emissions test.
17. Move vehicle to test area without starting the engine.
18. Perform FTP emissions test.

D. While on the FTP test cycle all tailpipe gaseous emissions were collected along with instantaneous particulate number emissions. Fuel economy and GHG emissions (CO_2, N_2O, and methane) was also collected. For particulate emissions, characterization

included solid particle number (>23 nm in diameter), PM mass for each individual phase of the FTP cycle, real-time soot mass emissions, and particle size distributions.

E. Additional emission measurements included carbonyl compounds, benzene, toluene, ethylbenzene, m/p/o-xylenes, and 1,3-butadiene.

F. The test matrix was designed to provide for randomization of the test fuels within the test vehicles.

3.3.5 Emissions Testing

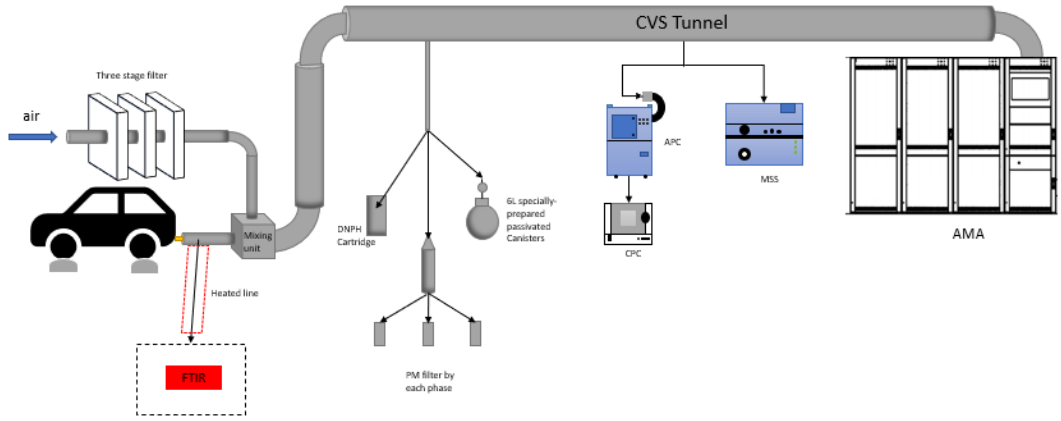

Figure 3-3: Schematic experimental setup

Table 3-7: Summary of measurement technique for all emissions

Emissions	Measurement technique
THC	Flame Ionization detection (FID)
CO	NDIR (nondispersive IR measurement)
CO2	NDIR
NOx	Chemiluminescence
NO	Chemiluminescence
NO2	Chemiluminescence
N2O	FTIR
CH4	FID + methane cutter (Cutter FID SL)
NMHC	Difference of THC and CH4
PM	Gravimetric Teflon filter
NH3	FTIR
BTEX	GC/MS/FID
Formaldehyde	DNPH cartridges
Acetaldehyde	DNPH cartridges
Carbonyls	DNPH cartridges
Particle Number	TSI CPC
Particle Size Distribution	TSI EEPS
AMA N2O	The AVL Quantum Cascade Laser (QCL)*

*No valid bag data.

Raw emissions

Vehicle emissions measurements were conducted in CE-CERT's Vehicle Emissions Research Laboratory (VERL). The centerpiece of the VERL is a 48-inch Burke E. Porter single-roll electric chassis dynamometer, capable of testing vehicles weighing up to 12,000 lbs.

Raw N_2O, NH_3 as well as CO, CO_2, NOx was measured through Fourier-transform infrared (FTIR) spectroscopy. FTIR is a powerful spectral detection technology that

has been recommended by the US Environment Protection Agency for monitoring air pollutants. FTIR spectra are composed of absorption peaks generated from infrared radiation absorption during the vibration transition of asymmetric dipole moment polyatomic molecules, and a wide variety of gaseous pollutants can be measured by FTIR technology due to their physical structures. FTIR has high sensitivity, permitting the detection of changes in gas concentration at the ppb (parts per billion, volume concentration) level.

The FTIR used in this campaign was a Horiba FTX-ONE-CS with a rate of one scan per 0.2 seconds, a cell volume of approximately 65 milliliters, and a pathlength of 2.4 meters.

3.3.6 Data Processing and calculations

Data Processing Procedure

1) Raw FTIR data (NH_3, NO, NO_2, CO, CO_2, N_2O) collected after each test from the Horiba FTX-ONE-CS instrument as an Excel spreadsheet.
2) Raw data is converted from parts per million (PPM) on a second-by-second basis to grams per second on a second-by-second basis
    a. First, raw data is converted from PPM to volume fraction by dividing each individual second-by-second data by a million.
    b. Then use the flow rate from FTIR data sheet to change data set to g/s using equation 1.

Equation 1:

$$\frac{Flow\ Rate\ \times\ Volume\ Fraction\ \times\ Density}{60}$$

3) Align raw data based on RPM.
4) FTIR only collects a fraction of the emissions emitted. Therefore, find the total CO_2 emitted by adding the CO_2 data set from the constant volume sampler (CVS) emissions tunnel with the FTIR CO_2 emissions data set. Then to find actual emissions, divide the total CO_2 with the FTIR CO_2 and multiply that ratio with the FTIR emissions data set.
5) Now with the actual emissions data, find the mass of emissions of each pollutant in each phase since time in each phase is known.
6) Find mass of emissions per mile for each pollutant, using known miles traveled in each phase.
7) Lastly, find weighted mass of each exhaust pollutant using equation 2 (Composite calculations for FTP exhaust emissions).

Equation 2:

$$pollutant\ mass(weighted) = 0.43\left(\frac{m_c}{D_{ct} + D_{cs}}\right) + 0.57\left(\frac{m_h}{D_{ht} + D_{hs}}\right)$$

Where:

M_c = the combined mass of emissions from phase 1 and phase 2.

D_{ct} = the measured driving distance in phase 1.

D_{cs} = the measured driving distance in phase 2.

M_h = the combined mass of emissions from phase 2 and phase 3.

D_{ht} = the measured driving distance in phase 2.

D_{hs} = the measured driving distance in phase 3.

3.4 Results

3.4.1 NH_3 Emissions

These two sections (3.4.1 and 3.4.2) present the statistical results for NH_3 emissions and N_2O emissions for the two ethanol fuels (E10 and E15). A statistical inferential analysis, T-test, was used to determine the statistical significance of differences in NH_3 and N_2O emissions rates between the two fuels. The results are considered to be statistically significant for $p \leq 0.05$ or marginally statistically significant for $0.05 < p \leq 0.1$ (Table 3-8 and Table 3-9). Differences found to be statistically significant infers that the differences probably represent a true effect from the fuel change (Warren, 2019). Marginally statistically significant differences imply that there could still be a real effect from the fuel change, but at a lower confidence level (Warren, 2019).

The NH_3-w (weighted NH_3) emissions from the 20-vehicle ethanol test are represented in Figure 3-4. The error bars represent one standard deviation from the triplicate test results for each one of the twenty vehicles.

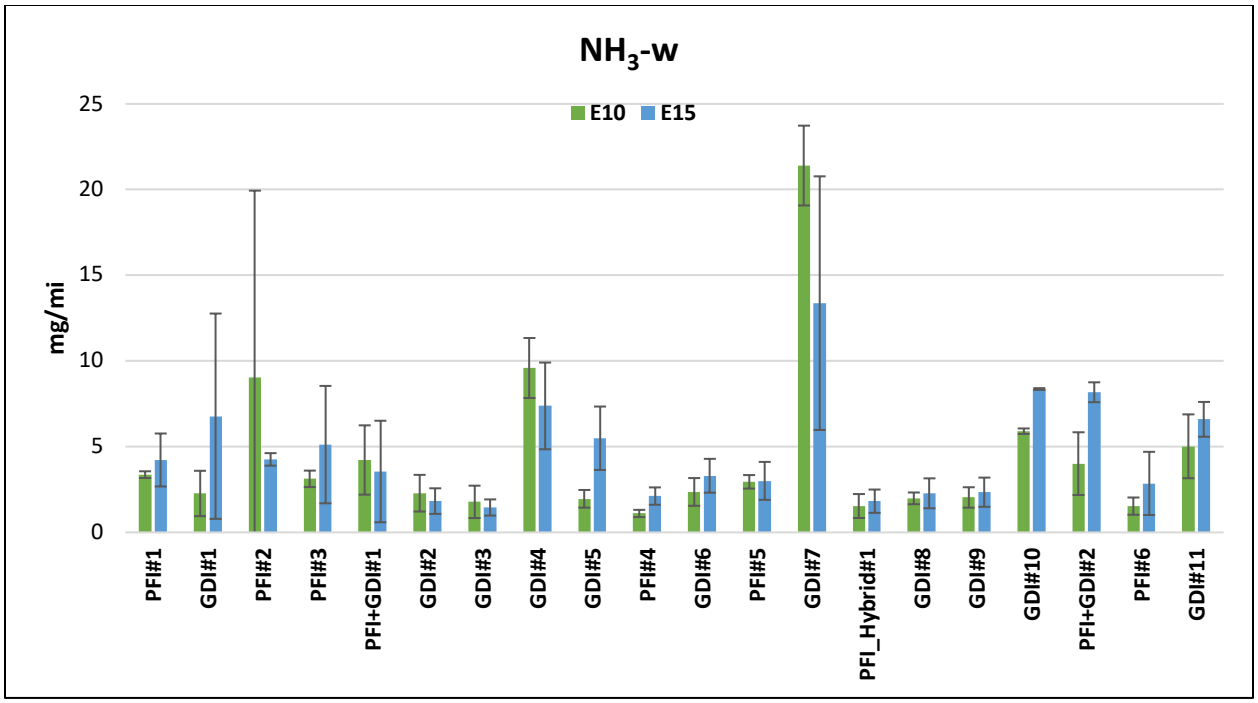

Figure 3-4: Average NH_3 Weighted Emission Results

Table 3-8 summarizes the statistical significances for NH_3 test results for the twenty-vehicle fleet.

For the NH_3-w emissions, GDI#5 and PFI+DFI#2 showed statistically significant differences, and PFI#4 showed a marginally statistically significant difference between E10 and E15 fuel. For the NH_3-w emissions**,** NH_3 emissions for E15 is greater than E10 by 95%, 68%, and 63% for GDI#5, PFI_DFI#2, and PFI#4, respectively.

For phase 1, cold-start, NH_3 emissions, GDI#10, PFI+GDI#2 and GDI#11 showed marginally statistically significant difference and GDI#5 showed a statistically significant

difference between E10 and E15. For cold-start, NH_3 emissions for E15 is greater than E10 by 119%, 87%, 86%, and 157% for GDI#10, PFI#2, GDI#11, and GDI#5, respectively.

For phase 2, hot-running, NH_3 emissions, GDI#5 and PFI+DFI#2 showed statistically significance, PFI#4 showed marginally statistically significance. For the GDI#5 NH_3 hot-running emissions, E15 is 32% higher than E10, for PFI_DFI#2 hot-running NH_3 emissions, E15 is 74% higher than E10, for PFI#4 hot-running NH_3 emissions, E15 is 106% higher than E10.

For phase 3, hot-start, NH_3 emissions, PFI#4 showed a marginally statistically significant difference with E15 being 23% higher compared to E10.

Table 3-8: NH_3 T-test p values

		t-test p value - w	t-test p value - ph1	t-test p value - ph2	t-test p value - ph3
	Vehicle#	NH_3	NH_3	NH_3	NH_3
Ram1500	PFI#1	0.395	0.446	0.512	0.330
Honda fit	GDI#1	0.272	0.459	0.645	0.319
Jeep compass	PFI#2	0.490	0.100	0.385	1.000
Nissan Rogue	PFI#3	0.374	0.140	0.121	0.531
Toyota Rav4	PFI+GDI#1	0.762	0.382	0.657	0.699
Honda civic	GDI#2	0.574	0.353	0.878	0.448
Mazda3	GDI#3	0.619	0.374	0.705	0.663
Ford Fusion	GDI#4	0.321	0.528	0.381	0.927
Chevrolet Impala	GDI#5	0.033	0.032	0.011	0.968
Chevrolet Spark	PFI#4	0.082	0.349	0.071	0.087
KIA Optima	GDI#6	0.270	0.219	0.665	0.145
Jeep Cherokee	PFI#5	0.938	0.582	0.906	0.259
Nissan Armada	GDI#7	0.147	0.886	0.155	0.235
Toyota Prius	PFI_Hybrid#1	0.683	0.444	0.221	0.236
GMC Acadia	GDI#8	0.616	0.523	0.363	0.223
Buick Enclave	GDI#9	0.635	0.633	0.764	0.302
Chevrolet Colorado	GDI#10	0.000	0.068	0.642	0.840
Ford F-150	PFI+GDI#2	0.020	0.068	0.006	0.423
Hyundai Accent	PFI#6	0.296	0.509	0.272	0.708
Chevrolet Suburban	GDI#11	0.268	0.053	0.772	0.146

** **Statistically significant and** **Marginally statistically significant**

Table 3-9 summarizes every test vehicle NH_3 emissions for each phase and for both fuels. This table shows highest levels of NH_3 emissions during the first phase and second phase of the FTP drive cycle for both E10 and E15 for 35 out the 40 tests. Figure 3-4 shows GDI#7 with significantly higher NH_3-w emissions compared to the rest of the fleet with phase 2 accounting for 64% and 58% of the total NH_3 emissions for the E10 and E15 fuel, respectively. This trend is the same for GDI#4, the next highest emitter of NH_3, showing 56% and 49% of NH_3 emissions occurred during phase 2 for E10 and E15 fuels, respectively. PFI+GDI#1 E10 fuel showed significantly higher NH_3 emissions with 70% of the total NH_3 emissions occurring during phase 1. This is contrary to a similar study (Durbin et. al., 2002), where the highest NH_3 emissions occurred during the third phase (hot start) of the FTP cycle. This is possibly due to the big difference in age of vehicles and differences in catalyst standards in both these studies. Overall, in this study, the average NH_3-w for vehicles fueled with E10 gasoline was 4.38 mg/mi and E15 was 4.72 mg/mi.

Table 3-9: Total NH_3 emissions in each phase

Year/Make/Model	Fuel	NH_3 Emissions (mg/mile)			
		NH_3-1	NH_3-2	NH_3-3	NH_3-w
PFI#1	E10	6.36	2.29	3.14	3.37
PFI#1	E15	9.90	2.83	2.58	4.23
GDI#1	E10	1.60	2.37	2.59	2.27
GDI#1	E15	1.40	3.32	17.42	6.78
PFI#2	E10	3.85	12.97	5.51	9.04
PFI#2	E15	8.03	2.10	5.51	4.26
PFI#3	E10	2.89	2.61	4.27	3.13
PFI#3	E15	8.58	1.36	9.60	5.12
PFI+GDI#1	E10	11.42	2.22	2.57	4.23
PFI+GDI#1	E15	6.55	3.08	2.19	3.55
GDI#2	E10	3.79	2.07	1.56	2.29
GDI#2	E15	2.30	1.95	1.23	1.83
GDI#3	E10	3.77	1.17	1.45	1.78
GDI#3	E15	2.16	1.32	1.18	1.45
GDI#4	E10	4.34	13.39	6.39	9.59
GDI#4	E15	3.15	9.51	6.56	7.38
GDI#5	E10	2.17	1.43	2.81	1.96
GDI#5	E15	17.88	1.98	2.77	5.49
PFI#4	E10	1.82	0.91	0.94	1.11
PFI#4	E15	1.24	2.97	1.19	2.12
GDI#6	E10	2.54	2.43	2.09	2.36
GDI#6	E15	6.82	2.02	3.07	3.30
PFI#5	E10	3.64	2.60	3.10	2.95
PFI#5	E15	5.25	2.66	1.96	3.01
GDI#7	E10	9.29	32.87	8.92	21.40
GDI#7	E15	8.69	19.55	5.24	13.38
PFI_Hybrid#1	E10	1.08	1.98	1.05	1.54
PFI_Hybrid#1	E15	0.85	0.85	4.39	1.82
GDI#8	E10	2.48	1.96	1.67	1.99
GDI#8	E15	4.18	1.44	2.44	2.28
GDI#9	E10	2.72	1.78	2.02	2.04
GDI#9	E15	3.98	1.70	2.34	2.35
GDI#10	E10	3.71	5.65	8.05	5.91
GDI#10	E15	14.58	6.20	7.77	8.36

PFI+GDI#2	E10	6.87	2.78	4.18	4.01
PFI+GDI#2	E15	17.38	6.08	5.18	8.18
PFI#6	E10	1.14	1.75	1.42	1.53
PFI#6	E15	1.40	4.15	1.52	2.86
GDI#11	E10	3.04	6.67	3.42	5.02
GDI#11	E15	7.60	7.38	4.37	6.60

3.4.3 N_2O Emissions

The N_2O-w (averaged weighted N_2O) emissions test results for the twenty vehicles are presented in Figure 3-5. Error bars represent one standard deviation from the triplicate test results.

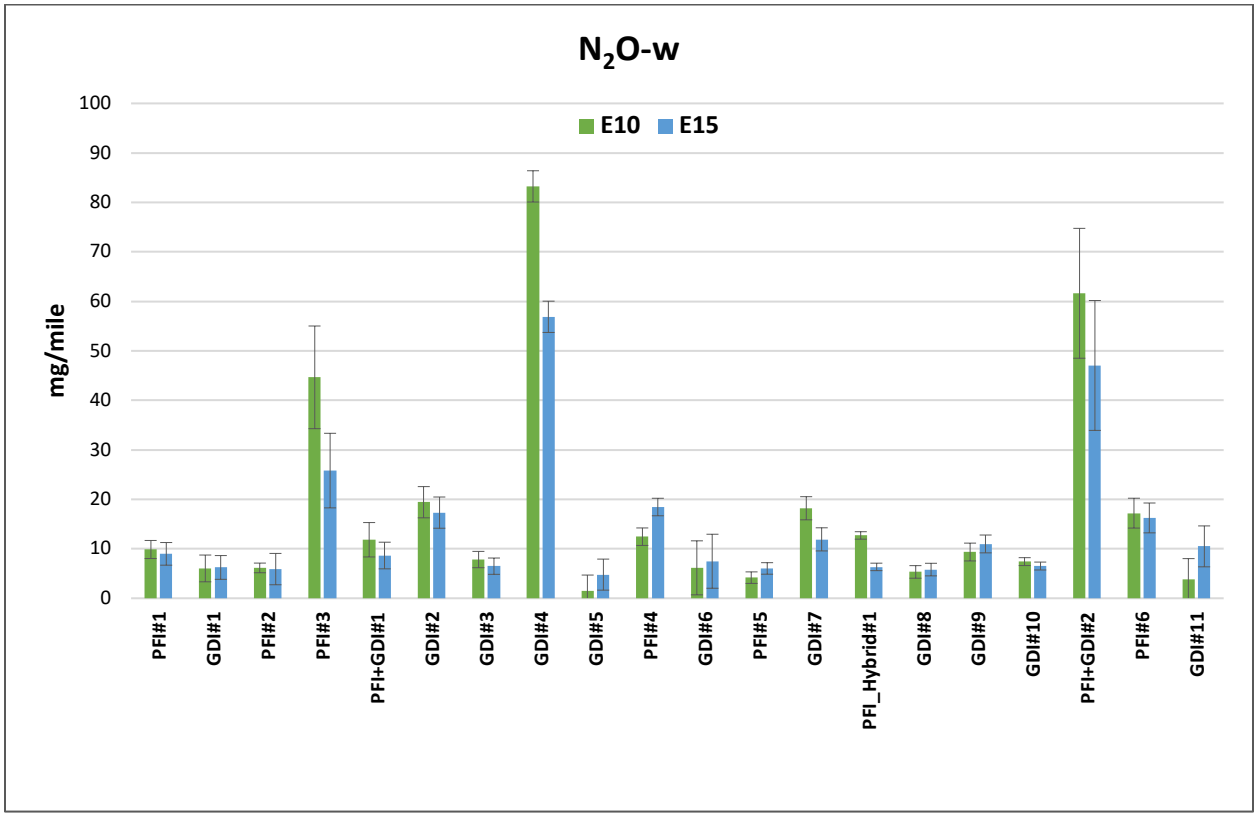

Figure 3-5: Average N_2O Weighted Emission Results

Table 3-10 summarizes the statistical significances for N_2O test results for the twenty-vehicle fleet.

For the N_2O-w emissions, GDI#4 and GDI#7 showed statistically significant, PFI#3, PFI#4 and GDI#11 showed marginally statistically significance between E10 and E15 fuel. For the GDI#4 N_2O-w emissions, E15 is 38% lower than E10, for GDI#7 N_2O-w emissions, E15 is 42% lower than E10, for PFI#3 N_2O-w emissions, E15 is 53% lower than E10, for PFI#4 N_2O-w emissions, E15 is 39% higher than E10, for GDI#11 N_2O-w emissions, E15 is 92% higher than E10.

For phase 1, cold-start, N_2O emissions, GDI#4, GDI#7, GDI#8 and GDI#11 showed marginally statistically significance between E10 and E15. For GDI#4 cold-start N_2O emissions, E15 is 25% lower than E10, for GDI#7 cold-start N_2O emissions, E15 is 30% higher than E10, for GDI#8 cold-start N_2O emissions, E15 is 27% higher than E10, for GDI#11 cold-start N_2O emissions, E15 is 86% higher than E10.

For phase 2, hot-running, N_2O emissions, GDI#4, PFI#4 and PFI+DFI#2 showed statistically significance between E10 and E15. For the GDI#4 N_2O hot-running emissions, E15 is 41% lower than E10, for PFI#4 hot-running N_2O emissions, E15 is 86% higher than E10, for PFI_GDI#2 hot-running N_2O emissions, E15 is 109% lower than E10.

For phase 3, hot-start, GDI#2, PFI#4 and GDI#10 showed statistically significant, PFI#3 and GDI#4 showed marginally statistically significance between E10 and E15 fuel. For the PFI#3 N_2O hot-start emissions, E15 is 111% lower than E10, for GDI#2 hot-start N_2O

emissions, E15 is 111% lower than E10, for GDI#4 hot-start N_2O emissions, E15 is 54% lower than E10, for PFI#4 hot-start N_2O emissions, E15 is 53% higher than E10, for GDI#10 hot-start N_2O emissions, E15 is 138% lower than E10.

Table 3-10: N_2O T-test p values

		t-test p value - w	t-test p value - ph1	t-test p value - ph2	t-test p value - ph3
	Vehicle#	N_2O	N_2O	N_2O	N_2O
Ram1500	PFI#1	0.630	0.457	0.112	0.978
Honda fit	GDI#1	0.930	0.425	0.512	0.344
Jeep compass	PFI#2	0.908	0.764	0.374	0.264
Nissan Rogue	PFI#3	0.064	0.247	0.218	0.055
Toyota Rav4	PFI+GDI#1	0.278	0.300	NA	0.817
Honda civic	GDI#2	0.490	0.531	NA	0.027
Mazda3	GDI#3	0.362	0.246	0.389	0.780
Ford Fusion	GDI#4	0.016	0.084	0.006	0.059
Chevrolet Impala	GDI#5	0.185	0.196	NA	0.227
Chevrolet Spark	PFI#4	0.050	0.167	0.037	0.044
KIA Optima	GDI#6	0.714	0.683	0.258	0.625
Jeep Cherokee	PFI#5	0.106	0.128	NA	0.254
Nissan Armada	GDI#7	0.023	0.072	NA	0.369
Toyota Prius	PFI_Hybrid#1	0.172	0.190	0.089	0.512
GMC Acadia	GDI#8	0.733	0.081	NA	0.479
Buick Enclave	GDI#9	0.198	0.793	NA	0.210
Chevrolet Colorado	GDI#10	0.520	0.749	NA	0.012
Ford F-150	PFI+GDI#2	0.293	0.273	0.019	0.599
Hyundai Accent	PFI#6	0.751	0.754	0.796	0.948
Chevrolet Suburban	GDI#11	0.058	0.054	NA	0.112

** Statistically significant and Marginally statistically significant

Table 3-11 summarizes every test vehicle total N_2O emissions for each phase and for both fuels. Phase 1 of the FTP cycle generally showed high emissions of N_2O, phase 2 showed very low N_2O emissions, and phase 3 showed low N_2O emissions. Figure 3-5 shows PFI#3, GDI#4, and PFI+GDI#2 with significantly higher N_2O-w compared to the rest of the fleet. PFI#3 shows high NH_3 emissions with 81% and 92% of the total NH_3 emissions occurring during phase 1 for E10 and E15 fuels. GDI#4 shows high NH_3 emissions with 69% and 67% of the total NH_3 emissions occurring during phase 1 and 39% and 32% of the total NH_3 emissions occurring during phase 3 for E10 and E15 fuels. PFI+GDI#2 is very similar to GDI#4 with the majority of N_2O emissions occurring in phase 1 and phase 2. The 1992 study by Hirano et. al. suggested that N_2O emissions is mostly formed at lower temperatures that would be found as the catalyst warms up to its operating temperature, which explains the high N_2O emissions during phase 1 in this study. In some cases, phase 3 showed high N_2O emissions, which is likely because phase 1 and phase 3 representing starting conditions compared to phase 2, which represents hot stabilized driving.

Overall, in this study, the average N_2O-w emissions was 17.45 mg/mi for vehicles fueled with E10 gasoline that contained 6.25 ppm of sulfur on average and average N_2O-w emissions was 14.41 mg/mi for vehicles fueled with E15 gasoline that contained 4.47 ppm of sulfur on average. These findings are in agreement with a past study (Huai, et al., 2004) that showed that increases in sulfur content in gasoline were found to increase N_2O emissions over the FTP cycle.

Table 3-11: Total N_2O emissions in each phase

Year/Make/Model	Fuel	N_2O Emissions (mg/mile)			
		N_2O-1	N_2O-2	N_2O-3	N_2O-w
PFI#1	E10	33.31	0.24	10.24	9.86
PFI#1	E15	29.50	0.13	10.13	8.98
GDI#1	E10	17.92	0.22	8.03	6.03
GDI#1	E15	24.40	0.10	4.13	6.23
PFI#2	E10	22.62	0.00	5.28	6.14
PFI#2	E15	24.98	0.01	2.67	5.90
PFI#3	E10	160.31	4.93	32.02	44.65
PFI#3	E15	112.40	0.00	9.13	25.80
PFI+GDI#1	E10	54.46	0.00	1.92	11.83
PFI+GDI#1	E15	38.64	0.00	2.29	8.64
GDI#2	E10	92.60	0.00	0.91	19.41
GDI#2	E15	83.37	0.00	0.26	17.31
GDI#3	E10	26.31	0.31	8.09	7.83
GDI#3	E15	19.15	0.17	8.88	6.49
GDI#4	E10	208.87	4.87	136.14	83.23
GDI#4	E15	162.48	3.23	78.40	56.88
GDI#5	E10	7.51	0.00	0.00	1.56
GDI#5	E15	22.72	0.00	0.26	4.78
PFI#4	E10	25.39	0.25	25.69	12.44
PFI#4	E15	29.16	0.64	44.02	18.44
GDI#6	E10	25.00	0.01	3.52	6.15
GDI#6	E15	32.88	0.06	2.29	7.48
PFI#5	E10	19.82	0.00	0.21	4.17
PFI#5	E15	27.05	0.00	1.51	6.03
GDI#7	E10	77.46	0.00	7.75	18.19
GDI#7	E15	57.00	0.00	0.31	11.90
PFI_Hybrid#1	E10	54.44	2.67	0.06	12.70
PFI_Hybrid#1	E15	26.81	1.20	0.57	6.34
GDI#8	E10	17.14	0.00	6.48	5.33
GDI#8	E15	22.52	0.00	4.11	5.80
GDI#9	E10	42.02	0.00	2.40	9.34
GDI#9	E15	43.11	0.00	7.49	10.98
GDI#10	E10	28.41	0.00	5.55	7.41

GDI#10	E15	30.15	0.00	1.01	6.52
PFI+GDI#2	E10	106.30	4.26	136.00	61.63
PFI+GDI#2	E15	68.86	1.26	116.85	47.05
PFI#6	E10	79.18	0.12	2.59	17.20
PFI#6	E15	74.63	0.09	2.57	16.24
GDI#11	E10	18.67	0.00	0.02	3.88
GDI#11	E15	46.71	0.00	2.91	10.49

3.4.4 Correlation with NH_3 Precursor Emissions

An analysis was taken to determine if there is a correlation between post-catalyst emissions of NH_3 and NH_3 precursor compounds (CO and NOx). Figure 3-6 shows the relationship between NH_3 and NH_3 precursors (CO, NOx) after the TWC for the FTP for GDI#7. Graph (b) shows NH_3 and NOx having a correlation during the phase 2 of the FTP cycle (500-1500 seconds), where NH_3 peaks follow NOx peaks. Graph (d) shows NH_3 and NOx having a more consistent correlation during entire FTP cycle with a Pearson correlation constant R=0.68. Graph (a) does not show a strong correlation between NH_3 and CO for the E10 fuel, but the E15 fuel in graph (c) shows some correlation between NH3 and CO peaks after startup.

Figure 3-7 shows the relationship between NH_3 and NH_3 precursors (CO, NOx) after the TWC for the FTP for PFI+GDI#2 for only the E15 fuel. Graph (a) shows some correlation between NH_3 and CO with some correlating emissions peaks during phase 2 and phase 3. Graph (b) shows a stronger correlation between NH_3 and NOx with correlating emissions peaks during phase 1 and phase 2 with a Pearson correlation constant R=0.68.

GDI#7 and PFI+DFI#2 suggest that NH_3 emissions are more correlated with NOx emissions than CO emissions in this study. These results were opposite of the Livingston, et al. (2009) results, in which there was a high correlation with CO and NH_3 (R = 0.56) and no correlation with NOx and NH_3 (R = -0.02).

GDI#7 and PFI+DFI#2 show E15 fuels having higher NH_3 correlation with CO and NOx than E10 fuels, which validates the previous findings in this study that showed E15 fuels emitting higher NH_3-w emissions compared to E10. Truyen, et al. (2015) ethanol blend study showed that CO emissions decreased as ethanol blend levels increased from E10 to E15 and NOx emissions increased from E10 to E15. This is a plausible explanation for the NOx and NH_3 correlation in this paper, since NH_3 formation is dependent on the presence of NOx and CO, as NH_3 can formed with the presence of just NOx and hydrogen as seen in chemical reaction 2b. This agrees with previous papers showing that NH_3 emissions are produced by the reaction of CO and NOx in the exhaust gas in the TWC instead of combustion in the engine cylinder (Liu, et al., 2021).

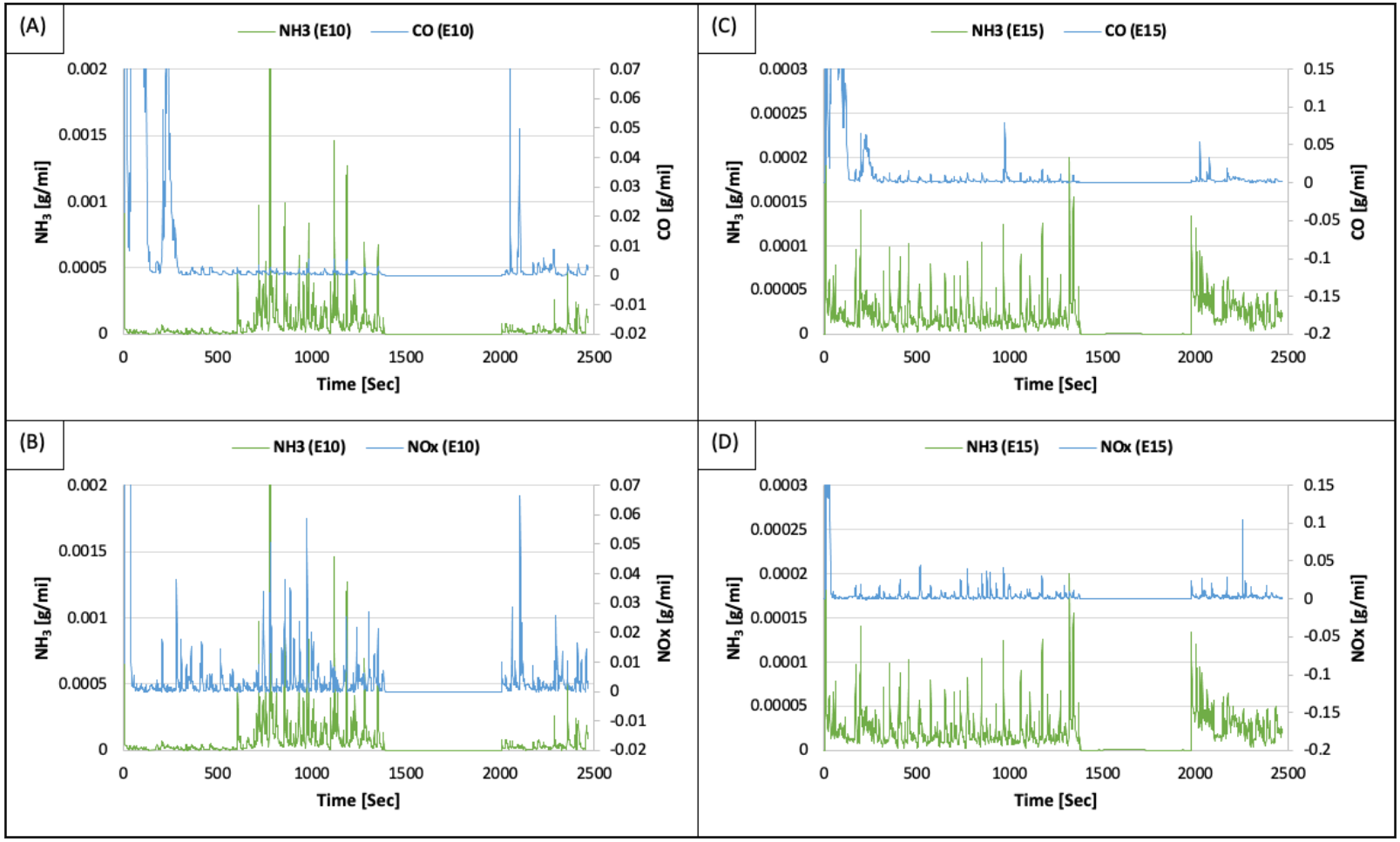

Figure 3-6: (a) NH_3 and CO emissions after TWC for E10 fuel, (b) NH_3 and NOx emissions after TWC for E10 fuel, (c) NH_3 and CO emissions after TWC for E15 fuel, and (d) NH_3 and NOx emissions after TWC for E15 fuel of GDI#7

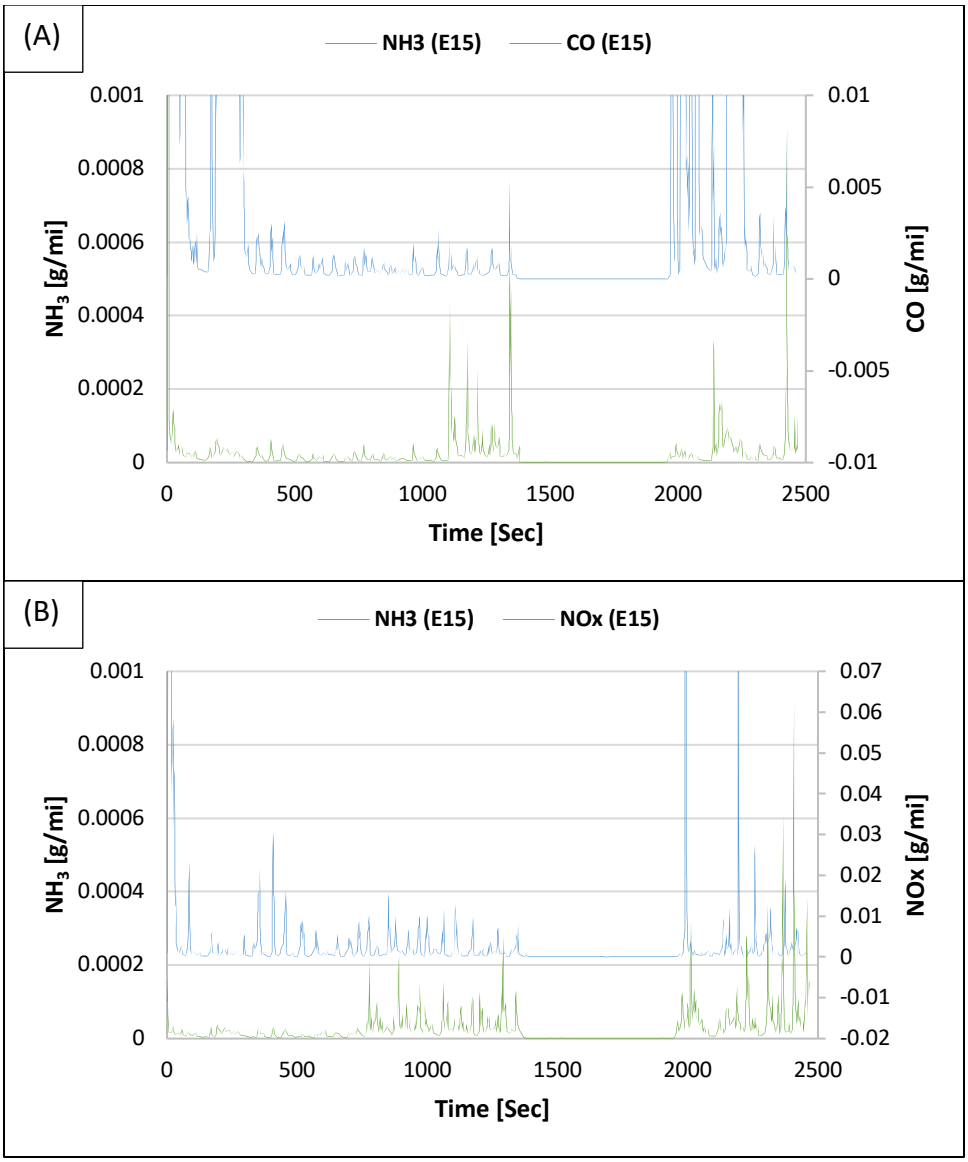

Figure 3-7: (a) NH_3 and CO emissions after TWC for E15 fuel, and (d) NH_3 and NOx emissions after TWC for E15 fuel of PFI+GDI#2

3.4.5 Correlation with N_2O Precursor Emissions

Analysis was undertaken to determine if a correlation existed between post-catalyst emissions of N_2O and the N_2O precursor compound NOx. Correlation plots between N_2O and NOx emissions were generated for the three phases of the FTP cycle for E10 and E15 fuels in Figure 3-8. A Pearson correlation coefficient was calculated for all three phases of the FTP cycle for E10 and E15 fuels, as shown in Table 3-12. The Pearson correlation show that only phase 1 of the FTP cycle for both E10 and E15 fuels showed strong N_2O and NOx correlations. E10 fuel shows the greatest correlation, R = 63, compared to E15 fuel, R = 53. This correlation between N_2O and NOx during phase 1 is likely due to the cold start, which generally emits higher NOx as seen in a previous study (Pielecha, et. al., 2021). A previous study (Huai, et al., 2004), showed that N_2O forms primarily during the catalyst warm-up from 250-450 ℃ and then declines as temperature gets closer to the equilibrium temperature of catalyst, which is likely contributing to the high correlation in phase 1 of the FTP cycle.

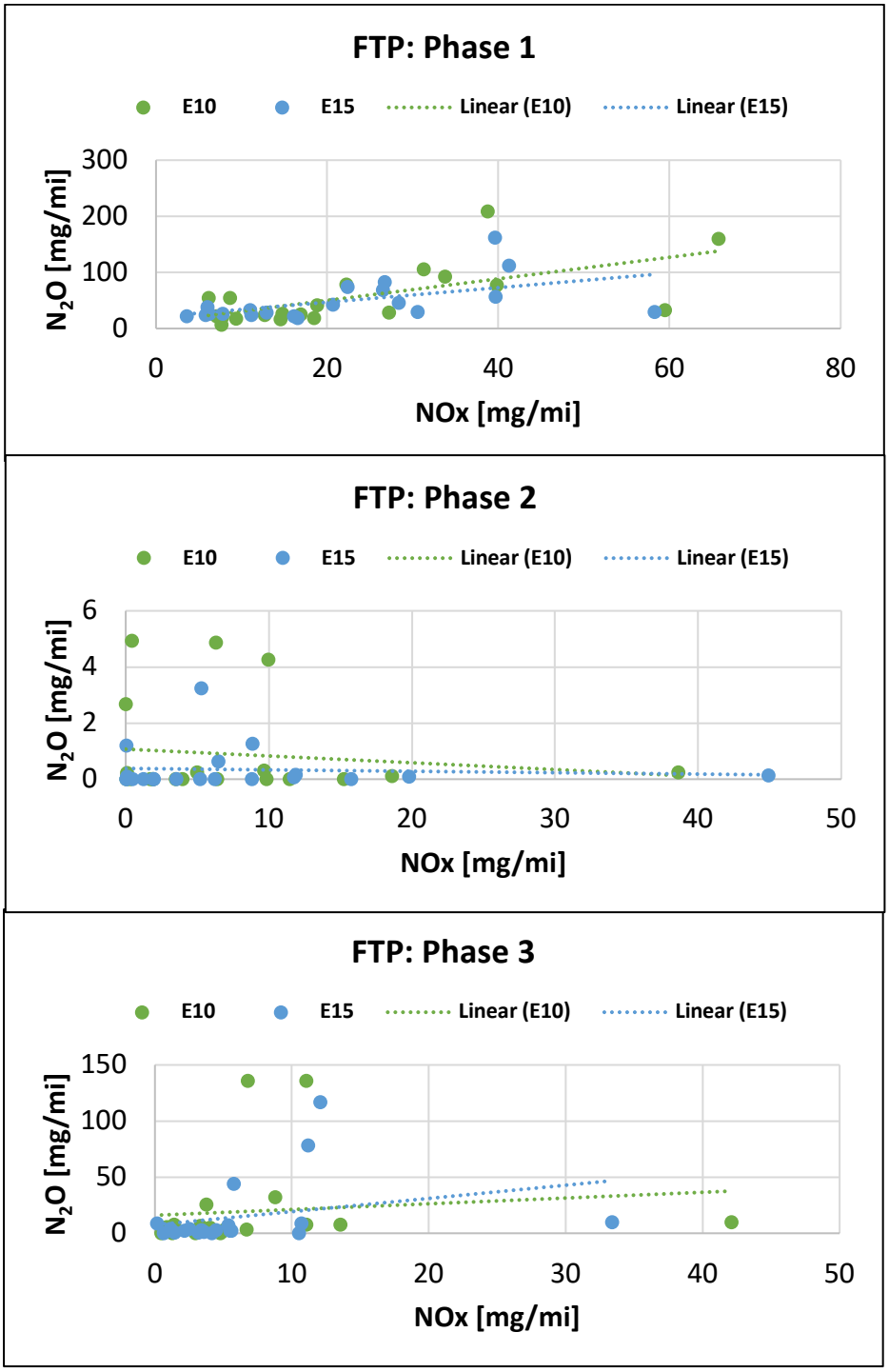

Figure 3-8: Correlation between N_2O vs NOx emissions

Table 3-12: Pearson Correlation between N_2O and NOx emissions

	Pearson Correlation:		
	Phase 1	Phase 2	Phase 3
E10	0.63	-0.13	0.11
E15	0.53	-0.07	0.28

3.4.6 Effects of Emissions Control Technology

The average NH_3 emissions in each emissions technology group are summarized in Figure 3-9. NH_3 emissions from E15 gasoline are higher in all four emissions technology groups (SULEV30, ULEV50, ULEV70 and ULEV125) compared to the E10 gasoline. Table 3-13, the emissions standards, in order of decreasing stringency for tailpipe emissions of NMOG, NOx and hydrocarbons are SULEV30, ULEV50, ULEV70 and ULEV125.

In this study, E15 fuels show clearly higher NH_3 emissions for all technology groups with significantly higher NH_3 emissions for SULEV30 and ULEV125 compared to E10. E10 fuel shows a huge increase in NH_3 emissions between SULEV30 and ULEV50, while E15 fuel shows a slight decrease. ULEV50 and ULEV70 show similar NH_3 emissions when comparing each fuel separately, which is due to the similar NOx and CO regulation for both technology groups (Figure 3-9). Then E10 and E15 fuels for the ULEV125 emissions technology group emit higher NH_3 emissions than the three more stringent emissions standard groups. This significant increase in NH_3 emissions for both E10 and

E15 gasolines for the ULEV125 emissions group is most likely from the difference in exhaust emissions limits, where ULEV125 permits significantly higher CO and NOx compared to the previous emission technology groups. ULEV70 permits 70 mg/mi NOx and 1.7 mg/mi CO, ULEV125 permits 125 mg/mi NOx and 2.1 mg/mi CO. The relationship between the technology groups and NH_3 emissions is likely a result of the increased stringency on precursor NH_3 tailpipe emissions (CO and NOx) from ULEV160 to SULEV20 as seen in Table 3-13, resulting in lower NH_3 emissions.

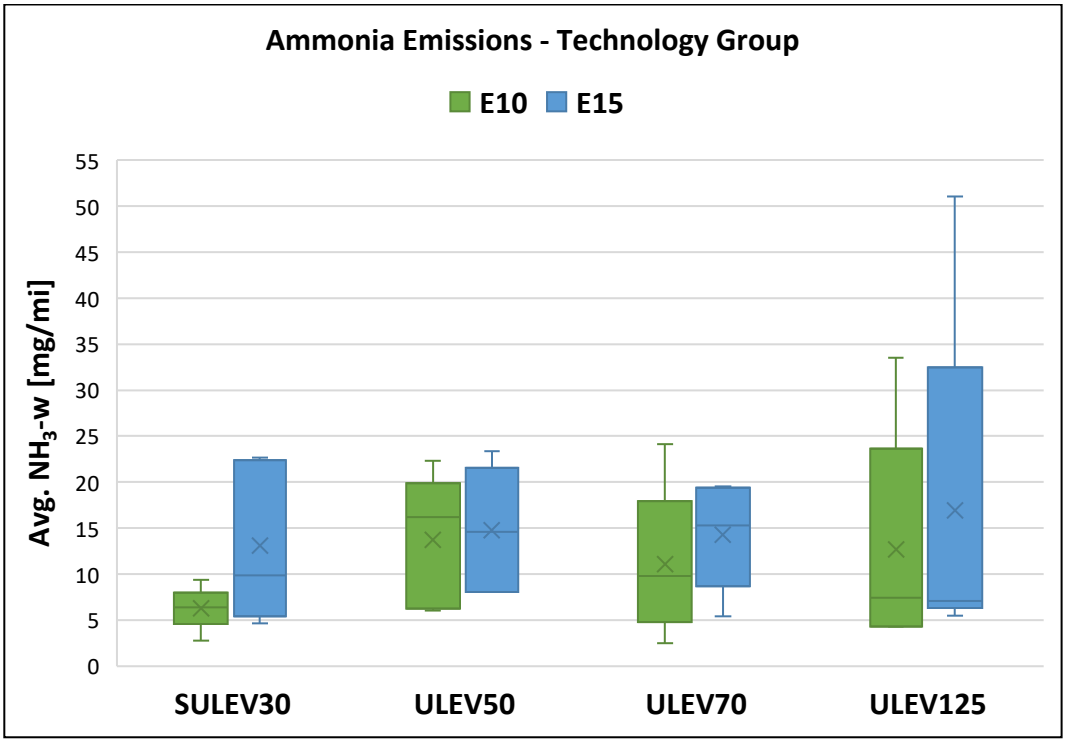

Figure 3-9: Average NH_3-w and emissions technology standards

Table 3-13: California LEV III/EPA Tier 3 150,000-Mile Exhaust Emission Limits (MECA, 2021)

Vehicle Class	Certification Level	NMOG+NOx (mg/mi)	CO (g/mi)
PCs, LDTs, MDPVs (up to 10,000 lbs. GVWR for MDPVs; up to 8500 lbs. GVWR for PCs, LDTs)	LEV160/Bin160	160	4.2
	ULEV125/Bin125	125	2.1
	ULEV70/Bin70	70	1.7
	ULEV50/Bin50	50	1.7
	SULEV30/Bin30	30	1.0
	SULEV20/Bin20	20	1.0

Figure 3-10 shows N_2O emissions are higher for all technology groups for the E10 fuels compared to E15. ULEV50 and ULEV70 shows N_2O emissions to be slightly higher and SULEV30 and ULEV125 shows N_2O emissions to be significantly higher for the E10 fuels than the E15. Several observations have been presented that show a direct increase of N_2O emissions from vehicles equipped with TWC, but the high NO reduction efficiency of the TWC decreases the formation of N_2O (Jobson, et al., 1994). This is a plausible explain for the gradual increase of N_2O emissions with the exception for the E10 fuel in the SULEV30 technology group. Table 3-13 shows an increased stringency in NOx from ULEV125 to SULEV30, which follow the trend of the gradual decrease in N_2O emissions.

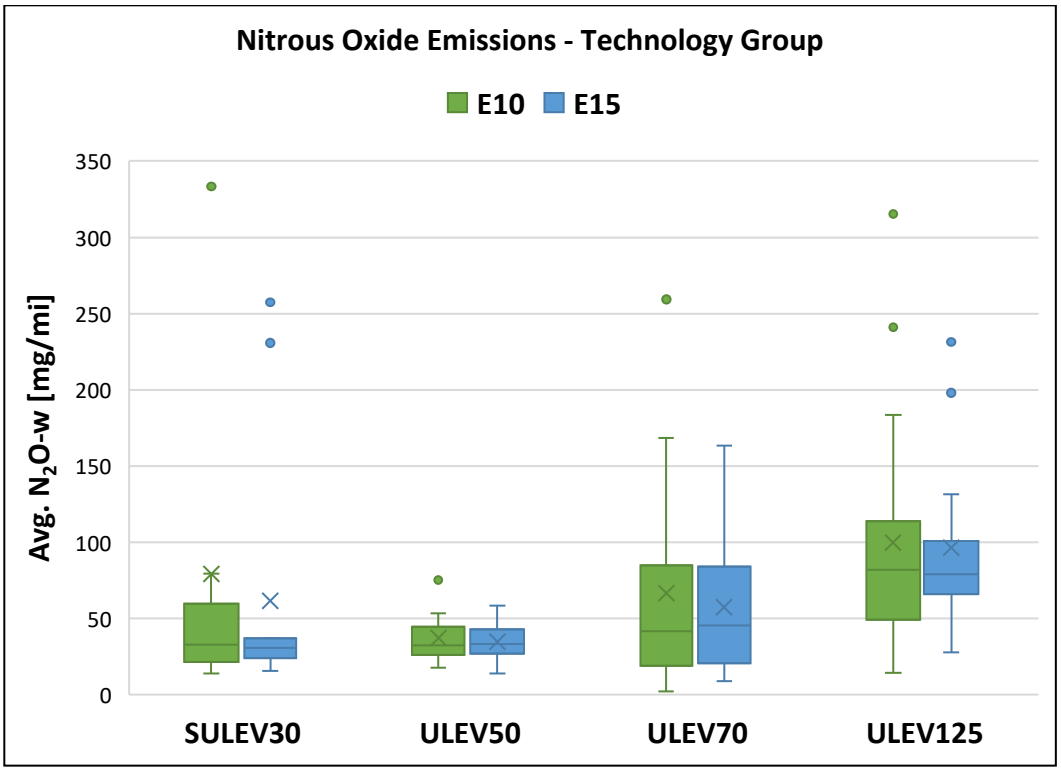

Figure 3-10: Average N_2O-w and emissions technology standards

3.4.7 Linking NH_3 Emissions with Air/Fuel Ratio (λ)

The comparison between NH_3 emissions and the AFR, lambda (λ), was studied for all 20 vehicles (E10 and E15) summarized in Table 3-14. Figure 3-11 show the real-time AFR and NH_3 data for GDI#5, GDI#10, and PFI#5. These three vehicles show the general AFR and NH_3 trends to be consistent with all 20 vehicles, where most of the NH_3 emissions occur when the AFR was slightly less than 1. Figure 3-11 (a) and (b) shows that when AFR is much higher or lower than 1 that NH_3 emissions was at their minimum for both E10 and E15 fuels. Similar to Suarez-Bertoa, et al. (2014), Huai et al., (2003),

Heeb et al., (2006) and Fraser and Cass (1998), this study shows a similar trend where the NH_3 concentrations were generally highest for rich combustion ($\lambda < 1$).

A vehicle operating at a rich AFR emits precursor NH_3 emissions (CO emissions) that eventually form NH_3 in the TWC (Fraser and Cass, 1998). This is seen in graph (b) of Figure 3-12, where a significant amount of CO emissions was formed when the AFR was less than 1. GDI#5 shows that 98% of the total CO was produced during the FTP cycle when the AFR was less than 1. It can be assumed that vehicles equipped with TWC running at a rich AFRs are the main source of ammonia emissions (Fraser and Cass, 1998). Therefore, the increase in NH_3 emissions with increasing vehicles speed and engine load is apparent, since the AFR will likely be in a rich condition (Kean et. al., 2009). However, there have been studies where high NH_3 emissions can be found at lean combustion ($\lambda > 1$) (Baum et al., 2001). NH_3 emissions are not regulated for LDV, therefore the lambda control is dependent on the strategy used by manufacturers to focus on compliance with NOx and CO standards, which is a possibility for increases in NH_3 emissions for lean conditions (Suarez-Bertoa, et al. 2014).

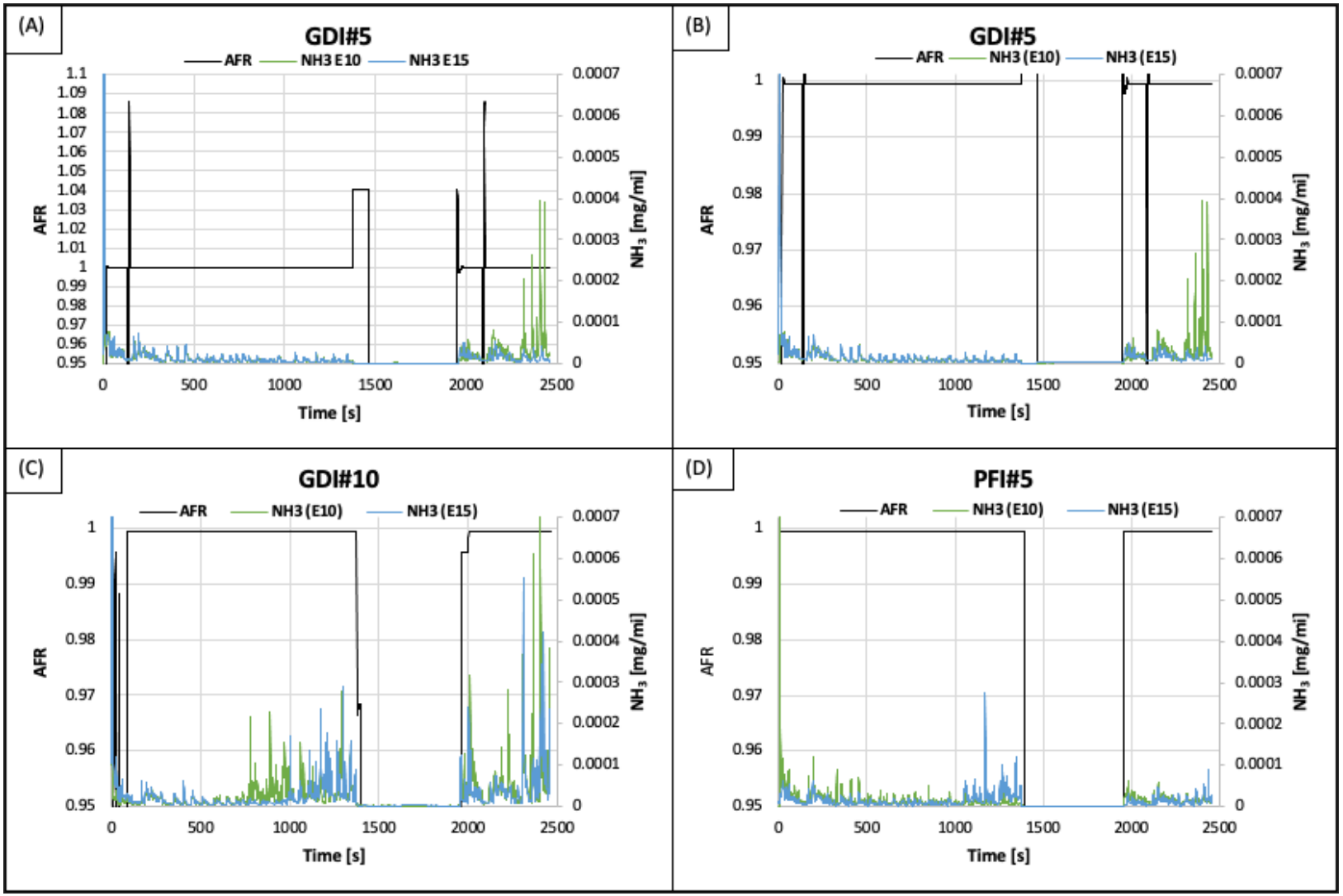

Figure 3-11: (a) GDI#5 Real-time AFR and NH_3, (b) GDI#5 Real-time AFR (<1), (c) GDI#10 Real-time AFR and NH_3, (d) PFI#5 Real-time AFR and NH_3

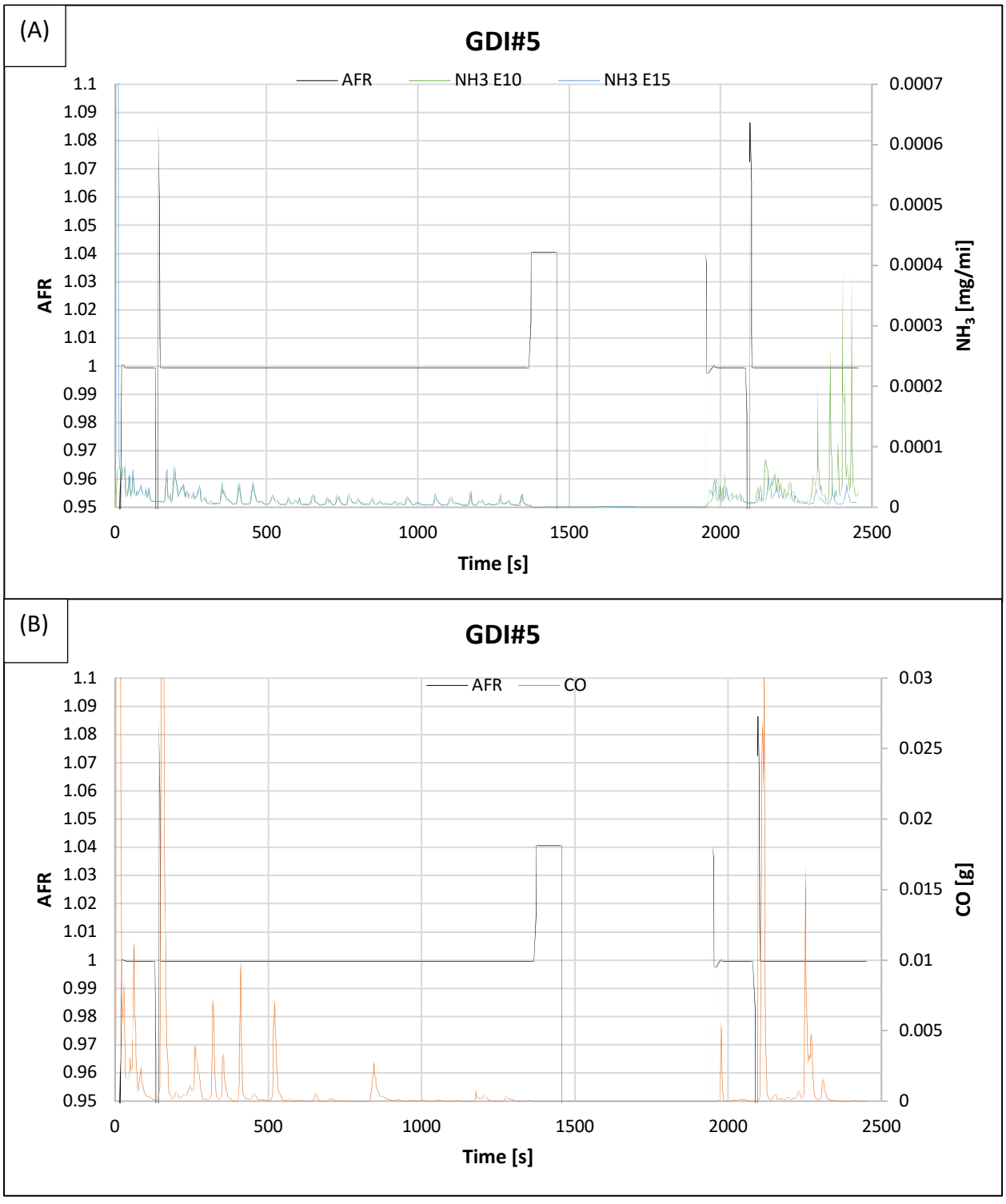

Figure 3-12: (a) GDI#5 Real-time AFR and NH_3, (b) GDI#5 Real-time AFR and CO

Table 3-14: Summary of NH_3-w and AFR

	Avg. NH_3-w E10	Air–fuel equivalence ratio (λ)-E10	Avg. NH_3-w E15	Air–fuel equivalence ratio (λ)-E15
PFI#1	3.37	NA	4.23	NA
GDI#1	2.27	NA	6.78	NA
PFI#2	9.04	NA	4.26	NA
PFI#3	3.13	1.00	5.12	1.00
PFI+GDI#1	4.23	0.94	3.55	0.94
GDI#2	2.29	1.10	1.83	1.09
GDI#3	1.78	NA	1.45	NA
GDI#4	9.59	0.98	7.38	0.98
GDI#5	1.96	0.99	5.49	0.98
PFI#4	1.11	0.99	2.12	1.00
GDI#6	2.36	0.98	3.30	0.98
PFI#5	2.95	1.01	3.01	1.00
GDI#7	21.40	0.90	13.38	0.92
PFI_Hybrid#1	1.54	1.00	1.82	0.99
GDI#8	1.99	0.96	2.28	0.96
GDI#9	2.04	0.98	2.35	0.97
GDI#10	5.91	0.99	8.36	0.99
PFI+GDI#2	4.01	0.98	8.18	0.98
PFI#6	1.53	1.13	2.86	1.12
GDI#11	5.02	1.00	6.60	1.00

3.4.8 Effects of Odometer Reading as a Proxy for TWC Age

Figure 3-13 shows NH3 emissions as a function of odometer readings. Similar to Livingston, et al., 2009 study, the lowest NH_3 emissions were associated with the high odometer (>50,000 miles) and low odometer (<20,000 miles) vehicles for both the E10 and E15 fuel blends. Using odometer reading as an indicator of catalyst age, Figure 3-13 suggests that lower NH_3 emissions is associated with the newest and oldest catalyst, while suggesting the highest NH_3 emissions is associated with catalyst between newest and oldest (Livingston, et al., 2009). Therefore, the Pearson Correlation displayed in Table 3-17, show there is no direct relationship between NH_3 and odometer reading (R=0.05, R=-0.04). However, Liu, et al. (2021) and Farren, et al. (2020) showed that as vehicle mileage increases, the amount of emitted NH3 emissions also increases. This is likely caused by the degradation of the catalyst, as seen in Huai, et al., 2003 study.

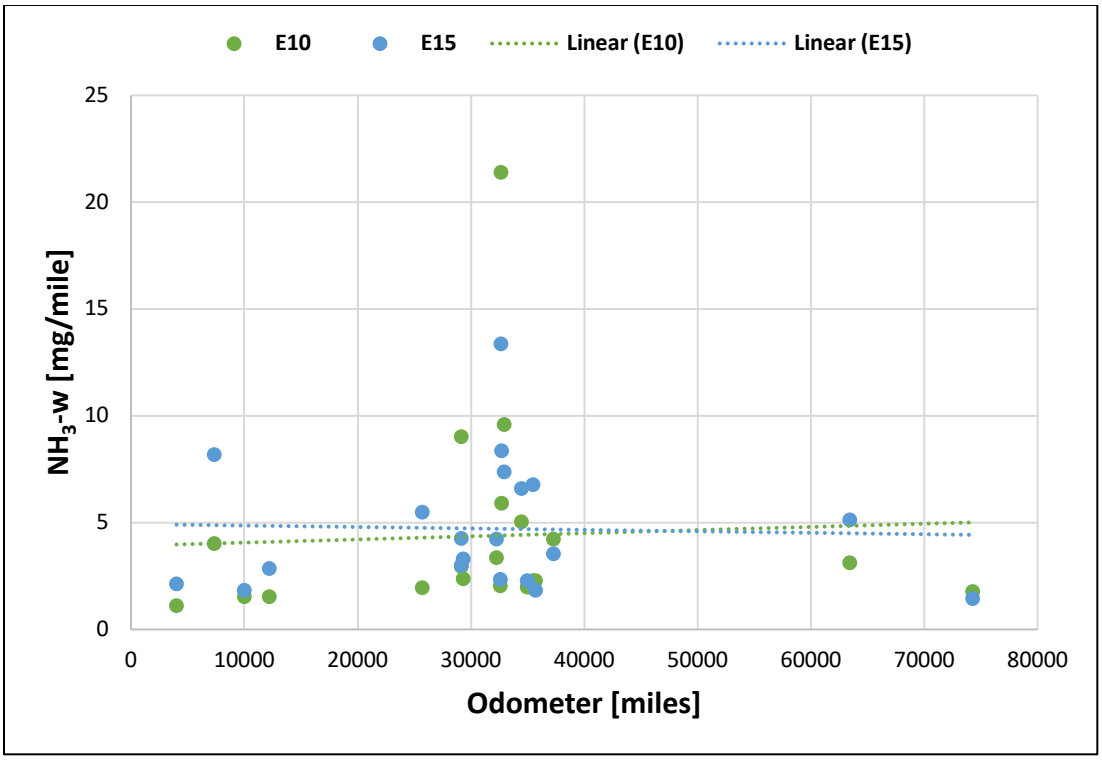

Figure 3-13: Comparison of NH_3-w and odometer reading

Table 3-15: Pearson Correlation of NH_3-w and odometer reading

E10	E15
0.05	-0.04

Figure 3-14 depicts N_2O emissions as a function of odometer reading and Table 3-19 show that there is no correlation between N_2O emissions and odometer reading for both E10 and E15 fuels (R = -0.04, R = -0.15). A previous study also showed no correlation (Barton and Simpson, 1994), while other studies showed a significant correlation (Pringent and De Soete, 1989). These previous studies were with older vehicles using less effective emission technology, different fuel compositions, and emissions instruments

affecting N_2O emissions. It is possible that this study has too small of a sample size to affect the results.

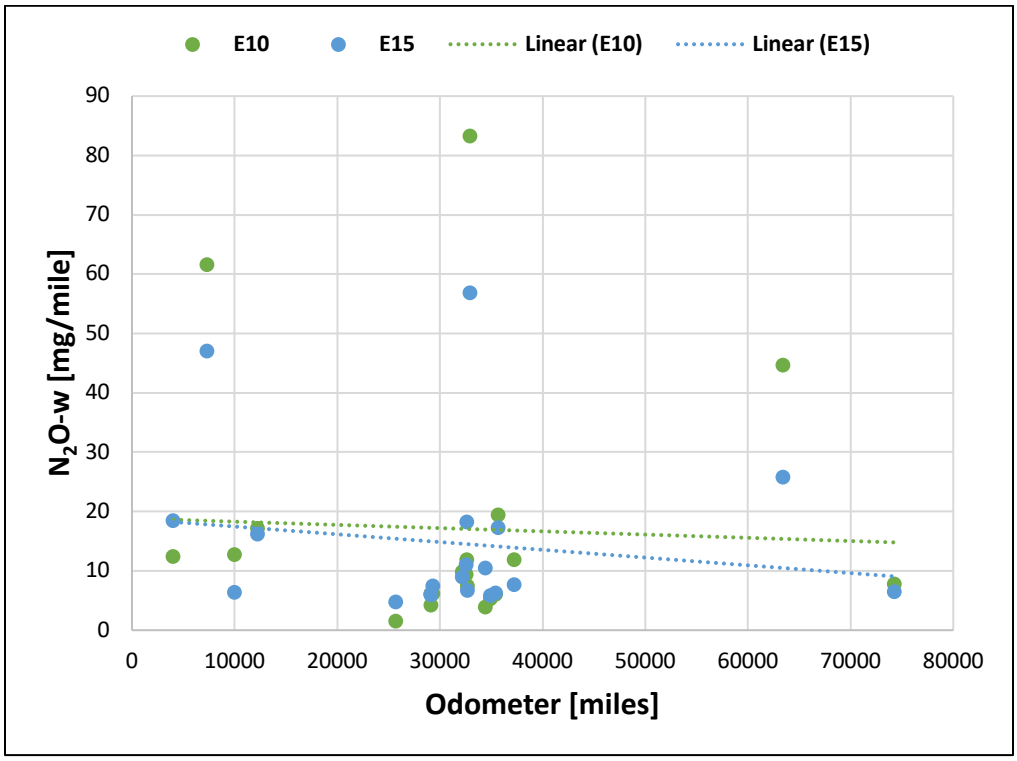

Figure 3-14: Comparison of N_2O-w and odometer reading

Table 3-16: Pearson Correlation of N_2O-w and odometer reading

E10	E15
-0.04	-0.15

3.4.9 Vehicle Weight and NH_3-w Emissions

According to the vehicle weight and NH_3 emissions data plot (Figure 3-15), there is a correlation as vehicle weight increases, NH_3 emissions increases for both the E10 (R=0.58) and E15(R=0.63) gasoline with E10 having a greater NH_3 increase (Table 3-17). This direct correlation is due to less stringent emission technology grouping as vehicles get larger and heavier, where heavier vehicles also require more aggressive accelerations to move their weight.

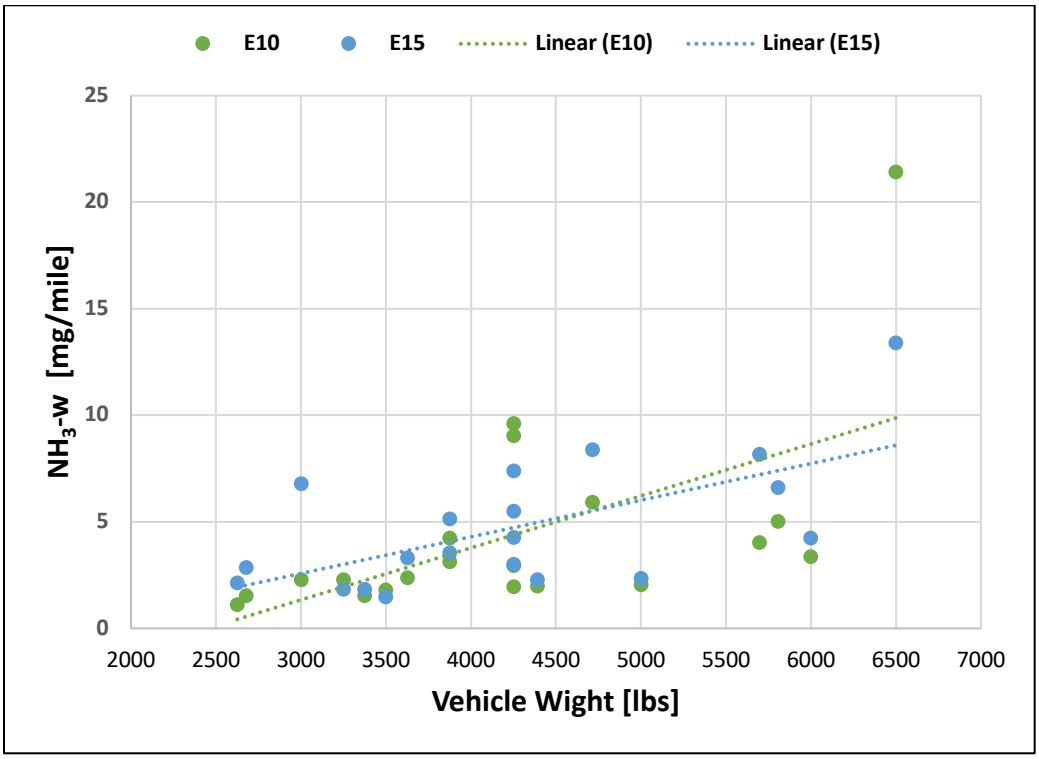

Figure 3-15: Vehicle weight and NH_3-w emissions

Table 3-17: Pearson Correlation Between vehicle weight and NH_3 emissions

	E10 (Avg. NH_3-w FTP mg/mile)	E15 (Avg. NH_3-w FTP mg/mile)	Vehicle Weight
E10 (Avg. NH_3 FTP mg/mile)	1		
E15 (Avg. NH_3 FTP mg/mile)	NA	1	
Vehicle Weight	0.58	0.63	1

3.4.10 Fuel Injection Type (DFI and SFI)

Figure 3-16 compares the NH_3 emissions of the direct fuel injection (DFI) and port fuel injection (PFI) vehicles with E10 and E15 fuels. It is observed that DFI results in higher NH_3 emissions compared to PFI for both E10 and E15 fuels. The NH_3-w for DFI E10 and E15 fuels emitted 5.21 mg/mile and 5.76 mg/mile, respectively, while the NH_3-w for the PFI E10 and E15 fuels emitted 3.24 mg/mi and 3.25 mg/mile of NH_3 emissions, respectively. According to Cole et. al. (1998), a study of gasoline direct-injection engines, tailpipe NOx emissions from DFI vehicles were 2.9 to 9.5 times more than those from the PFI vehicles, not meeting tier II (2004) emission standards, while it did meet the limit for CO. This study shows NOx emissions for DFI vehicles being 8%-13% lower and CO emissions being slightly higher (2 - 6%) compared to PFI vehicles. Since NOx and CO are precursor emissions, it is possible that the slightly elevated CO emissions is sufficient to produce higher NH_3 for the DFI vehicles compared to the PFI vehicles.

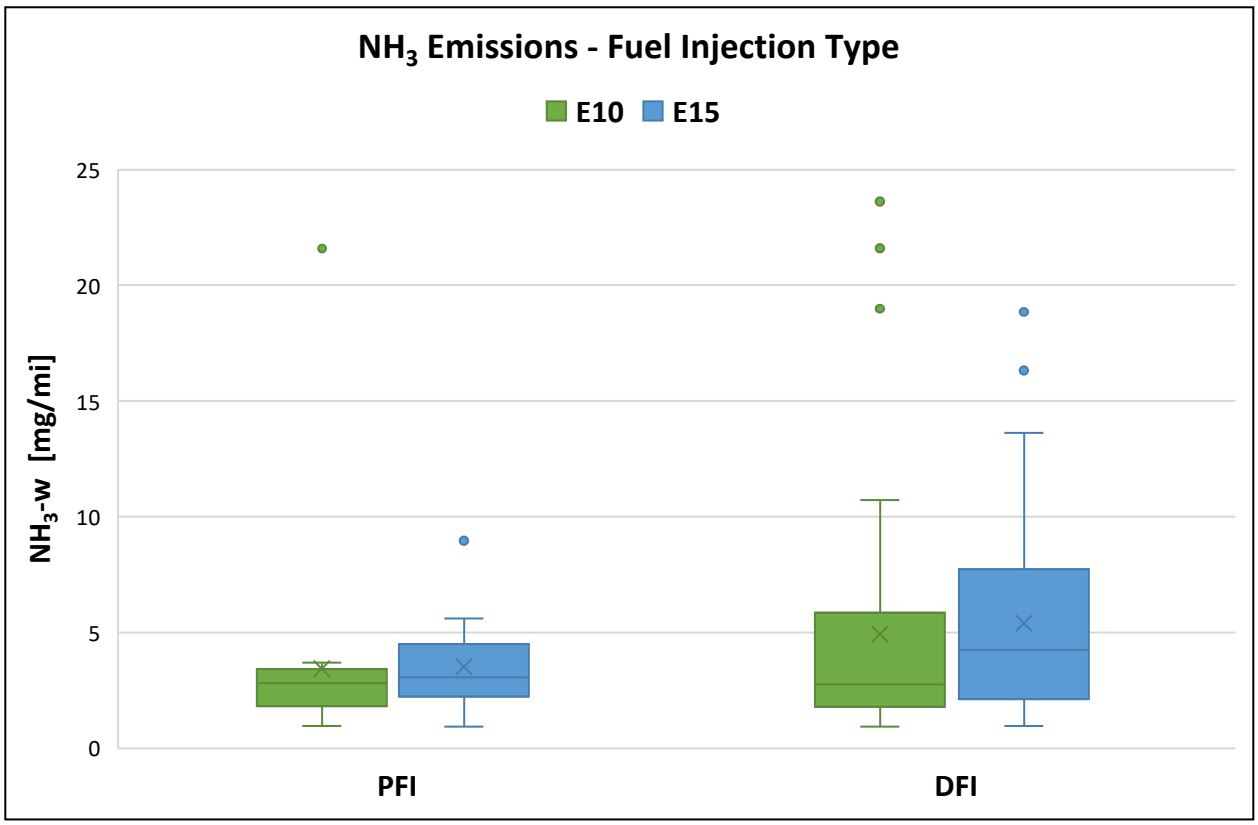

Figure 3-16: NH_3-w emissions and fuel injection type

Figure 3-17 compares the N_2O emissions for the DFI and PFI vehicles with E10 and E15 fuels. PFI vehicles showed significantly higher N_2O emissions compared to DFI vehicles. The N_2O for DFI E10 and E15 fuels emitted 57.65 mg/mile and 56.75 mg/mile, respectively, while the weighted average of the PFI E10 and E15 fuel emitted 95.98 mg/mi and 74.39 mg/mile of NH_3 emissions, respectively. This study shows NOx emissions for PFI vehicles being 8%-13% higher than DFI vehicles. This likely contributed to the higher N_2O emissions from the PFI vehicles compared to the DFI

vehicles, since N_2O emissions are formed from the reaction of NOx in exhaust emissions treatment systems as seen in Suarez-Bertoa, et al., 2016 study.

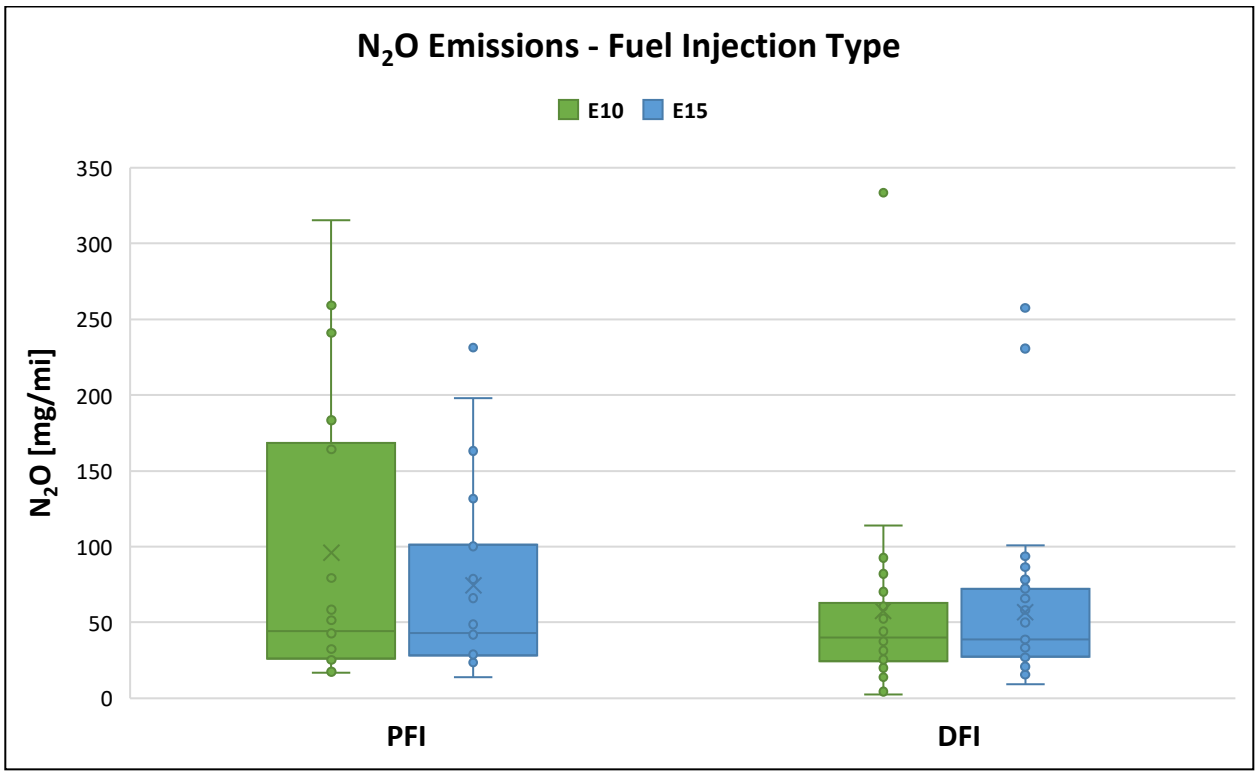

Figure 3-17: N_2O-w emissions and fuel injection type

3.4.11 Naturally aspirated and Turbocharged engines

Figure 3-18 shows a comparison of NH_3 emissions for naturally aspirated and turbocharged engine air intake systems with E10 and E15 fuels. It is observed that for naturally aspirated engines, E15 produced higher NH_3 emissions, where for turbocharged engine E10 produced higher NH_3 emissions. The data shows that turbocharged engines resulted in much higher overall NH_3 emissions compared to naturally aspirated engines

for both E10 and E15 fuels. The weighted average NH_3 emissions for the turbocharged E10 and E15 fuels emitted 5.01 mg/mile and 5.60 mg/mile, respectively, while the naturally aspirated E10 and E15 fuels emitted 4.33 mg/mile and 4.64 mg/mile, respectively. These results are consistent with those from Suarez-Bertoa, et al., 2014, a European study, which also showed NH_3 emissions to be significantly higher for turbocharged engines compared to naturally aspirated engines.

According to Mahmoudi, et al. (2017) in their engine air intake system emissions study, turbocharged engine resultant emissions of CO and NOx proved to be higher in terms of their concentrations in the exhaust plumes compared to naturally aspirated engines. That study showed that turbocharged vehicles with E10 and E15 fuel to be 28-32% and 20-22% higher NOx and CO emissions than naturally aspirated vehicles. Both resultant emissions are precursor emissions required for NH_3 production in the TWC, as shown in the chemical reactions 1, 2a and 2b, likely contributing to the higher NH_3 emissions in the turbocharged engines compared to the naturally aspirated engines.

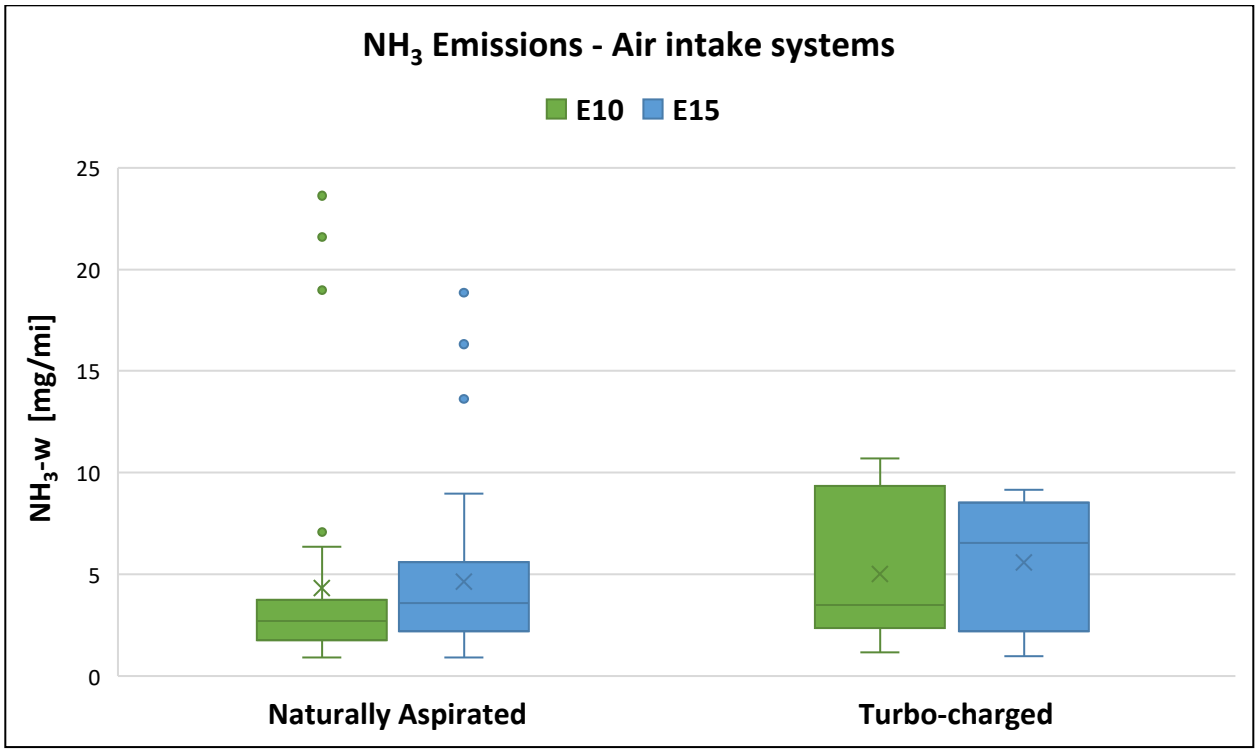

Figure 3-18: NH_3-w and air intake systems

Figure 3-19 shows a comparison of N_2O-w emissions for naturally aspirated and turbocharged engine air intake systems with E10 and E15 fuels. It is observed that turbo-charged vehicles produce significantly higher N_2O-w emissions compared to naturally aspirated vehicles for both E10 and E15 fuels. The N_2O-w for the turbocharged E10 and E15 fuel emitted 81.89 mg/mile and 77.29 mg/mile, respectively, while the naturally aspirated E10 and E15 fuel emitted 72.20 mg/mile and 66.88 mg/mile, respectively. NOx emissions for the turbocharged E10 and E15 fuels were 28% and 32% higher compared to the naturally aspirated vehicles. This high increase in NOx emissions due to the turbocharger is likely the reason for the high N_2O emissions from the turbocharged vehicles since NOx is a precursor to N_2O in the catalyst (Suarez-Bertoa, et al., 2016).

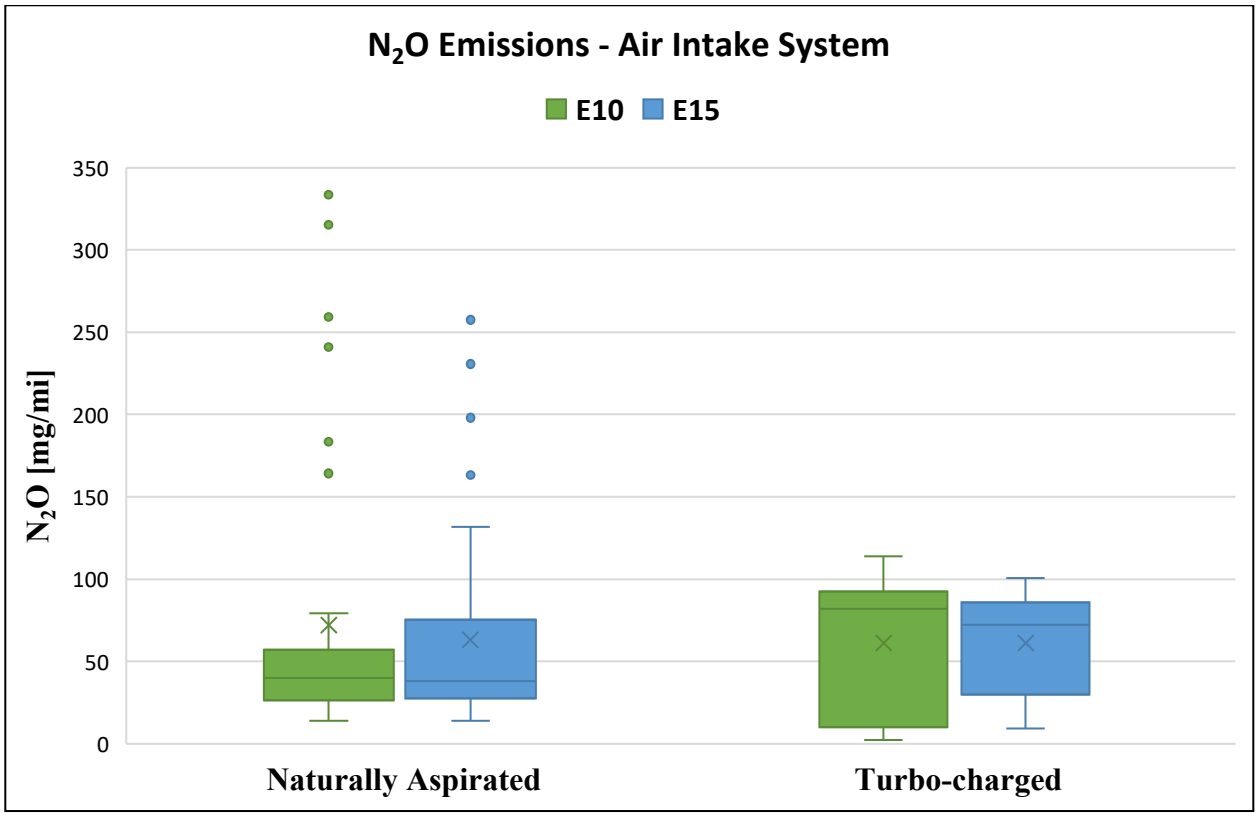

Figure 3-19: N_2O-w and air intake systems

3.5 Discussion

In this study, the NH_3-w emissions from this 20-vehicle fleet were compared and analyzed with previous studies (Pierson and Brachaczek, 1983; Fraser and Cass, 1998; Moechli et. al., 1996; Kean et. al. 2000; Baum et. al., 2001; Durbin et. al., 2002; Emmenegger et. al., 2004; Durbin et. al., 2004, Huai et al., 2003; Livingston et. al., 2009; Kean et. al., 2009; Suarez-Bertoa and Storga, 2016; Wang, et. al., 2019) as illustrated in Figure 3-20 and described in Table 3-18. This study had very similar NH_3 emissions

results to Pierson and Brachaczek (1983), Suarez-Bertoa and Storga (2016), Wang, et. al. (2019). The Pierson and Brachaczek (1983) NH_3 emissions tunnel study showed similar results to this paper most likely because less than 10% of vehicles were equip with TWCs. Since the majority of NH_3 emissions is produced in the TWC, the resulting NH_3 emissions should be low in that particular study. The Suarez-Bertoa and Storga (2016) chassis dynamometer study had similar NH_3 emissions results as this paper because this 2016 study was conducted with a fleet of light-duty hybrid electric vehicles over a WLTC cycle. Hybrid vehicles generally produce less NH_3 precursor emissions resulting in low NH_3 emission levels, which was seen in this study. The Wang, et. al. (2019) chassis dynamometer study also had similar NH_3 emissions results as this study likely because the China-6 compliant cars over the WLTC cycle are equipped with TWCs and have similar manufacture year as this study. Lastly, the Durbin et. al. (2004) and Huai et al. (2003) chassis dynamometer FTP tests had somewhat similar NH_3 emissions results that are worth mentioning. This is likely because this emissions test in 2004 was tested over the FTP cycle with vehicles that were equipped with TWCs under less stringent emissions standards, which is probably why these early tests showed higher NH_3 emissions (Durbin et. al., 2004, Huai et al., 2003)

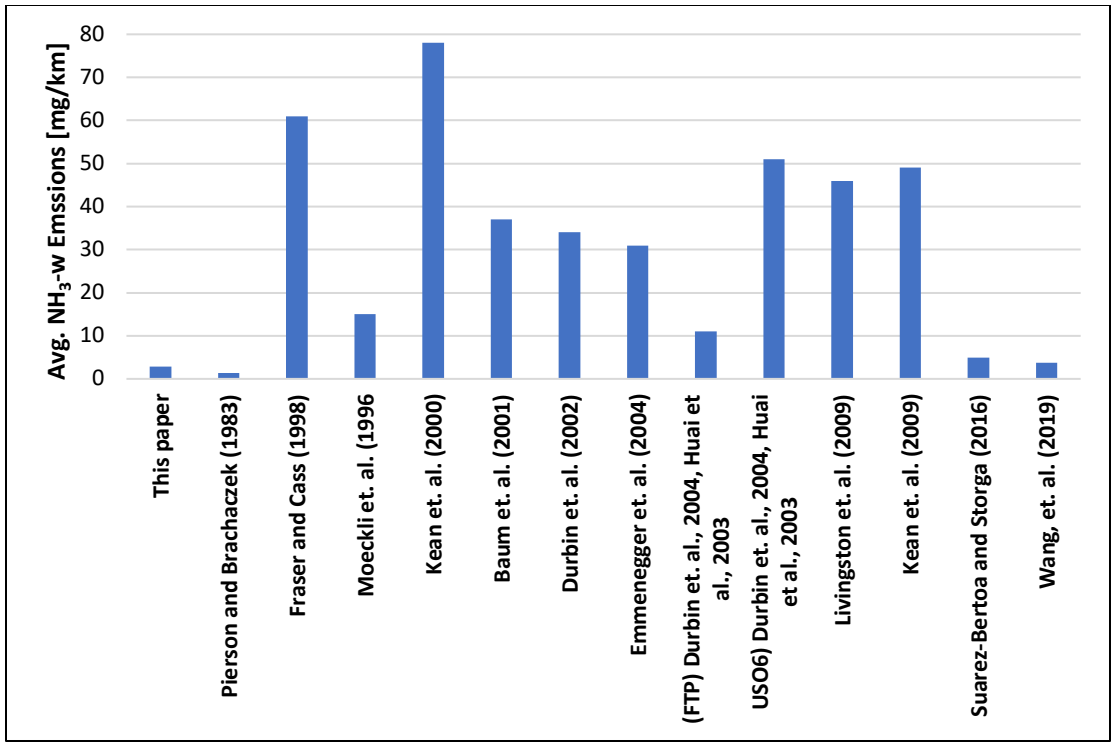

Figure 3-20: NH_3 results comparison between this study and other publications

Table 3-18: Comparison of on-road and dynamometer-based NH_3-w emissions measurement light-duty vehicles

Location	Authors	NH_3 [mg/km]	Methodology	Notes	Year
Riverside, CA	This paper	2.83	Chassis Dynamometer (FTP)	20 vehicle fleet (year 2016-2020) equip with TWCs	2021
Allegheny Mountain Tunnel, PA	Pierson and Brachaczek (1983)	1.3	Tunnel	Very few (<10%) three-way catalyst (TWC) equipped vehicles	1981
Van Nuys Tunnel, CA	Fraser and Cass (1998)	61	Tunnel	81% of vehicles were TWC equipped	1993
Gubrist Tunnel, Switzerland	Moeckli et. al. (1996	15	Tunnel	Authors have greater confidence in mg km−1 than mg kg−1	1995
Caldecott Tunnel, CA	Kean et. al. (2000)	78	Tunnel	Warmed-up vehicles traveling at highway speeds up 4% grade	1999
Freeway On-Ramp, CA	Baum et. al. (2001)	37	Remote Sensing	Remote sensing study of warmed-up vehicles	1999
Riverside, CA	Durbin et. al. (2002)	34	Chassis Dynamometer (FTP)	Mixed fleet of 39 vehicles on FTP driving cycle	2001
Riverside, CA	(FTP) Durbin et. al., 2004, Huai et al., 2003	11	Chassis Dynamometer (FTP)	Dynamometer study of twelve 2000–2001 vehicles on FTP cycle	2002
Riverside, CA	(US06) Durbin et. al., 2004, Huai et al., 2003	51	Chassis Dynamometer (US06)	Dynamometer study of twelve 2000–2001 vehicles on US06 cycle	2002
California South Coast Air Basin	Livingston et. al. (2009)	46	Chassis Dynamometer (FTP)	Fleet of 41 light and medium-duty recent model year and technology vehicles	2009
Caldecott Tunnel, CA	Kean et. al. (2009)	49	Remote Sensing	Light-duty and heay-duty vehicles traveling uphill equip with a catalyst	2001
Caldecott Tunnel, CA	Suarez-Bertoa and Storga (2016)	5	Chassis Dynamometer	Nine modern light duty vehicles tested over the NEDC with catalyst	2006
Beijing, China	Wang, et. al. (2019)	3.7	Chassis Dynamometer (WLTC)	7 China-6 compliant cars were measured	2019

N_2O-w emissions from this 20-vehicle fleet were compared and analyzed with previous studies (Behrentz et. al., 2004; Becker et. al. 2000; Ballantyne et. al, 1994; Huai et. al., 2003; Sjodin et. al., 1995; Jimenez et. al., 2000), as illustrated in Figure 3-21 and described in Table 3-19. This study shows similar N_2O emissions results to Becker et. al. (2000) and Jimenez et. al. (2000). Becker et. al. (2000) N_2O emissions study showed similar results likely due to both studies using the same testing method that is dynamometer and FTIR spectroscopy with LDVs. Jimenez et. al. (2000) showed N_2O emissions slightly higher than this study probably since the study was conducted in 1996 with lower efficiency catalyst-equipped vehicles.

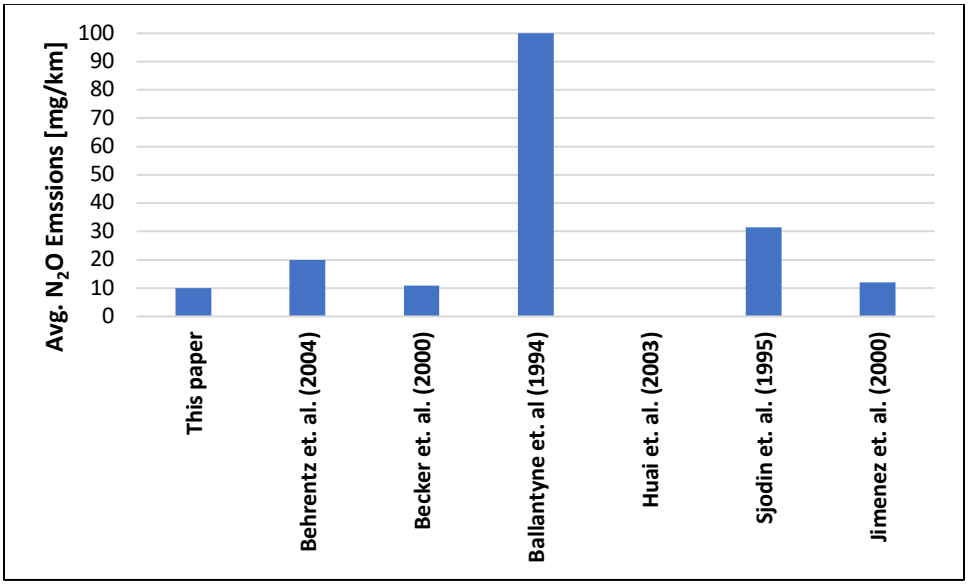

Figure 3-21: N_2O results comparison between this study and other publications

Table 3-19: Comparison of on-road and dynamometer-based N_2O-w emissions measurement light-duty/medium duty vehicles

Location	Authors	N_2O [mg/km]	Methodology	Notes	Year
Riverside, CA	This paper	9.9	Chassis Dynamometer (FTP)	20 vehicle fleet (year 2016-2020) equip with TWCs	2021
El Monte, CA	Behrentz et. al. (2004)	20	Chassis Dynamometer (FTP)	37 LDVs (1986-2001)	2004
Wuppert al, Germany	Becker et. al. (2000)	11	Chassis dynamometer (FTP)	Dynamometer test for 26 LDVs using alternative fuels (85% methanol and 85% ethanol)	2000
Canada	Ballantyne et. al (1994)	100	Chassis dynamometer (FTP)	9 aged catalyst and 5 new catalysts	1994
Riverside, CA	Huai et. al. (2003)	1.37E-05	Chassis dynamometer (FTP)	5 CNG, 3 LPG, and 2 gasoline vehicles	2003
Sweden	Sjodin et. al. (1995)	32	Tunnel	4000 vehicles per hour	1995
Los Angelos, CA	Jimenez et. al. (2000)	12	Tunnel	tunable infrared laser differential absorption spectroscopy (TILDAS)	2000

Figure 3-20, Figure 3-21, Table 3-18 and Table 3-19 show NH_3-w and N_2O-w emissions reported from different studies with varying vehicles fleets. The average NH_3-w and N_2O-w emissions have similar results as some previous studies, while the other studies had significantly different results. Differences in the average NH_3-w and N_2O-w emissions as presented above are likely due to differences in vehicle fleets (i.e., vehicle types, model year, emissions technology, driving style/conditions (cold start/hot start), catalyst age) and testing methodologies (Livingston et. al., 2009).

3.6 Conclusion

Chassis dynamometer NH_3 and N_2O emissions testing was conducted for a fleet of twenty light-duty vehicles carried out using an FTIR over an FTP cycle. This study compared the use of E10 and E15 gasoline and its relation to N_2O and NH_3 emissions. The overall NH_3 emissions was higher with E15 gasoline compared to E10. Of the NH_3 precursor emissions, CO and NOx, it was found that NOx has a greater correlation with NH_3 emissions for both E10 and E15 fuels. GDI#7 being the biggest emitter of NH_3, showed that E15 fuels produced high levels of both CO and NOx emissions that match NH_3 emission peaks. Emissions technology standards showed that E15 fuels emitted greater NH_3 compared to E10 fuels in all technology groups. Rich AFR ($\lambda < 1$) was also seen as indicator for high NH_3 emissions. Odometer reading was used as an indicator of TWC age, and it showed that highest NH_3 emissions were associated with catalyst with intermediate ages, between 20,0000 miles to 50,0000 miles (Livingston, et al., 2009). Heavier vehicles had higher NH_3 emissions for both fuels. DFI vehicles produced higher

NH_3 emissions, while E15 fuels still emitted higher NH_3 emissions for both DFI and SFI. Lastly, turbocharged engines produce much higher precursor NH_3 emissions, resulting in higher NH_3 emissions for both E10 and E15 fuels.

Overall N_2O-w emissions were higher with E10 fuels than the E15 fuels. N_2O showed significant correlations with NOx emissions in phase 1 of the FTP cycle for both E10 and E15 fuels. ULEV70 and ULEV125 emissions technology groups show higher N_2O emissions compared to SULEV30 and ULEV50, likely due to the more stringent NOx standards. PFI vehicles showed much higher N_2O emissions than the DFI vehicles, where PFI vehicles also showed higher NOx emissions than the DFI vehicles. Lastly, turbocharged vehicles emitted significantly higher N_2O emissions for both E10 and E15 fuels compared to the naturally aspirated vehicles.

3.7 References

Ballantyne, Vera F., et al. "Nitrous Oxide Emissions from Light Duty Vehicles." SAE Technical Paper Series, 1994.

Barton P., and J. Simpson. "The effects of aged catalysts and cold ambient temperatures on nitrous oxide emissions." Mobile sources emissions division, 1994.

Battye, W. "Evaluation and improvement of ammonia emissions inventories." Atmospheric Environment, vol. 37, no. 27, 2003, pp. 3873-3883, https://www.sciencedirect.com/science/article/pii/S1352231003003431.

Baum, Marc M., et al. "Multicomponent Remote Sensing of Vehicle Exhaust by Dispersive Absorption Spectroscopy. 2. Direct On-Road Ammonia Measurements." Environmental Science & Technology, vol. 35, no. 18, 2001, pp. 3735-3741.

Becker, K.H, et al. "Contribution of vehicle exhaust to the global N2O budget." Chemosphere - Global Change Science, vol. 2, no. 3-4, 2000, pp. 387-395, www.sciencedirect.com/science/article/abs/pii/S1465997200000179.

Behera, Sailesh N., and Mukesh Sharma. "Investigating the potential role of ammonia in ion chemistry of fine particulate matter formation for an urban environment." Science of The Total Environment, vol. 408, no. 17, 2010, pp. 3569-3575, www.sciencedirect.com/science/article/pii/S0048969710003955.

Behrentz, Eduardo, et al. "Measurements of nitrous oxide emissions from light-duty motor vehicles: a pilot study." Atmospheric Environment, vol. 38, no. 26, 2004, pp. 4291-4303, www.sciencedirect.com/science/article/abs/pii/S1352231004004303.

Borsari, Vanderlei, and João V. Assunção. "Ammonia emissions from a light-duty vehicle." Transportation Research Part D: Transport and Environment, vol. 51, 2017, pp. 53-61, www.sciencedirect.com/science/article/pii/S1361920916304151.

Cadle, Steven H., and Patricia A. Mulawa. "Low-molecular-weight aliphatic amines in exhaust from catalyst-equipped cars." Environmental Science & Technology, vol. 14, no. 6, 1980, pp. 718-723.

California Air Resource Board. California Air Resource Board, ww2.arb.ca.gov/about. Accessed 5 July 2021.

Cole, Roger L., et al. "Exhaust Emissions of a Vehicle with a Gasoline Direct-Injection Engine." SAE Technical Paper Series, vol. 107, 1998, pp. 1696-1706, www.jstor.org/stable/44746573.

Dale, Bruce, and David Pimental. "Does Ethanol Make Economic and Environmental Sense?" Americas Quarterly, 11 Dec. 2008, www.americasquarterly.org/does-ethanol-make-economic-and-environmental-sense/.

Durbin, Thomas D., et al. "The effect of fuel sulfur on NH3 and other emissions from 2000–2001 model year vehicles." Atmospheric Environment, vol. 38, no. 17, 2004, pp. 2699-2708, www.sciencedirect.com/science/article/pii/S1352231004001530.

---. "Estimates of the emission rates of ammonia from light-duty vehicles using standard chassis dynamometer test cycles." Atmospheric Environment, vol. 36, no. 9, 2002, pp. 1475-1482, www.sciencedirect.com/science/article/pii/S1352231001005830.

Emmenegger, L., et al. "Measurement of ammonia emissions using various techniques in a comparative tunnel study." International Journal of Environment and Pollution, vol. 22, no. 3, 2004, p. 326, www.inderscienceonline.com/doi/abs/10.1504/IJEP.2004.005547.

Farren, Naomi J., et al. "Underestimated Ammonia Emissions from Road Vehicles." Environmental Science & Technology, vol. 54, no. 24, 2020, pp. 15689-15697, pubs.acs.org/doi/full/10.1021/acs.est.0c05839.

Fraser, Matthew P., and Glen R. Cass. "Detection of Excess Ammonia Emissions from In-Use Vehicles and the Implications for Fine Particle Control." Environmental Science & Technology, vol. 32, no. 8, 1998, pp. 1053-1057, pubs.acs.org/doi/full/10.1021/es970382h.

Heeb, Norbert V., et al. "Three-way catalyst-induced formation of ammonia—velocity- and acceleration-dependent emission factors." Atmospheric Environment, vol. 40, no. 31, 2006, pp. 5986-5997.

Hirano, H., et al. "Mechanisms of the various nitric oxide reduction reactions on a platinum-rhodium (100) alloy single crystal surface." Surface Science, vol. 262, no. 1-2, 1992, pp. 97-112, www.sciencedirect.com/science/article/pii/003960289290463G.

Huai, Tao, et al. "Estimates of the emission rates of nitrous oxide from light-duty vehicles using different chassis dynamometer test cycles." Atmospheric

Environment, vol. 38, no. 38, 2004, pp. 6621-6629, www.sciencedirect.com/science/article/abs/pii/S1352231004006909#bib20.

---. "Investigation of NH3Emissions from New Technology Vehicles as a Function of Vehicle Operating Conditions." Environmental Science & Technology, vol. 37, no. 21, 2003, pp. 4841-4847.

---. Analysis of Nitrous Oxide and Ammonia Emissions from Motor Vehicles. College of Engineering-Center for Environmental Research and Technology University of California, Riverside, 2003.

Jimenez, J.L., et al. "Cross road and mobile tunable infrared laser measurements of nitrous oxide emissions from motor vehicles." Chemosphere - Global Change Science, vol. 2, no. 3-4, 2000, pp. 397-412, www.sciencedirect.com/science/article/pii/S1465997200000192.

Jobson, Edward, et al. "Nitrous Oxide Formation Over Three-Way Catalyst." SAE Technical Paper Series, 1994, www.jstor.org/stable/44612362.

Kean, A.J., et al. "Trends in on-road vehicle emissions of ammonia." Atmospheric Environment, vol. 43, no. 8, 2009, pp. 1565-1570, www.sciencedirect.com/science/article/pii/S1352231008008881.

Kean, Andrew J., et al. "On-Road Measurement of Ammonia and Other Motor Vehicle Exhaust Emissions." Environmental Science & Technology, vol. 34, no. 17, 2000, pp. 3535-3539, pubs.acs.org/doi/abs/10.1021/es991451q.

Liu, Yingshuai, et al. "Research on ammonia emissions from three-way catalytic converters based on small sample test and vehicle test." Science of The Total Environment, vol. 795, 2021, p. 148926, www.sciencedirect.com/science/article/pii/S004896972103998X. Accessed 28 July 2021.

Livingston, Cody, et al. "Ammonia emissions from a representative in-use fleet of light and medium-duty vehicles in the California South Coast Air Basin." Atmospheric Environment, vol. 43, no. 21, 2009, pp. 3326-3333, www.sciencedirect.com/science/article/pii/S1352231009003240.

Mahmoudi, Amir R., et al. "Simulating the effects of turbocharging on the emission levels of a gasoline engine." Alexandria Engineering Journal, vol. 56, no. 4, 2017, pp. 737-748, www.sciencedirect.com/science/article/pii/S1110016817300960.

MECA. "U.S. EPA Tier 3 and California LEV III Rulemakings | MECA." Manufacturers of Emission Controls Association | MECA, 2021, www.meca.org/regulation/epa-tier-3-and-california-lev-iii-rulemakings.

Moeckli, Marc A., et al. "Emission Factors for Ethene and Ammonia from a Tunnel Study with a Photoacoustic Trace Gas Detection System." Environmental Science & Technology, vol. 30, no. 9, 1996, pp. 2864-2867, pubs.acs.org/doi/full/10.1021/es960152n.

Pielecha, Jacek, et al. "Testing and evaluation of cold-start emissions from a gasoline engine in RDE test at two different ambient temperatures." Open Engineering, vol. 11, no. 1, 2021, pp. 425-434.

Pierson, William R., and Wanda W. Brachaczek. "Emissions of ammonia and amines from vehicles on the road." Environmental Science & Technology, vol. 17, no. 12, 1983, pp. 757-760, pubs.acs.org/doi/pdf/10.1021/es00118a013.

Prigent, Michel, and Gérard De Soete. "Nitrous Oxide N2O in Engines Exhaust Gases-A First Appraisal of Catalyst Impact." SAE Technical Paper Series, 1989.

Shores, Richard C., et al. "Ammonia Emissions from the EPA's Light Duty Test Vehicle." SAE Technical Paper Series, 2001.

Sjödin, Åke, et al. "Estimations of Real-World N2O Emissions from Road Vehicles by Means of Measurements in a Traffic Tunnel." Journal of the Air & Waste Management Association, vol. 45, no. 3, 1995, pp. 186-190.

Suarez-Bertoa, R., and C. Astorga. "Unregulated emissions from light-duty hybrid electric vehicles." Atmospheric Environment, vol. 136, 2016, pp. 134-143, www.sciencedirect.com/science/article/pii/S1352231016303041.

Suarez-Bertoa, R., et al. "Ammonia exhaust emissions from spark ignition vehicles over the New European Driving Cycle." Atmospheric Environment, vol. 97, 2014, pp. 43-54, www.sciencedirect.com/science/article/pii/S1352231014005809#bib4. Accessed 22 July 2021.

Suarez-Bertoa, Ricardo, et al. "On-road measurement of NH3 and N2O emissions from a Euro V heavy-duty vehicle." Atmospheric Environment, vol. 139, 2016, pp. 167-175, www.sciencedirect.com/science/article/pii/S1352231016303181.

Truyen, Pham Huu, et al. "INFLUENCE OF E10, E15 AND E20 FUELS ON PERFORMANCE AND EMISSIONS OF IN-USE GASOLINE PASSENGER CARS." ASEAN Engineering Journal, vol. 4, 2015,

www.researchgate.net/publication/340023625_Influence_of_E10_E15_and_E20_fuels_on_performance_and_emissions_of_in-use_gasoline_passenger_cars.

Wallington, T.J., and P. Wiesen. "N2O emissions from global transportation." Atmospheric Environment, vol. 94, 2014, pp. 258-263, www.sciencedirect.com/science/article/pii/S1352231014003653#bib17.

Wang, Xin, et al. "Ammonia emissions from China-6 compliant gasoline vehicles tested over the WLTC." Atmospheric Environment, vol. 199, 2019, pp. 136-142, www.sciencedirect.com/science/article/pii/S1352231018307994.

Warren, Matthew. "Psychologists Love To Report “Marginally Significant” Results, According To A New Analysis." Research Digest, 12 Mar. 2019, digest.bps.org.uk/2019/03/12/psychologists-love-to-report-marginally-significant-results-according-to-a-new-analysis/.

Żółtowski, Andrzej, and Wojciech Gis. "Ammonia Emissions in SI Engines Fueled with LPG." Energies, vol. 14, no. 3, 2021, p. 691.